Technische Universität Graz

Institut für Chemische Verfahrenstechnik und Umwelttechnik

Kinetic study of the self-condensation of acetone in a water/toluene system

Sandrina Stocker, BSc

Graz, November 2020

Sandrina Stocker, BSc

Kinetic study of the self-condensation of acetone in a water/toluene system

Master Thesis

zur Erlangung des akademischen Grades eines

Diplom-Ingenieur

in

Verfahrenstechnik

eingereicht an der

Technischen Universität Graz

Betreuer:

Univ.-Prof. Dr.-Ing. habil. Zeiner, Tim

Dipl.-Ing. Nagl, Roland, BSc

Institut für Chemische Verfahrenstechnik und Umwelttechnik

Graz, November 2020

Deutsche Fassung:

Beschluss der Curricula-Kommission für Bachelor-, Master- und Diplomstudien vom 10.11.2008

Genehmigung des Senates am 1.12.2008

EIDESSTATTLICHE ERKLÄRUNG

Ich erkläre an Eides statt, dass ich die vorliegende Arbeit selbstständig verfasst, andere als die angegebenen Quellen/Hilfsmittel nicht benutzt, und die den benutzten Quellen wörtlich und inhaltlich entnommenen Stellen als solche kenntlich gemacht habe.

Graz, am …… ……

(Unterschrift)

Englische Fassung:

STATUTORY DECLARATION

I declare that I have authored this thesis independently, that I have not used other than the declared sources / resources, and that I have explicitly marked all material which has been quoted either literally or by content from the used sources.

Graz, …… ……

date (signature)

Danksagung

An dieser Stelle möchte ich mich bei allen bedanken, die mir bei der Erstellung dieser Arbeit geholfen und mich während meines Studiums unterstützt haben.

Mein Dank gilt Herrn Univ.-Prof. Dr.-Ing. habil. Tim Zeiner, der mir die Teilnahme an diesem Projekt und die damit verbundene interessante Aufgabenstellung ermöglicht hat. Außerdem möchte ich mich bei meinem Betreuer DI Roland Nagl, BSc für die Unterstützung bei der Erstellung der Arbeit und die Hilfe bei Herausforderungen bedanken. Mein Dank gilt auch dem Laborteam des ICVT, das meinen Arbeitsalltag spannender und lustiger gemacht hat.

Ein besonderer Dank gilt meinen Eltern, die nicht nur während meines Studiums, sondern bei allen Entscheidungen hinter mir stehen, mir Kraft geben und für mich sogar ans andere Ende der Welt fliegen. Außerdem möchte ich meiner Oma danken, die mir beigebracht hat, das Beste aus allem zu machen.

Meinen Freunden, insbesondere meinem Freund, möchte ich für das Verständnis und den Rückhalt danken, den ich in den letzten Jahren stets bekommen habe. Mein Dank gilt auch all meinen Studienkollegen, die meine Studienzeit vom Anfang bis zum Ende mit schönen Erinnerungen gefüllt haben.

Kurzfassung

Die Reaktivextraktion ist ein wichtiger Trennprozess in der chemischen Industrie. Ziel dieser Arbeit ist es, experimentelle Daten zu sammeln, um Reaktivextraktionsprozesse modellieren zu können.

Die Kinetik der Aldolselbstkondensation von Aceton in einem Wasser/Toluol System wurde untersucht. Als Reaktionsprodukt bildet sich Diacetonalkohol unter Verwendung von Natriumhydroxid (NaOH) als Katalysator. Experimente zu Reaktionskinetik, Flüssig-Flüssig-Gleichgewicht und Grenzflächenspannung im extraktiven quaternären System (Wasser/Toluol/Aceton/Diacetonalkohol) und dem Stoffübergang bei 25°C und 40°C werden im Rahmen dieser Arbeit durchgeführt und diskutiert.

Die Modellierung der Kinetik ergibt eine Reaktion zweiter Ordnung für die Hinreaktion und eine Reaktion erster Ordnung für die Rückreaktion. Die Ergebnisse der Gleichgewichtsversuche zeigen, dass die Löslichkeit von Aceton in beiden Phasen fast gleich groß ist, während die Löslichkeit von Diacetonalkohol in der wässrigen Phase etwas höher ist. Dies zeigt sich auch in den Stoffübergangsversuchen in der Nitsch Zelle. Für die Grenzflächenspannung ergeben sich geringere Werte bei höherem Anteil der Übergangskomponente. Die Werte der Grenzflächenspannung ändert sich zwischen 25°C und 40°C nicht signifikant, da das bestimmende System Wasser/Toluol ist. In der Nitsch Zelle wurden Versuche zum diffusiven Stoffübergang an der Grenzfläche und zum Stoffübergang an der Grenzfläche mit überlagerter Reaktion durchgeführt. Die Versuche bei rein diffusivem Stoffübergang zeigen einen steigenden, parabelförmigen Verlauf der Übergangskomponente bis zum Erreichen des Gleichgewichtes. Die Versuche mit überlagerter Reaktion zeigen einen S-förmigen Verlauf in der organischen Phase, der vom Stofftransport der wässrigen Phase in die organische Phase bestimmt wird.

Abstract

Reactive extraction is an important separation process in the chemical industry. This thesis aims to acquire experimental data to model mass transfer in reactive extraction processes.

The kinetic of the self-condensation of acetone in a water/toluene system is determined. The reaction product is diacetone alcohol. At 25°C and 40°C reaction kinetic experiments, LLE experiments for the quaternary system (water/toluene/acetone/diacetone alcohol) and mass transfer experiments were conducted. Sodium hydroxide (NaOH) was chosen as catalyst.

The model for the reaction kinetics is based on a second order forward reaction and a first order reverse reaction. For the liquid-liquid-equilibrium the data show that acetone is distributed almost equally between the two phases and the solubility of diacetone alcohol is higher in the aqueous phase. This is also shown by the mass transfer experiments in a Nitsch cell. The interfacial tension of the liquid-liquid-equilibrium samples were measured. The interfacial tension decreases with an increasing amount of target component. The phase forming components are water and toluene, hence between 25°C and 40°C the values of the interfacial tension are almost the same. In a Nitsch cell diffusive interfacial mass transfer and interfacial mass transfer with the overlaid reaction of the self-condensation of acetone was examined. The comparison shows that the composition of the target component over time is different for both cases. The mass transfer experiments result in an increasing, parabolic development of the concentration until the equilibrium is reached. The experiments with overlaid reaction show an s-shaped development of diacetone alcohol in the organic phase. This results from the mass transfer from the aqueous phase to the organic phase.

Content

1 Introduction

Liquid-liquid-extraction is one of the most common and relevant separation processes in the chemical and pharmaceutical industry.

A special form of the liquid-liquid-extraction is the reactive extraction. In this case the transmitting component in the system is chemically modified in favor of the separation process. This allows for separation of mixtures that cannot be achieved by a standard extraction, for example azeotropic mixtures. [1]

To save time and effort whilst finding the most suitable process, nowadays computer simulations are very common in the industry. With rigorous simulations it is possible to predict the development of the bulk phase concentrations of an extractive process, as well as to weigh the alternatives. It can also bring a financial advantage, due to the fact that complicated and expensive laboratory experiments can be avoided. [2]

To establish a suitable thermodynamic model for a reactive liquid-liquid-extraction, different kinds of experimental data are necessary. The reaction has to be studied to determine the reaction rate law and the temperature dependency. Moreover, the liquid-liquid-equilibrium (LLE) of the reactive system as well as its associated interfacial tension has to be determined experimentally. Only with this data a thermodynamic model, which links simultaneous reaction and extraction, can be validated.

The chosen reaction for these experiments is the aldol self-condensation of acetone in the quaternary system water/toluene/acetone/diacetone alcohol. The aldol self-condensation is a catalytic reaction, where acetone dimerizes to diacetone alcohol (DAA) and can subsequently form mesityl oxide (MO) and water [3]. Diacetone alcohol is a common solvent in the chemical and pharmaceutical industry and environmentally friendlier compared to acetone due to its low volatility. It is used as a cleaning solvent for cellulose acetate, nitrocellulose and epoxy resin, as well as, in hydraulic fluids, as bactericide to staphylococcus and in styrene-butadiene latex paints. Mesityl oxide is used as a solvent for phenol-formaldehyde resins, in PVC compositions and as urea derivatives as feed for cattle, sheep and poultry. [3]

Previous works within this project have investigated the reaction kinetics for the aldol self-condensation and equilibria data for ternary systems. Within this thesis experimental data are collected to establish a kinetic model for the aldol self-condensation of acetone in a quaternary system [4].

Furthermore, experiments to determine the liquid-liquid equilibria in the quaternary system and experiments in a Nitsch cell to determine the mass transfer within the phases are conducted. Within the scope of this project the collected data will be used to develop a computer-based model to simplify applications in reactive extraction.

2 State of the art

This chapter gives an overview of reactive extraction, aldol self-condensation of acetone, reaction kinetics, liquid-liquid equilibria (LLE), interfacial tension and the Nitsch cell.

2.1 Reactive extraction

Reactive extraction is a form of extraction where the target component is chemically changed. This kind of extraction is usually a fluid-fluid extraction, in which the component is transferred from an aqueous phase to an organic phase.
Applications for reactive extraction are separation processes which involve thermally instable substances or unintended by-products at high temperatures. Furthermore, reactive extraction is employed for mixtures in which one of the components has a very high or a very low boiling point, contains a very small amount of a target component or for azeotropic mixtures. [1]

Other examples where reactive extraction is used are separation of carboxylic acids and metal salt extraction. The latter is used to separate metals from wastes or diluted leaching liquor. It is based on the different distribution of metal salts in water and organic phases. The separation of carboxylic acids in aqueous phases is complicated due to its low activity coefficient. The activity coefficient describes the deviation of an ideal and a real mixture. [5]–[7]

The self-condensation of acetone takes place in the aqueous phase. Solvent and feed are not or only slightly miscible. Therefore, a miscibility gap emerges. To increase the mass transfer, it is important to increase the mass transfer area. This can be obtained by dispersion of one phase into small droplets. The distribution coefficient is crucial to determine the separation factor. The distribution coefficient indicates the distribution of the target component between the phases. [1]

The ingoing stream loaded with solutes is called feed whilst the outgoing stream which is enriched with solutes after the process is called extract. The raffinate is an outgoing stream, which is almost free from solutes.

In Figure 2-1 the scheme of a reactive extraction is shown. After the extraction an ion exchanger is often used to recreate a certain salt form. The re-extraction uses ions, concentrated acids or salts as stripping-agents. To improve the product quality a reflux is fed back to the scrubber. The raffinate stream is loaded with residues of solvent. The scrubber conditions are different to the extraction and re-extraction conditions. Therefore, certain process parameters like temperature, concentrations or pH-value have to be adjusted accordingly. [1], [5]

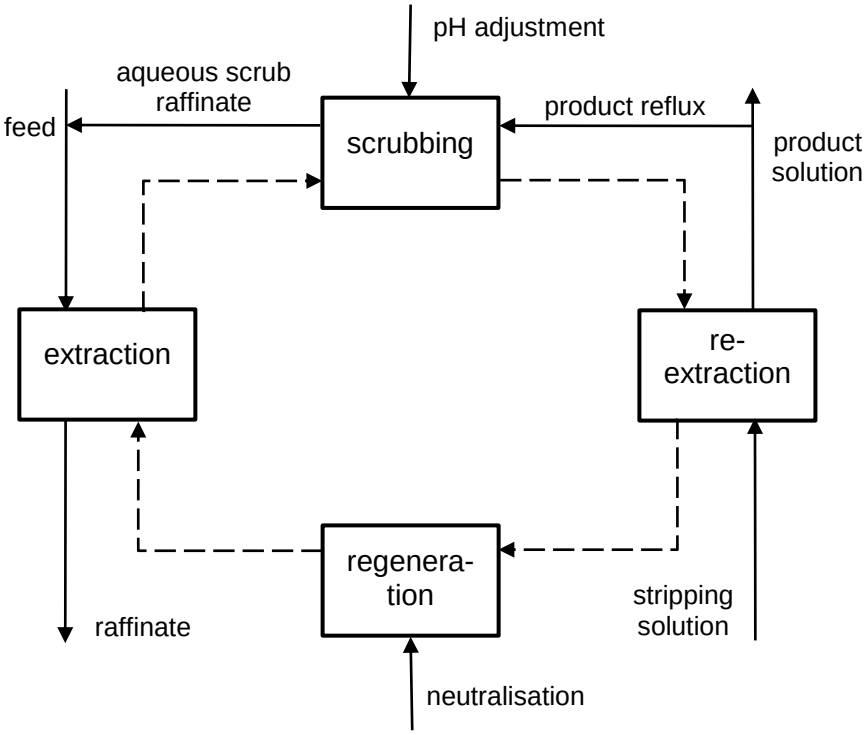

Figure 2-1: Scheme of a reactive extraction with scrubbing section and pH adjustment according to [5].

Reactive extraction is a viable alternative to common distillation, because it is viable at ambient temperature and environment-friendly due to its low energy consumption. It is often conducted prior to a rectification. [1]

2.2 Self-condensation of acetone

The self-condensation of acetone is a catalyzed aldol condensation reaction, where two acetone molecules form one diacetone alcohol molecule. Furthermore, mesityl oxide can be formed from diacetone alcohol in a subsequent elimination reaction. [8]

During the first step of the reaction, two acetone molecules dimerize to 4-methyl-4-hydroxy-2-pentanone (diacetone alcohol). In the second step of the reaction, 4-methyl-3-penten-2-one (mesityl oxide) is formed by an elimination process, where water is eliminated from the diacetone alcohol molecule. This elimination is an *E1cB* mechanism. *E1* denotes an elimination process where the rate-determining step involves only one molecule. *cB* stands for conjugate base, since the elimination starts with a deprotonation and the leaving group (OH^-) is lost from the conjugate base. The choice of the catalyst and process parameters influences the formation of mesityl oxide in this reaction. [4], [9], [10]

In Figure 2-2 the reaction mechanism is shown. In the first step diacetone alcohol is formed out of two acetone molecules. During the subsequent step water is eliminated and mesityl oxide is formed. [9]

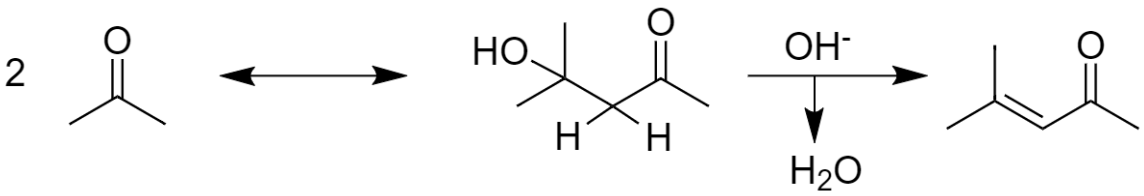

Figure 2-2: Reaction of the aldol self-condensation of acetone with diacetone alcohol as aldol with two α-H-atoms for deprotonation and elimination of water to mesityloxide.

The aldol which is formed during the first step has two α-H-atoms, which can be withdrawn as protons from the base. The pK_a value is ~19. Therefore, this elimination can only take place with a strong base. For weak bases it only happens slowly or not at all. The selectivity depends on the chosen catalyst. The stronger the base, the faster is the reaction. [3], [4]

For the formation of diacetone alcohol as the main product, the reaction has to be stopped after the first step. One way is to remove the catalyst to avoid the condensation of water. Adding water shifts the equilibrium to the side of diacetone alcohol. Therefore, mainly diacetone alcohol is formed with a minimal amount of by-products. [3]

Other by-products that could be formed during the aldol self-condensation are phorones, mesitylene, isophorones, and 3,5-xylenol. The formation can be influenced

by the choice of the catalyst and experimental parameters, like temperature and pressure. [3]

The reaction of the aldol-condensation can also take place as an acid-catalyzed reaction. The same product forms as with the base-catalyzed reaction. [8]

2.3 Reaction kinetics

The field of reaction kinetics is crucial for designing a process. It gives information about the reaction rate and the equilibrium as well as the conversion of a reaction. Influence factors on the reaction are for example temperature, pressure, solvents and catalysts. [11]

The reaction rate *r* is defined as the change of the concentration over time. Equation 2-1 depicts a simple irreversible reaction with two educts A and B and two products C and D. The reaction rates of the different components are calculated by equations 2-2 to 2-5.

$$aA + bB \rightarrow cC + dD \tag{2-1}$$

The reaction rate of each component results in:

$$-r_A = -\left(\frac{dc_A}{dt}\right) \tag{2-2}$$

$$-r_B = -\left(\frac{dc_B}{dt}\right) \tag{2-3}$$

and

$$r_C = \left(\frac{dc_C}{dt}\right) \tag{2-4}$$

$$r_D = \left(\frac{dc_D}{dt}\right) \tag{2-5}$$

For determining a rate law, the reaction rate constant *k* and the reaction order *n* are needed. They can be empirically or arithmetically ascertained. [11]

For a reversible reaction $aA + bB \leftrightarrow cC + dD$ (2-6)

the rate law can then be determined as

$$-r_A = -\left(\frac{dc_A}{dt}\right) = k_1 * c_A^{\alpha} * c_B^{\beta} - k_2 * c_C^{\gamma} * c_D^{\delta} \quad (2\text{-}7)$$

The reaction order results in the sum of the exponents of the concentrations.

$$n = \alpha + \beta + \gamma + \cdots \quad (2\text{-}8)$$

The equilibrium constant can be obtained from the reaction rate constants k_1 and k_2.

$$K = \frac{k_1}{k_2} \quad (2\text{-}9)$$

In case of a heterogeneous reaction the catalyst is in a different state than the reaction mixture. The most common case is a solid catalyst in a liquid or gaseous phase.
The catalyst lowers the activation energy E_A of the reaction through weakening the bonding or changing the mechanism of the reaction. [11], [12]

The examined reactions for the purpose of this thesis are all catalyzed. To ensure reproducibility also for mass transfer experiments in the Nitsch cell, the catalyst has to be dissolved in the aqueous phase. This results in a homogeneously catalyzed reaction. To model the reaction kinetics, experiments with different temperatures and concentrations have to be examined.

2.3.1 Homogeneously catalyzed reactions

In a homogeneously catalyzed reaction the catalyst is in the same state as the reactant. The equations 2-10 and 2-11 show reactions from *A* to *R* with and without catalyst.

$$A \xrightarrow{k_1} R \quad (2\text{-}10)$$

$$A + C \xrightarrow{k_1'} R + C \quad (2\text{-}11)$$

C is the catalyst, which is not used up during the process. The reactions have different reaction rate constants, since the catalyst accelerates the reaction. Reaction 2-10 has a reaction rate constant k_1 and reaction 2-11 has a reaction rate constant k_1'. The reaction rate arises from the sum of k_1 and k'_1.

The reaction rates for the reactions from above result in:

$$-\left(\frac{dc_A}{dt}\right)_1 = k_1 * c_A \tag{2-12}$$

$$-\left(\frac{dc_A}{dt}\right)_2 = k'_1 * c_A * c_C \tag{2-13}$$

This means that the reactions would also take place without the catalyst. The reaction rate behaves in relation to the concentration of the catalyst. These equations are valid for irreversible reactions.

Adding formula 2-12 and 2-13 results in:

$$-\left(\frac{dc_A}{dt}\right) = k_1 * c_A + k'_1 * c_A * c_C = (k_1 + k'_1 * c_C) * c_A \tag{2-14}$$

Which, after integration, results in:

$$-ln\left(\frac{c_A}{c_{A0}}\right) = -ln(1 - X_A) = (k_1 + k'_1 * c_C) * t = k_{new} * t \tag{2-15}$$

With this formula 2-15 k_1 and k'_1 can be determined from various experiments with different amounts of catalysts. [11]

In case of the aldol self-condensation the reverse reaction has to be taken into account as well and the kinetic modeling is adapted accordingly as described in 4.1.3. [13]

2.3.2 Influence of temperature

The Arrhenius equation shows the correlation between reaction rate and temperature.

$$k = A * e^{\frac{-E_A}{RT}} \tag{2-16}$$

E_A is called the activation energy, R the gas constant, T the temperature and k the reaction rate constant. The activation energy indicates how much energy is needed to start a reaction, the unit is [J/mol]. A is called the frequency or pre-exponential factor. The unit is always the same as the reaction rate constant k, generally $[mol^{(n-1)}/(l^{(n-1)} * s)]$. Usually an increase of temperature also increases the reaction rate. The Arrhenius equation shows that this increase is not linear. The determination of the activation energy and the frequency factor is achieved experimentally by varying temperature and determining the reaction rate constants. [11], [12]

2.4 Liquid-liquid equilibria

For thermal separation processes heat and mass transfer proceed until the phase equilibrium is reached. The system has reached the equilibrium when there are no more mass or heat shifts between phases respectively the transfer through the phase boundary is reversible. For a closed system without any mass or energy transfer, the conditions for the equilibrium are constant pressure, temperature and chemical potential over time and location. [1]

$$dp = 0 \; or \; p_I = p_{II} = \cdots \tag{2-17}$$

$$dT = \; 0 \; or \; T_I = T_{II} = \cdots \tag{2-18}$$

$$d\mu = \; 0 \; or \; \mu_I = \mu_{II} = \cdots \tag{2-19}$$

To determine the degrees of freedom *F* of a system, the Gibbs phase-rule is used.

$$F = K - P + 2 \tag{2-20}$$

In equation 2-20 *K* stands for the number of components and *P* is for the number of phases. For a pure substance the system is fully defined at the triple point, since there are three phases and one component. A two-phase system with four components, as in the quaternary system of the aldol self-condensation, would yield four degrees of freedom. In this case more information is necessary to describe the system. This means thermodynamic parameters such as temperature, pressure, concentration or volume have to be set. [14]

2.4.1 Nernst law

Irrespective of the amount of phases the concentration between two liquid phases distributes in the same ratio, which is constant as long as temperature and pressure do not change. [1]

The activity of the component *i* according to Lewis is known as

$$a_i = \frac{f_i}{f_{0i}} = x_i * \frac{\varphi_i}{\varphi_{0i}} \tag{2-21}$$

and the activity coefficient is the ratio of fugacity coefficients

$$\gamma_i = \frac{\varphi_i}{\varphi_{0i}} = \frac{f_i}{x_i * f_{0i}} \tag{2-22}$$

Where a_i is the activity of i, γ_i is the activity coefficient for the component i, f_i is the fugacity for the component i and f_{0i} the fugacity for the pure component i, φ_i and φ_{0i} the fugacity coefficients for i in the mixture and for a pure component and x_i is the substance amount fraction. The fugacity is a measure of the deviation of the behavior of a real fluid from an ideal gas behavior. [15]

The activity is defined as

$$a_i = \gamma_i * x_i \tag{2-23}$$

The distribution of a solute substance i in two immiscible liquid solvents can be described as

$$\bar{\mu}_{0i,I} + RT \ln a_{i,I} = \bar{\mu}_{0i,II} + RT \ln a_{i,II} \tag{2-24}$$

Whereby R is the gas constant, T is the temperature, $\mu_{0,S}$ is the standard chemical potential and a_i is the activity of i.

For phase equilibrium the following relation is valid.

$$\mu_{i,I} = \mu_{i,II} \tag{2-25}$$

and therefore:

$$a_{i,I} = a_{i,II} \tag{2-26}$$

Nernst law can be applied for small concentrations $c_{i,I}$ and $c_{i,II}$ between the two phases.

$$\frac{c_{i,II}}{c_{i,I}} = \frac{c_{i,extract}}{c_{i,raffinate}} = K(\vartheta) \tag{2-27}$$

K is the phase equilibrium constant.

This law describes the equilibrium between raffinate and extract phase, if both solvents are immiscible. It is, however, only valid for small concentrations, for example for up to 100 µg/ml for metal ions. [1], [16]

2.4.2 Binary systems

The description of liquid-liquid systems requires concentrations of both liquid phases and mutual solubility in the equilibrium state.
For liquid-liquid extraction it is crucial that the solvents are not miscible. This property results in a miscibility gap in the phase diagram. There are different kinds of miscibility gaps according to the different behaviors. The extraction also depends on the width and the temperature range of this gap. [1], [14]

In Figure 2-3 plots of the solubility of different systems are shown. On the ordinate the temperature is plotted, whilst on the abscissa the mass fraction z is plotted. The first plot shows the system benzene/formic acid, which has an open miscibility gap and an upper critical solubility temperature. The plot in the middle shows water/di-n-propylamine, which has a lower critical temperature. The third system is water/nicotine, which shows a closed miscibility gap and an upper and lower critical temperature. [14]

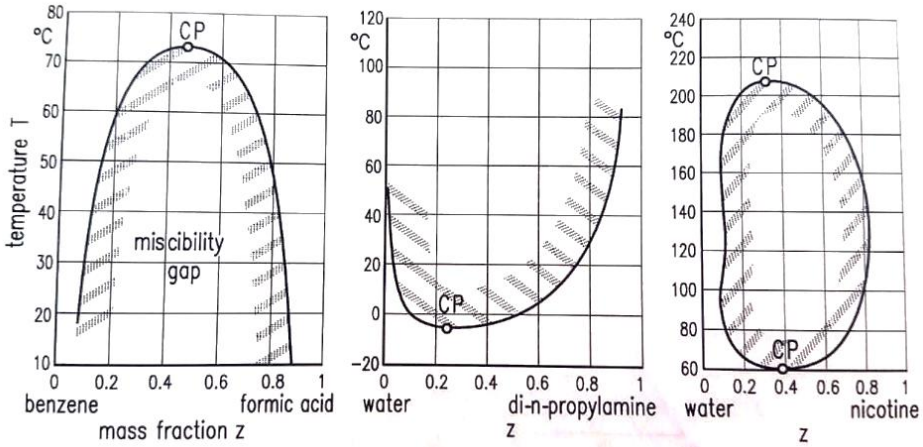

Figure 2-3: Binary miscibility gaps for different systems with upper, lower and both critical solubility temperatures according to [14].

2.4.3 Ternary systems

To depict the thermodynamics of an extraction process, a triangular concentration diagram is usually used. It has the advantage that all components are shown, as the raffinate and the extract are ternary mixtures. [14]

In this kind of diagram, the corners of the diagrams represent pure components and the sides of the triangle represent binary mixtures. The inner part of the triangle represents the ternary mixture. [12]

The binodal curve marks the border of the homogeneous area and the heterogeneous area. The area of the phase diagram which is enclosed by the binodal curve is the concentration range where the mixture falls apart into two conjugated liquid phases. These points are parts of the binodal curve. Outside that curve the mixture is homogeneous. [1]

In Figure 2-4 different kinds of miscibility gaps are shown. The homogeneous areas are marked with I, the two-phase areas are marked with II and the area with three phases is marked with III. Type A shows the most common miscibility gap between the components A and B. Type B and C show a closed system with miscibility gaps between the components A and B and A and C. Type C shows a system where the mixture separates into three phases in area III. Type D shows an open system with a miscibility gap between component B and C. [1]

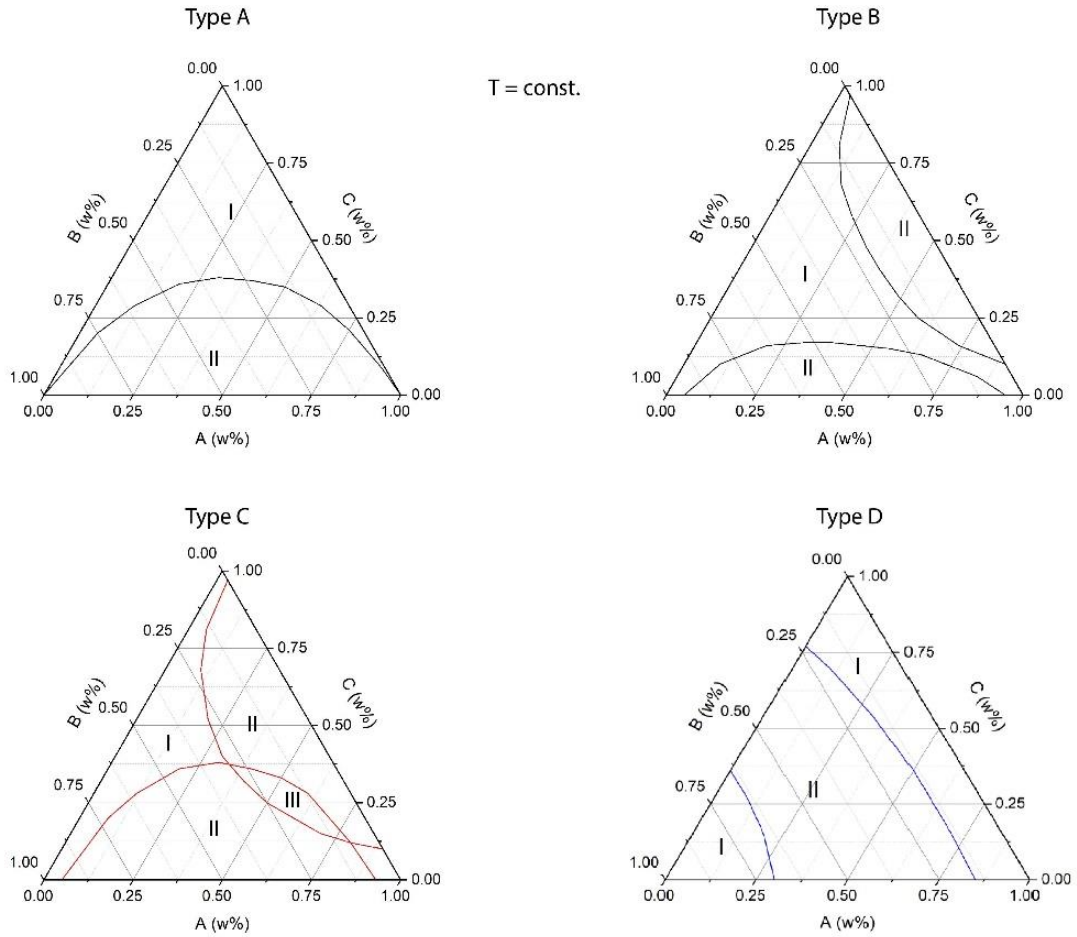

Figure 2-4: Four types of phase equilibria for ternary systems with partially immiscible components.

2.4.4 Quaternary systems

For a quaternary system the triangular diagram is extended to a tetrahedron diagram. As for the triangular diagram the corners are pure components and the sides are binary mixtures. The triangular areas are ternary systems. The inner part consists of the quaternary system. In this case the binodal curve extends to an area which spans the miscibility gap where the mixture separates into two or more phases. The shape of the miscibility gap depends on the ternary systems. In Figure 2-5 an example of a tetrahedron diagram for a quaternary system is shown. [17]

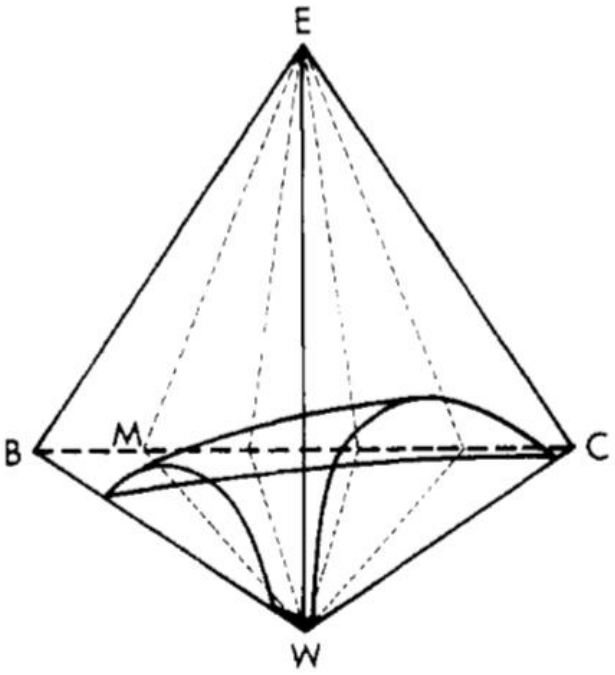

Figure 2-5: Schematic depiction of a quaternary system water(W)/ethanol(E)/1-butanol(B)/chloroform(C) according to [17].

2.5 Interfacial tension

In a liquid phase, molecules are surrounded by the same kind of molecules so that their gravitational attraction is canceled out. At a phase boundary the molecules are not surrounded by each other. The interface has less or different molecules on the other side depending on the medium of the second phase. There is a resulting force acting on the molecules of the phase boundary pulling to the inside of the liquid. This is the reason for phase boundaries as well as for formation of droplets. This phenomenon is called interfacial tension. The dimension of interfacial tension is [N/m]. To enlarge the interfacial area, the molecules have to be moved from the interior of the phase to the boundary. [15]

Molecular interactions hinder the motion of fluids. This explains the tenacity of a fluid, also called viscosity. To represent the viscosity, the viscosity coefficient η is used. The unit of this coefficient is [Pa*s]. η describes the resistance of the fluid to the movement

and is generally known as the dynamic viscosity. In order to obtain the kinematic viscosity υ, knowledge of the medium's density is required as shown in equation 2-28. The respective unit is [m^2/s]. [12]

$$\upsilon = \frac{\eta}{\rho} \tag{2-28}$$

In liquid media the viscosity decreases with rising temperature, due to the more intense movement of the molecules at higher temperatures. [18]

To increase the mass transfer in a system, the interfacial area of two immiscible phases has to be increased. The formation of small droplets will lead to an increase in the transfer area. That can be achieved by continuous stirring, packed columns or cross-flow reactors. [1]

2.6 Mass transfer

Reactive extraction as well as other thermal separation technologies are mass transfer operations. To determine the mass transfer in a system it is therefore essential to analyze and design a separation process. [1]

There are various methods to determine the mass transfer. One of which is per diffusion coefficient *D* in Fick's law.

$$j_i = -D_{ij} * \frac{dc_i}{ds} \tag{2-29}$$

The first Fick law (2-29) describes the component flux along the concentration gradient dc_i/ds. Whereby j_i is the flux of component *i* and D_{ij} is the binary diffusion coefficient of the component *i* and the medium *j*. The diffusion coefficient is dependent on temperature, pressure, concentration and components that diffuse in the system. [1]

Another way is via the mass transfer coefficient, which describes diffusion in multiphase systems. The flux equation for the mass transfer is

$$N_1 = k * \Delta c_1 = k * (c_{1i} - c_1) \tag{2-30}$$

Whereby N_1 is the flux at the interface, c_{1i} and c_1 are the concentrations at the interface and in the bulk phase and k is the mass transfer coefficient. The mass transfer coefficient k describes the rate for the transfer of a target component from the phase boundary into the bulk phase. A high value for k means that the transfer is fast.

This approach applies under the estimation that the concentration is constant for most of the phase's volume and the change in concentration is limited to the phase boundary. [19]

There are different theories to describe the mass transfer at fluid-fluid interfaces, which are commonly used in the industry. The two-film theory, which is based on diffusion across a thin film, and the penetration theory, which describes diffusion into a semi-infinite fluid, are the most common ones. The density gradient theory (DGT) is used within the scope of this project. This theory determines the gradient of the chemical potential within the interface as driving force for the mass transfer through the phase boundary. [18]–[20]

The two-film theory is the simplest way to describe mass transfer across liquid interfaces. But since the coefficients have to be determined empirically, the two-film theory mostly serves as a basis for other theories. [19]

2.6.1 Experimental determination of mass transfer

The most common way to determine interfacial mass transfer in liquid-liquid systems is with small batch vessels with two phases in a thermostatic condition. Subsequently samples from both phases are taken and analyzed.

Another way to determine mass transfer is nuclear magnetic resonance (NMR) spectroscopy. A small sample volume is put into a sample tube and shaken. After the equilibrium is reached, both phases are analyzed consecutively. The advantages of this method are that the sample volumes are smaller and the analysis method is not invasive, hence the samples can be reused. It is also faster than the common method and no calibration is needed, hence the work effort is much lower. [21]

Microfluids and Raman microspectroscopy are also used to determine mass transfer. This method is also fast and has the advantage of good fluid flow properties. Microfluids are mostly laminar, whereas macro fluids are more likely to develop a turbulent flow regime. For this method two fluids are fed into a micro H-cell. The dimensions of this cell are 1 m in length, 400 µm in width and 40 µm in height, with two inlets for the different fluids. One fluid is a mixture of at least two liquids of the investigated system and the second fluid is the target component. Due to the small volumes the retention time is small. The analysis of the samples is conducted via Raman microspectroscopy which is based on the scattering of light. This allows in situ analysis of the concentrations. The advantages of this method are, due to the fact that phase separation can be avoided, faster results with lower effort. [22]

2.7 Nitsch cell

To determine the diffusive mass transfer through the phase boundary and the influence of the chemical reaction on the mass transfer, experiments are performed in a Nitsch cell. This device ensures a stable phase boundary and therefore allows to minimize the calculative effort due to the known surface area. [23]

In Figure 2-6 the sketch of a Nitsch cell is shown. The equipment inside the cell is designed to keep the phase boundary stable and also to ensure homogeneous phases in both sections. To stabilize the phase boundary, stirring speeds are set so that the Reynold numbers in both phases are the same. [20], [24]

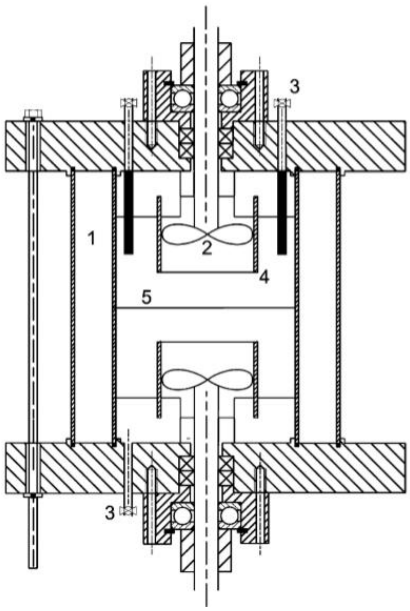

Figure 2-6: Sketch of a Nitsch cell with heating jacket (1), stirrer (2), sampling openings (3), flow breakers (4) and liquid–liquid interface (5) according to [24].

The Reynolds-number is defined as

$$Re = \frac{v*L*\rho}{\eta} = \frac{inertia\ force}{viscous\ forces} \tag{2-31}$$

where *v* is the velocity, *L* is a characteristic length, *η/ρ* is the kinematic viscosity. [12], [14]

The velocity is calculated from the diameter *d* and the rotational speed *n* of the stirrer.

$$v = \pi * d * n \tag{2-32}$$

3 Experimental methods

In this chapter preparing measures, setups and procedures for the conducted experiments regarding reaction kinetics, liquid-liquid equilibria and mass transfer are described.

3.1 Materials

The used materials for all experiments are given in Table 3-1. For the aqueous phases ultrapure water purified by Barnsted E-pure is used.

Table 3-1: Materials used with the purities.

Substance	Fabricator	Purity
Acetone	Honeywell	≥99,8%
Toluene	Honeywell	≥99,9%
Sodium hydroxide	Carl Roth	≥99%
Barium hydroxide	pro analysi MERCK	98%
Sulfuric acid	Chem-Lab	98%
o-Phosphoric acid	Carl Roth	≥85%
Hydrochloric acid	Chem-Lab	37%
Potassium hydroxide	Pro analysi MERCK	≥85%
Diacetone alcohol	Acros Organics	99%
Mesityl oxide	Alfa Aesar	≥90%
Tetrahydrofuran	Carl Roth	≥99,9%
Amberlyst 15	Sigma Aldrich	hydrogen form

3.2 Analytical methods

To analyze the samples, different methods for different purposes are used. Gas chromatography (GC) is used mainly for analyzation. Since water cannot be detected with

a GC, Karl Fischer titration is used to determine the amount of water in organic samples. For measuring the interfacial tension of the LLE samples, a spinning drop tensiometer is used.

3.2.1 Gas chromatography

All samples are analyzed by gas chromatography. The gas chromatograph Shimadzu Nexis GC-2030 is used. The specifications of the gas chromatograph are shown in Table 3-2.

Table 3-2: Operation parameters for GC analysis.

Column		
ZB-WAX plus	Length	30 m
	Diameter	0.25 mm
	Film thickness	0,5 µm
Method parameters		
Split Ratio	1:10	
Injection temperature	250 °C	
Injection pressure	40 kP	
Injection volume	1 µl	
Duration	22 min	
Detector	FID	280 °C

This device uses an FID (flame ionization detector) to analyze the samples. The samples are burnt with hydrogen and air. This method is applied for detecting organic substances. Water is not detectable by the FID [25]. The reactive samples are stored in the sample tray at 5°C.

3.2.2 Karl Fischer titration

Karl Fischer titration is used to determine the amount of water in the organic samples. Only small amounts of water can be determined with the SI analytics Titroline 7500 KF, which is used. All samples are measured at least twice.

The titration is based on a chemical redox reaction, where the conductivity is constantly measured, while I_2 is added. When an I_2 excess is reached, the tension decreases suddenly, which marks the end of the reaction.

$$2\,H_2O + SO_2 + I_2 \rightarrow SO_4^{2-} + 2I^- + 4H^+ \tag{3-1}$$

Sulfur dioxide and iodine only react when water is present. For every mole of water a mole of I_2 is consumed. [25]

3.2.3 Spinning drop tensiometry

To determine the interfacial tension of two liquids, a spinning drop tensiometer can be used. This device measures the drop size and the shape of a droplet in the heavy phase. During these experiments the aqueous phase is the heavy phase. The droplet is located in a rotating capillary to apply centrifugal forces and eliminate the gravitational force.

The spinning drop video tensiometer Dataphysics SVT 20 is used for this analysis.

Prior to the spinning drop tensiometry, the density and refractive index of the samples have to be measured. For the density measurement at a certain temperature (25°C or 40°C corresponding to the LLE temperature), the SVM 3000 from Anton Paar is used.

To measure the interfacial tension between the aqueous and the organic phase, a small droplet of the organic phase is put into a glass capillary filled with the heavy phase, the aqueous sample. The temperature can be set and controlled via a cryostat. The actual temperature is given in the software of the spinning drop tensiometer. When the cartridge is spinning, the camera is adjusted, so that the droplet is in the middle of the picture. In Figure 3-1 an example is shown.

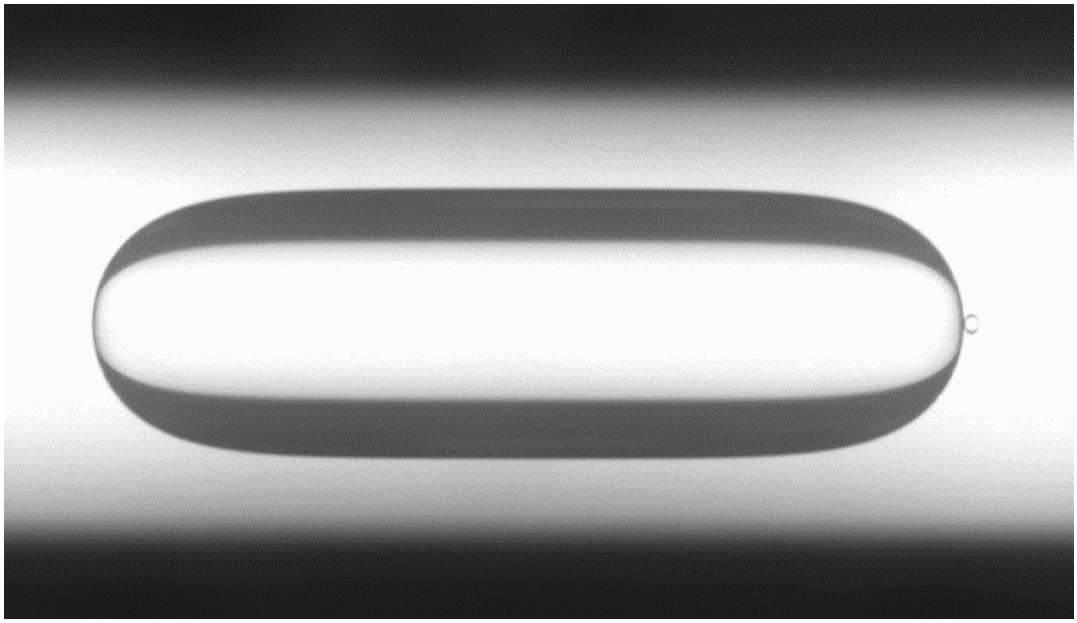

Figure 3-1: Droplet from the spinning drop tensiometry, LLE at 40°C, sample 10.

The software recognizes the shape and the ratio of the droplet. Pixel errors are also recognized. Methods according to Young-Laplace, Vonnegut or Cayias-Schechter-Wade can be chosen to evaluate the interfacial tension. For this work the Young-Laplace method is used.

This method is based on the Vonnegut correlation and is a viable method for low interfacial tensions. For a non-spherical shape, the Young-Laplace equation [26] is

$$\Delta P = \sigma * (\frac{1}{R_1} + \frac{1}{R_2}) \quad (3\text{-}2)$$

ΔP is the pressure difference between the phases, *σ* is the interfacial tension and R_1 and R_2 are the radii 1 and 2. The ratio is shown in Figure 3-2.

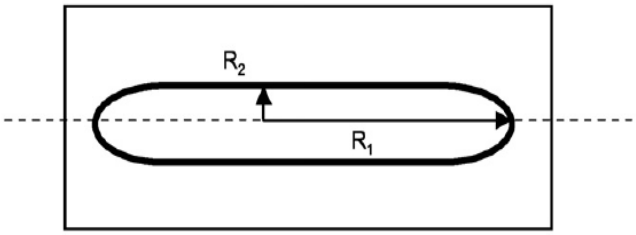

Figure 3-2: Cylindrical droplet shape in the spinning drop method according to [26].

This term is extended to (3-3), when hydrostatic pressure caused by a gravitational field and the force of a centrifugal field applies.

$$\sigma * \left(\frac{1}{R_1} + \frac{1}{R_2}\right) = \frac{2\sigma}{R_0} + \Delta\rho * g * y + \Delta\rho * g^* * \lambda \quad (3\text{-}3)$$

Where *g* is the gravity constant, *y* is the liquid column height relative to the sphere, *g** is the acceleration due to the rotational field (ω^2*λ) and *λ* is the potential distance.

Since the rotational field acceleration is determining in the spinning drop method, the gravitational term can be neglected. [26]

$$g^* \gg g \quad (3\text{-}4)$$

$$\sigma * \left(\frac{1}{R_1} + \frac{1}{R_2}\right) = \frac{2\sigma}{R_0} + \Delta\rho * \omega^2 * \lambda^2 \quad (3\text{-}5)$$

After usage the capillary is rinsed with solvent and dried in a vacuum oven at 75°C for 20 minutes.

3.3 Calibration

Prior to the experiments a calibration for all components, acetone, toluene, diacetone alcohol and mesityl oxide is carried out for the gas chromatograph. Nine different standards are prepared in a range from 50 ppm to 10,000 ppm and each standard is injected three times.

Previous experiments showed that DMSO (dimethyl sulfoxide) is not a suitable solvent, because the peaks of the gas chromatography are overlapping, result in a shoulder peak and cannot be analyzed correctly. Therefore, the chosen solvent is THF (tetrahydrofuran). Another experiment series is prepared with water as a solvent to evaluate the samples from the aqueous phase.

The conversion of the calibration lines is provided in mass-related ppm, mol/mol and mol/l for each component. In Figure 3-3 the calibration line for diacetone alcohol in mol/l is shown exemplarily. The coefficient of determination equals 0.9996, which indicates a good calibration line. The other data can be found in the Appendix B.

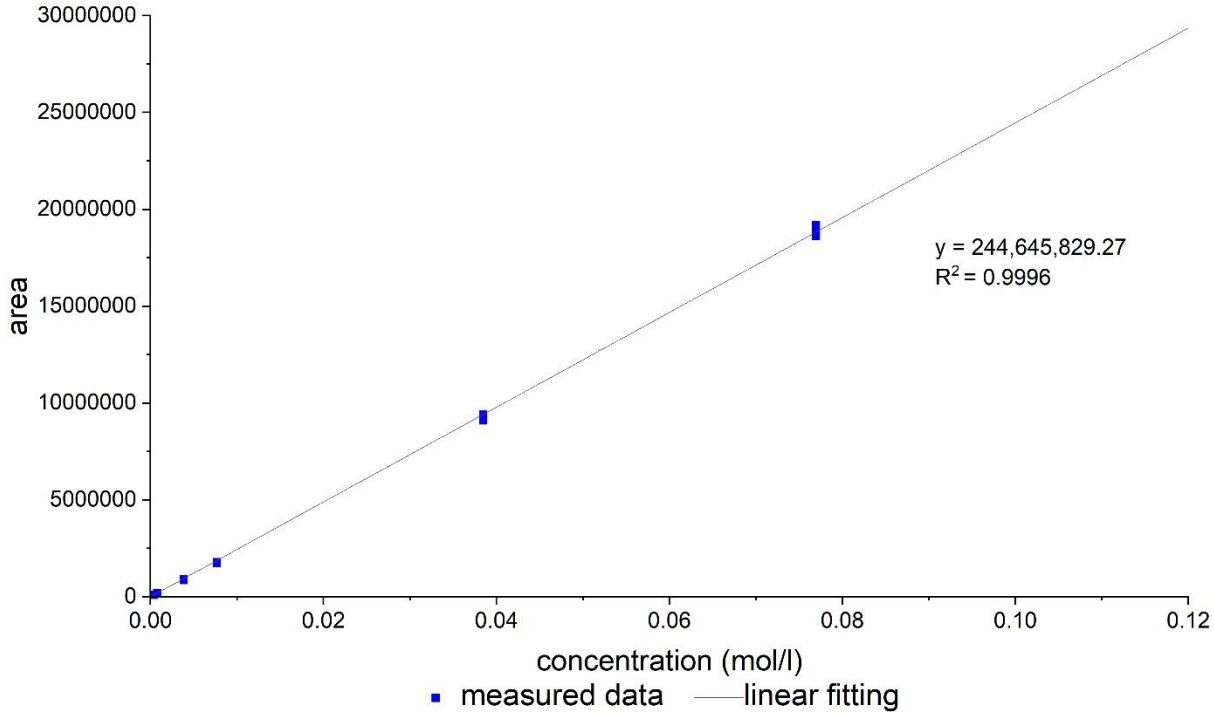

Figure 3-3: Calibration line for diacetone alcohol in THF in mol/l.

3.4 Error discussion

For every measured value there is a measurement inaccuracy. Experimental errors can be divided into systematic and random errors. Systematic errors originate from faulty devices or incorrect implementation of an experiment and therefore, can be avoided. Random errors cannot be corrected. They can occur from reading a scale or from measurement noise of analytical equipment. All used devices show random errors. [25]

The sources of errors are discussed in this section. The accuracy and deviation of all used scales are shown in Table 3-3.

Table 3-3: Accuracies of used scales.

Purpose	Device	Accuracy
Calibration standard	Sartorius BP 121 S	0.1 mg
Dilution	Sartorius 1801	0.1 mg
Components	Sartorius Universal U6100 S	0.01 g

The gas chromatograph has a certain measurement accuracy. To keep this error small, the calibration is repeated in frequent time gaps and after changes to the device have been made.

To minimize the analytical error, all stable samples are injected twice and the mean value is taken for further work. The error bars result from the standard deviation.

The calibration curve is fitted according to the results from the calibration standards without intercept. Therefore, small deviations can occur. To keep them as small as possible, the coefficient of determination R^2 should be close to 1.

NaOH is very hydroscopic. This can lead to agglomeration while weighing and mixing the component.

During the first experiments, discrepancies in the results are noticed. After a series of experiments, it is found that the error has been caused by deposition of basic catalyst on the column in the GC. Therefore, causing the samples to react further before being analyzed. This causes a significant increase of acetone and a decrease of diacetone alcohol in the results.

To avoid this problem, the reactive aqueous samples are neutralized before being analyzed in the GC. Amberlyst 15, an ion exchange catalyst, is used to neutralize the samples. The procedure is described in 3.5.2. The procedure cannot be automated in the laboratory, hence possible problems can occur. Due to the short time gaps, the amount of catalyst and the contact time are not exactly the same for all experiments. A point of reference is used for both parameters, time and mass. The pH value can only be measured by pH-indicator strips, which are not very accurate. The indicator is

always checked by the same person in order to reduce the inaccuracy. The influence of this procedure on the reaction progress is tested and documented.

Since the pH value is approximately 7 when filling the sample into the vial, the reaction does not proceed. This cannot be guaranteed, but the reaction is slowed down to a minimum. To ensure a deceleration of the reaction, the vials are additionally quenched with ice and cooled at 5 °C in the sample tray until analyzation. To determine the influence of this procedure, experiments are conducted and repeated with double injections.

For the kinetic experiments, a constant temperature is important. The temperature sensor measures within a deviation of 0.1°C. Any variations of the temperature have been documented.

Simplifications that are made for the calculation and modeling of the kinetics lead to errors. Choosing wrong starting values for models can also lead to errors. Therefore, starting values from the work of Maple and Allerhand [13] are chosen to begin with.

3.5 Kinetic study

This chapter describes the determination of the reaction kinetics.

3.5.1 Setup

To determine the reaction rates, constant temperature and pressure are crucial.

For these experiments a three-neck flask is placed on a heating plate. On top of the flask a reflux condenser is mounted to help control the temperature and condensate rising vapor. The reflux condenser is connected to a cryostat, which is set to 5°C. As coolant isopropyl alcohol is used.
The other two necks are used to measure the temperature and to take samples. A temperature sensor is measuring the temperature of the mixture constantly and controlling its set point.

The mixture is stirred with a magnetic stirrer at 1000 rpm at all times to ensure sufficient mixing between the two phases.

The setup is shown in Figure 3-4.

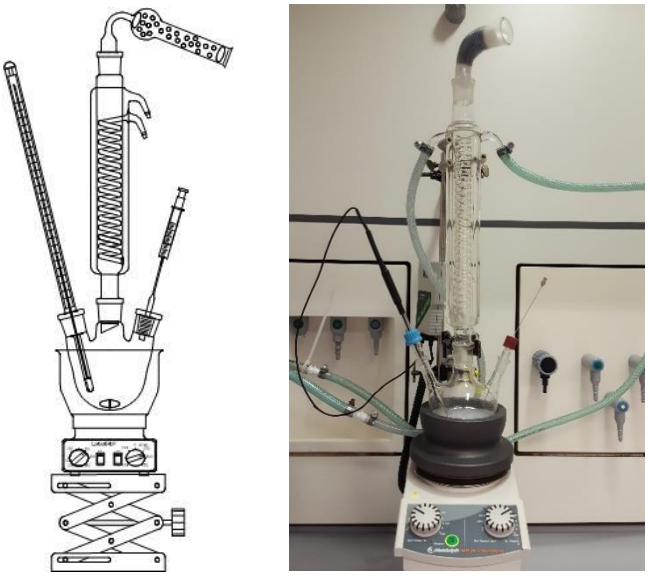

Figure 3-4: Kinetic experiment setup for the temperatures 25°C and 40°C.

3.5.2 Procedure

Firstly, the kinetic experiments are implemented. For this procedure different catalysts are tested to compare the different results with regard to the conversion and the selectivity. The basic catalysts are sodium hydroxide (NaOH), barium hydroxide ($Ba(OH)_2$) and potassium hydroxide (KOH). The acidic catalysts are sulfuric acid (H_2SO_4), o-phosphoric acid (H_3PO_4) and hydrochloric acid (HCl). All catalysts are tested at 40°C to compare the results and see whether diacetone alcohol is the sole product or if mesityl oxide is formed.

To ensure the reproducibility every experiment is examined twice.

As a reference the work of Kuśtrowski et al. [4] is used to examine the procedure and validate the methodology. During previous works within this project this experiment was already implemented for a catalyst screening with NaOH, $Ca(OH)_2$ and $Ba(OH)_2$, where NaOH is found to show the most preferable development of concentration. Since $Ca(OH)_2$ showed the slowest reaction rate it is excluded from further testing.

For the procedure the catalyst is dissolved in the aqueous phase. A mixture of toluene and water in a volume ratio of 1:1 is heated to the set temperature and stirred constantly at 1000 rpm. When the set temperature is reached, acetone is added to the mixture. This is the start of the reaction (t=0 s). From this point on, samples are taken in constant time gaps according to the duration of the GC analysis. The samples are put into precooled sample bottles to slow down the reaction immediately. After phase separation (< 1 min) the samples are transferred into the GC vials. The aqueous phase has to be neutralized first, to protect the column in the GC from basic residues. This is achieved by the use of an ion exchange catalyst. 1 g Amberlyst 15 is brought into contact with 3 ml of the aqueous phase until a pH of 8-7 is reached (< 2 min). During that time 1 ml of the organic phase is put into the GC vial. Afterwards 1 ml of the neutralized aqueous phase is put into another GC vial. The rest of the untreated mixture is put back in the flask, so that the volume change over time can be neglected. The GC vials are still cooled to make sure the reaction is not proceeding.

The experiments run for at least 3 hours to ensure that the equilibrium is reached. This has also been tested in preliminary experiments. In Table 3-4 the parameters of the catalyst screening experiments are shown.

After usage Amberlyst 15 is washed out and dried at 60°C to recover.

Table 3-4: Parameters for the catalyst screening for the kinetic experiments.

Substance	m	T	p	t
	[g]	[°C]	[atm]	[h]
NaOH	0.41	40	1	3
NaOH	2.05	40	1	3
NaOH	0.205	40	1	3
$Ba(OH)_2$	0.41	40	1	3
KOH	0.68	40	1	3
H_2SO_4	5.13	40	1	3
H_3PO_4	1.18	40	1	3
HCl	1.01	40	1	3

Afterwards experiments on the influence of the temperature and concentration are examined. To be able to model the kinetics accordingly, the experiments are examined only in the aqueous phase to disregard the influence of the mass transfer between the phases. The procedure remains the same.

3.6 Liquid-liquid equilibria

To establish a suitable thermodynamic model, data about the equilibrium state in the liquid-liquid-equilibrium (LLE) of the reactive system are necessary.

3.6.1 Setup

Prior to the mass transfer experiments in the Nitsch cell, the liquid-liquid equilibrium between the organic phase and the aqueous phase has to be determined. With this data the tie lines, the binodal curve and the shape of the miscibility gap in the tetrahedral diagram can be evaluated.

Eleven mixtures with an overall weight of 40 g are prepared in 100 ml Schott flasks. The water to toluene mass ratio is 1:1. The eleven mixing points in 3 planes and 3 to 5 tie lines per plane can be seen in Table 3-5.

Due to the small concentrations in preliminary experiments in the Nitsch cell, the concentrations for the mixing point are selected from the lower range of concentration.

Table 3-5: Mixtures for LLE experiments.

Sample	Plane	Tie line	(A+DAA)	Acetone	DAA	Water	Toluene	Overall
			[w%]	[g]	[g]	[g]	[g]	[g]
1	1	1	5	1.0	1.0	19.0	19.0	40
2	1	2	10	2.0	2.0	18.0	18.0	40
3	1	3	20	4.0	4.0	16.0	16.0	40
4	1	4	30	6.0	6.0	14.0	14.0	40
5	1	5	35	7.0	7.0	13.0	13.0	40
6	2	1	5	0.5	1.5	19.0	19.0	40
7	2	2	15	1.5	4.5	17.0	17.0	40
8	2	3	25	2.5	7.5	15.0	15.0	40
9	3	1	5	1.5	0.5	19.0	19.0	40
10	3	2	15	4.5	1.5	17.0	17.0	40
11	3	3	25	7.5	2.5	15.0	15.0	40

3.6.2 Procedure

The components are weighed with a scale with a deviation of 0.02 g. Afterwards all samples are stirred with 450 rpm for 5 hours to ensure a sufficient mass transfer area.

Subsequently the bottles are put into a tempered water bath (25°C or 40°C) for 68 hours to obtain phase separation. After 68 hours samples from both phases are taken. According to prior experiments the concentration is expected to be too high for the GC calibration. Hence, the samples have to be diluted. The organic phase is diluted with THF at a ratio of 1:100 and the aqueous phase is diluted with THF at a ratio of 1:20. An internal standard of DMSO is added to normalize the results after analyzation. To ensure the equilibrium after 68 hours, the bottles are left in the water bath for another 24 hours and analyzed afterwards.

To avoid errors from the analytic evaluation, every sample in the gas chromatograph is injected twice and the mean value is used for further calculations.

The concentration of water in the organic samples is determined by Karl-Fischer titration. This is also examined twice for every sample.

3.6.3 Interfacial tension

To determine the interfacial tension, all samples which reached the equilibrium are tested. After 92 hours in the tempered water bath, samples are taken and analyzed with the spinning drop tensiometer, which is described in 3.2.3.

Before measuring the interfacial tension, density and refraction of the samples have to be determined at the according temperature (25°C or 40°C). In Table B-6 and Table B-7 in Appendix B the according data are given. As described in 3.2.3 the SVT 20N is used to determine the interfacial tension. This device can be set to a specific temperature, so that the samples are examined at the experiment's temperature.

Rotational speeds of 5,000 to 18,000 rpm are used to keep the droplet of the light phase stable. The shape of the droplet changes with the rotational speed. The rotational speed is increased constantly. With every step at least five measurements are taken until the values are constant. This adds up to around 30 measurements per sample, which are averaged in the end.

3.7 Interfacial mass transfer

To examine the mass transfer, a Nitsch cell is used. The experiments are conducted at 25°C and 40°C.

3.7.1 Nitsch cell

The setup of the used Nitsch cell is shown in Figure 3-5. A glass cylinder isolates the inner cell from ambient conditions, especially the temperature. Two stirrers on top and bottom of the cell keep the axial flow constant and ensure a homogeneous distribution for each phase. The Nitsch cell has an inner diameter of 75 mm. To keep a stable flow

regime, internal fittings are installed. A flow tube with an inner diameter of 50 mm and 12 radially installed baffles prevent tangential and radial flow in the cell.

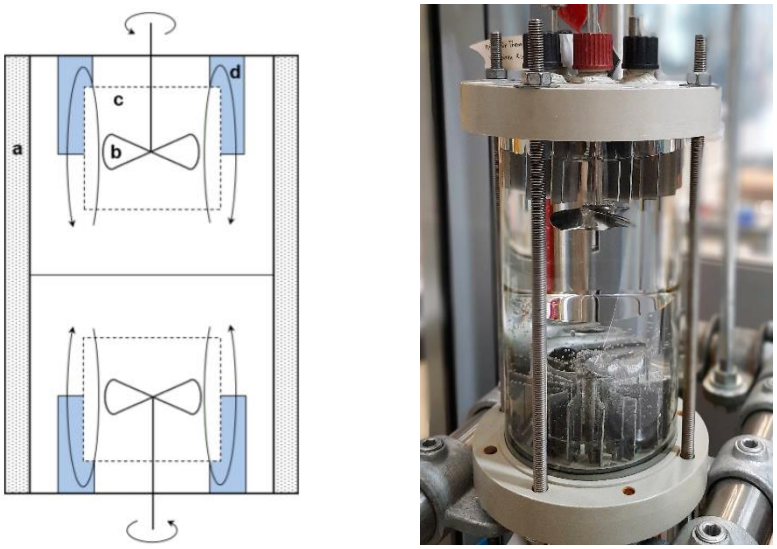

Figure 3-5: Sketch of a Nitsch cell according to [20]; (a) double-walled glass cylinder; (b) stirrer; (c) flow tube; (d) baffles and the Nitsch cell setup for experiments.

To keep the interface between the organic and the aqueous phase stable, a constant laminar flow regime is necessary. Both phases have to match the same Reynolds number, which is described in chapter 2.7, to reach this condition.

In this case, the kinematic viscosity is assumed to be constant for both phases and equal to the viscosity of the pure components at the according temperature. The bulk phase in the aqueous phase is water with a viscosity of 0.89 mPas. For the organic phase toluene is the phase forming component with a viscosity of 0.56 mPas. The velocity is calculated from the rotational speed of the stirrer. As a characteristic length the inner diameter of the cell is given.

To ensure both sufficient mixing and a stable and stationary interface, the rotational speeds of the stirrers are tested empirically. The highest possible rotational speed ratio to ensure a stable interface is chosen. This results in a stirrer speed of 175 rpm for the aqueous phase.

Seeing as the condition

$$Re_{aqu} = Re_{org} \quad ()$$

must be fulfilled. This results in

$$\frac{v_{aqu}}{v_{aqu}} = \frac{v_{org}}{v_{org}} \quad (3\text{-}7)$$

and the rotational speed of the stirrer in the organic phase can be put as

$$v_{org} = v_{aqu} * \frac{v_{org}}{v_{aqu}} \quad (3\text{-}8)$$

The rotational speed in the organic phase results in 127 rpm.

In Figure 3-6 the flow regime in the Nitsch cell is shown.

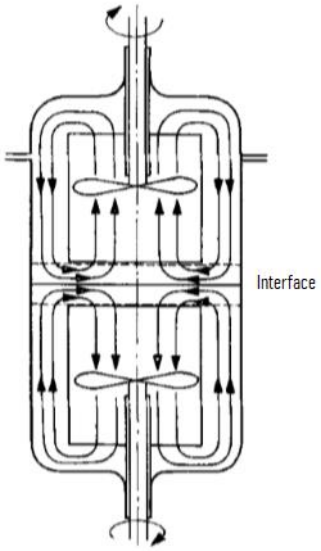

Figure 3-6: Flow regime in a Nitsch cell according to [23].

3.7.2 Procedure

At first a ternary system has to be in equilibrium to evaluate the mass transfer of the quaternary system water/toluene/acetone/diacetone alcohol. The procedure is explained exemplarily for the case of the experiment with water/toluene/acetone as ternary system and diacetone alcohol as target component.

In Table 3-6 the implemented experiments in the Nitsch cell to determine the mass transfer are shown.

After adjusting the Nitsch cell and the cryostat to the set temperature, the two phases are added. First the heavy, aqueous phase and then the top phase, here toluene, are filled into the Nitsch cell. The stirrer speed is set according to the conditions described in chapter 2.7. Both phases are stirred at a constant temperature for 5 hours. Afterwards the stirrers are turned off and the system is kept inoperative at a constant temperature overnight. During this time the equilibrium within the ternary system is reached.

The next day, the target component is added either in the top or the bottom phase, according to the experiment series. Before the component is added, sample 0 is taken from the ternary system to ensure the equilibrium state of the ternary system has been reached. During the mass transfer experiment, samples are taken from the organic and aqueous phase simultaneously. At first the time intervals are shorter and with running time the interval increases, due to the slower mass transfer resulting from the decreasing concentration gradient. After 8 hours the last sample is taken and the experiment can be stopped.

The concentrations of the components are above the calibration limits of the GC. Hence, all samples are diluted. The organic samples are diluted with THF at a ratio of 1:100 and the aqueous samples are diluted at a ratio of 1:10. For the reactive experiments the dilution of the organic phase is 1:10 and the aqueous phase is analyzed without further dilution.

The water concentrations in the organic samples are determined with Karl Fischer titration. All analyses are double determinations to minimize error sources.

Table 3-6: Mass transfer experiments in the Nitsch cell.

Experi-ment	T	Ternary system	Target component	Injection phase	Catalyst
	[°C]				
1	25	W/T/Acetone	DAA	top	-
2	25	W/T/Acetone	DAA	bottom	-
3	25	W/T/DAA	Acetone	top	-
4	25	W/T/DAA	Acetone	bottom	-
5	40	W/T/Acetone	DAA	top	-
6	40	W/T/Acetone	DAA	bottom	-
7	25	W/T/Acetone	-	bottom	NaOH
8	40	W/T/Acetone	-	bottom	NaOH

4 Results and Discussion

In this chapter the results of the experiments are shown and discussed.

4.1 Kinetic study

Within the kinetic study a catalyst is chosen, the reaction kinetics are determined and modeled, and the influence of the temperature is examined.

4.1.1 Screening of catalysts

The aldol self-condensation of acetone is a reaction that can be induced with an acidic as well as a basic catalyst. To determine the catalyst with the best results regarding reaction rate and yield of DAA, experiments with different kind of catalysts are made. All experiments are conducted at a temperature of 40°C in a system with both phases, water and toluene. The catalyst is only present in the aqueous phase, where the reaction takes place, and therefore diacetone alcohol forms.

Selectivity and yield of DAA with different basic and acidic catalysts were determined in the work of Salvapati et al. [3]. Based on that the catalysts NaOH, $Ba(OH)_2$, H_2SO_4, H_3PO_4, HCl and KOH are chosen to compare different outcomes.

Challenging conditions regarding the reactive substances and the catalyst caused some difficulties with the analytical method. Due to the different substances, especially NaOH which is dissolved in the aqueous phase, the results are distorted. The assumption is that the substances deposited on the liner and the column in the GC, which would cause further reactions during the analysis. Due to this the amount of diacetone alcohol in the results seemingly reduces over time. After these experiments, the liner is replaced to avoid similar problems during subsequent experiments.

Figure 4-1 shows developments of the concentration in the aqueous phase in [mmol/l]. Figure 4-2 shows the mass transfer from the aqueous phase to the organic phase in

[mmol/l], where the concentration increases until the equilibrium between the two phases is reached.

The experiments that show almost no formation of DAA due to the analytical problem described above, are excluded in both diagrams.

The experiments that are conducted with KOH show an unusual development of DAA concentration. The concentration increases beyond the equilibrium first, but subsequently decreases before finally reaching the equilibrium. In this case, the strong activity of the catalyst leads to a very high reaction rate. Therefore, the initial formation of diacetone alcohol seems to be faster than the mass transfer into the organic phase, hence the process is mass transfer limited.

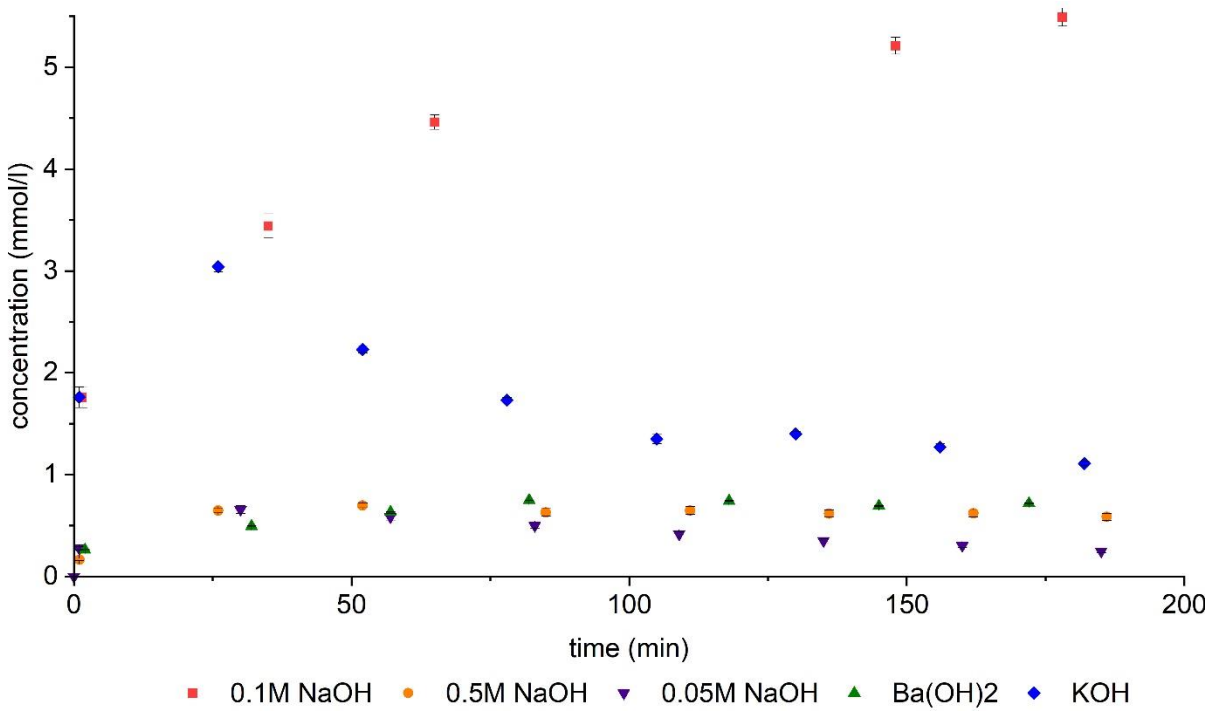

Figure 4-1: DAA concentration over time in [mmol/l] for different catalysts in the aqueous phase.

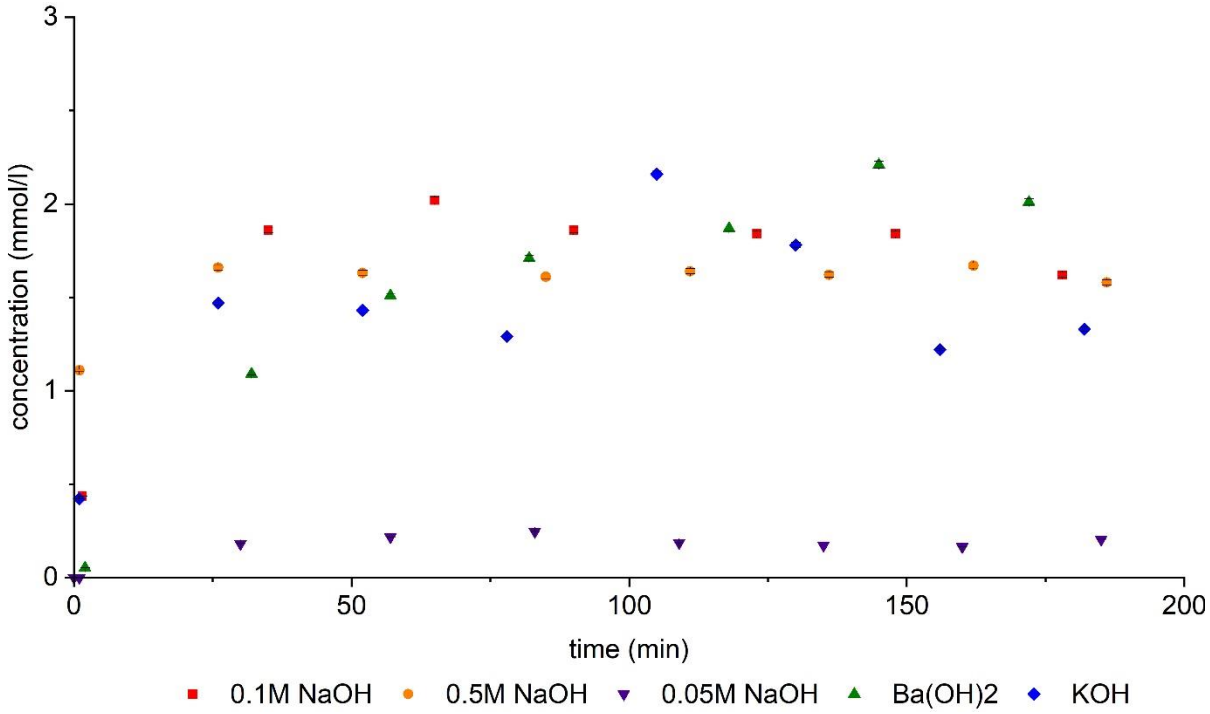

Figure 4-2: DAA concentration over time in [mmol/l] for different catalysts in the organic phase.

The experiment with 0.41g NaOH (0.05M) shows the most promising results. The acidic catalysts show almost no yield of DAA. KOH, as described before, causes a very fast formation of DAA and therefore a mass transfer limited procedure. The formation of DAA with $Ba(OH)_2$ as catalyst proceeds slower and therefore, reaching the equilibrium takes longer. Moreover, experiments with different amounts of NaOH are conducted to determine the optimal amount of catalyst. Due to the analysis method the time gaps cannot be smaller than 25 minutes. The beginning period of the experiment is crucial, because the concentration gradient is bigger than at the end. To describe this period sufficiently, a small amount of NaOH has to be chosen, because then the reaction proceeds slower and the development of concentration of DAA can be observed. NaOH with a concentration of 0.05M is chosen as a catalyst to perform the kinetic experiments and furthermore the modeling of the reaction kinetics, as well as the reactive mass transfer experiments in the Nitsch cell.

4.1.2 Experiments

The reaction rate is determined through experiments in the aqueous phase with NaOH as a catalyst at temperatures of 25°C and 40°C and with different starting amounts of acetone, 3 w%, 6 w% and 12 w%. The different amounts of acetone are important for the reaction rate. The influence of the amount of reactant can be considered in the rate law separately, otherwise it would be implemented in *k'*.

In Figure 4-3 the DAA concentration over time of the aldol self-condensation of acetone at 25°C with 6 w% starting concentration of acetone and 0.05M NaOH as catalyst is shown exemplarily. All other results can be found in Appendix C1.

Diacetone alcohol is formed during the reaction. At the beginning, the slope of the curve is steeper because of the higher concentration gradient. When reaching the equilibrium state, the concentration gradient and the reaction rate decrease.

The amount of acetone in the system is very high. The conversion of acetone, however, is very low, hence almost no changes of the composition of acetone over time are observed. For a better overview, only the DAA concentration over time is shown.

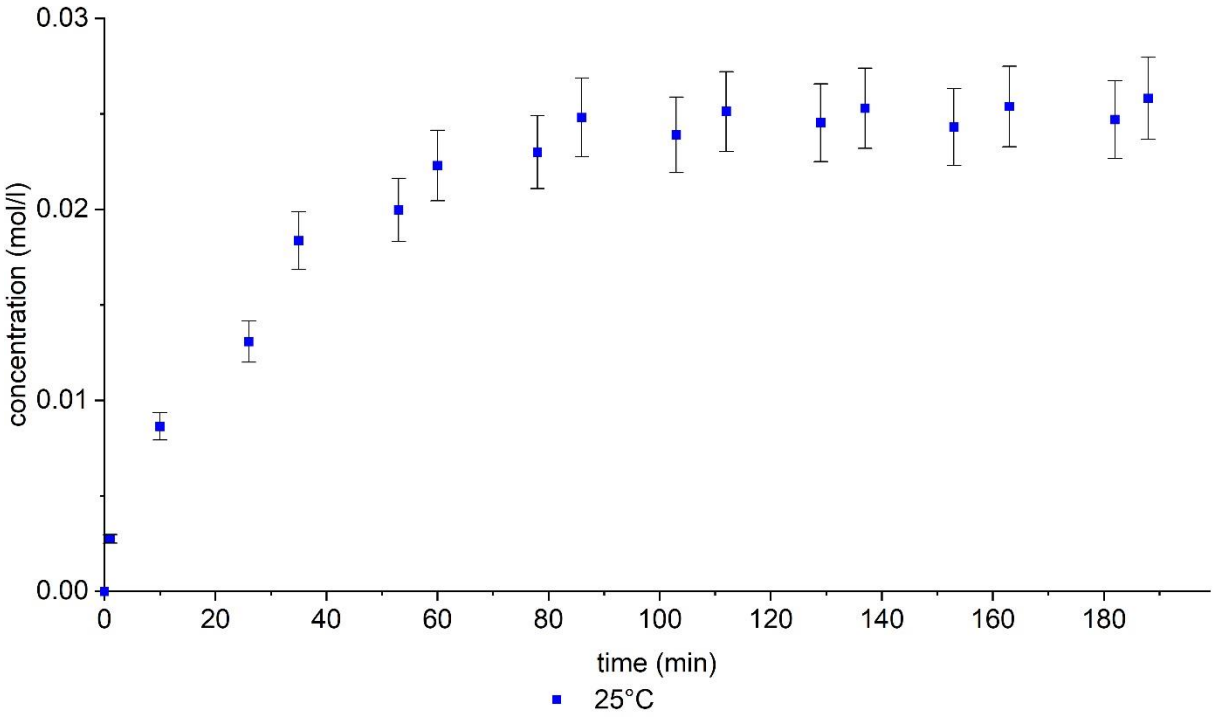

Figure 4-3: DAA concentration over time at a temperature of 25°C and 1 atm with 6 w% starting concentration of acetone and 0.05M NaOH as catalyst.

At a higher temperature the reaction rate increases. This is shown in Figure 4-4. It shows that the equilibrium is reached at 25°C after 2 hours and after 1.5 hours at 40°C. DAA is formed faster, hence in the beginning the slope of the experiment is steeper at 40°C than at 25°C. With 1.88% the conversion at 40°C is lower than at 25°C, where the conversion results in 2.50%. This is in good agreement with the results of Kuśtrowski et al. [4].

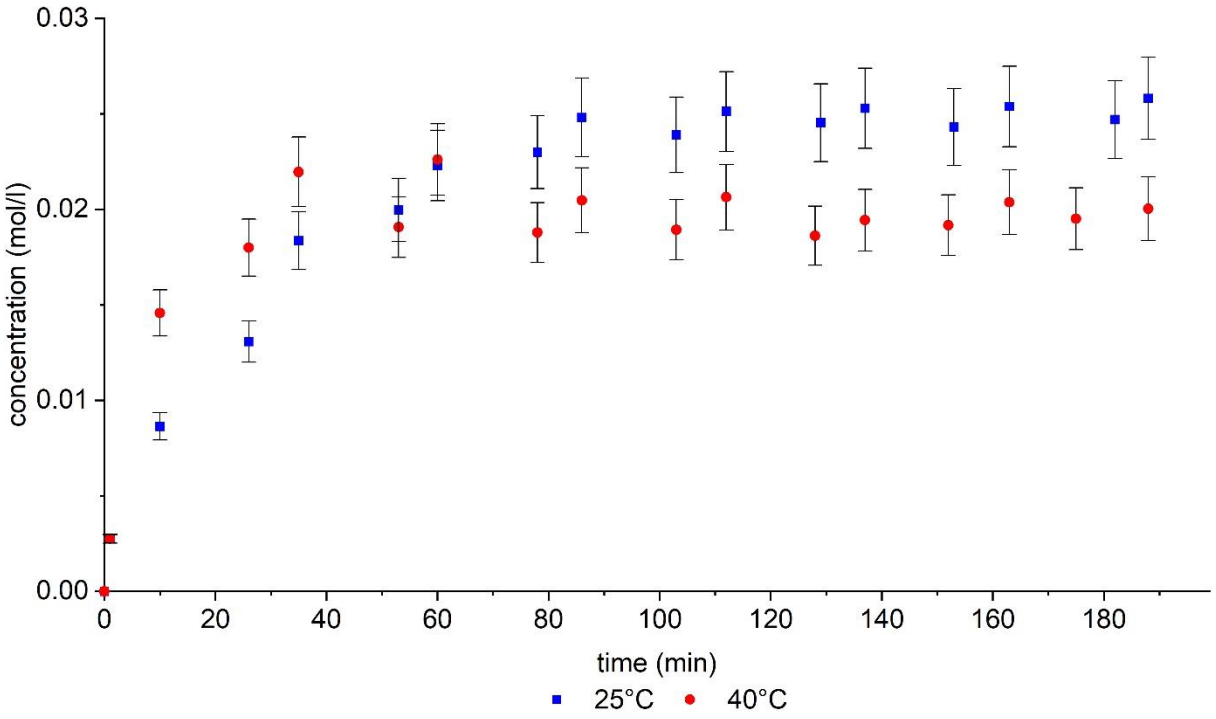

Figure 4-4: DAA concentration over time at a temperature of 25°C and 40°C at 1 atm with 6 w% starting concentration of acetone and 0.05M NaOH as catalyst.

4.1.3 Rate law

To model the reaction kinetics of a system, a mathematical model is established. The rate of reaction is dependent on the concentration of the components and the reaction rate constants. The values of the constants are fitted to the experimental data.

As described in chapter 2.2, the chemical equation for an aldol self-condensation is based on the following form:

$$2A \overset{OH^-}{\longleftrightarrow} C \tag{4-1}$$

For the self-condensation of acetone, *A* stands for acetone and *C* stands for diacetone alcohol.

According to the chemical equation, the reaction rate for component *C* may be written as an equation with k_1 and the concentration of *A* to the square for the forward reaction, and k_2 and the concentration of *C* for the reverse reaction.

$$r_C = \frac{dc_C}{dt} = k_1 * c_A^2 - k_2 * c_C \tag{4-2}$$

These assumptions result from the reaction equation and have been validated in the works of Maple and Allerhand [13], Podrebarac et al. [9] and Kuśtrowski et al. [4].

For the calculations the volume can be assumed to be constant, since the sample volume during the experiments is very small in relation to the overall volume.
Additionally, at the time t=0 the concentration of *C* is 0.

The concentration c_A of component *A* at the time *t* is defined as:

$$c_A = c_{A0} - 2 * c_C \tag{4-3}$$

$$c_{C0} = 0 \tag{4-4}$$

When in equilibrium, the reaction rates of the forward and the reverse reaction are equal, and therefore the overall reaction rate is 0. The equilibrium concentration $c_{C\infty}$ can be defined with k_1 and k_2.

$k_1 * (c_{A0} - 2 * c_{C\infty})^2 = k_2 * c_{C\infty}$ (With this, the equation for the reaction rate can be rearranged and integrated. When equations 4-3 and 4-4 are applied to equation 4-2, the following approach results:

$$\frac{dc_C}{dt} = k_1 * \left[(c_{A0} - 2 * c_C)^2 - \frac{c_C}{c_{C\infty}} * (c_{A0} - 2 * c_{C\infty})^2\right] \tag{4-6}$$

After integration this results in:

$$c_{Ct} = \frac{{c_{A0}}^2 * c_{C\infty} * (e^{\tau} - 1)}{e^{\tau} * {c_{A0}}^2 - 4 * {c_{C\infty}}^2} \tag{4-7}$$

with

$$\tau = \frac{k_1 * t * ({c_{A0}}^2 - 4 * {c_{C\infty}}^2)}{c_{C\infty}} \tag{4-8}$$

The reaction rate constants k_1 and k_2 can be determined by measuring values for c_C.

For that purpose, the least squares method is applied by minimizing the residual sum between measured and calculated values for c_C. Starting values for this operation are taken from previous works within this project and furthermore from the work of Maple and Allerhand [13].

For an initial mass concentration of acetone of 6 w% at 25°C, the result of the modeling is shown exemplarily in Figure 4-5. All results can be seen in the Appendix C1.

The dots in the diagram are the measured points from the experiment and the line is the fitted curve of the model. The deviation with a mean of $7.81*10^{-4}$ [mol/l] results from the simplifications and assumptions of the model. For all experiments the first measuring point is above the curve of the model. This results from the model, which factors in the equilibrium very strongly. Therefore, the measuring points at the beginning of the experiment, before equilibrium is reached, are underestimated, while the measuring points close to the equilibrium or in equilibrium are fitted very well. To counteract this effect, the values in equilibrium state are weighted differently.

In Table 4-1 the results of all experiments for the reaction rate constants k1 and k2 are shown.

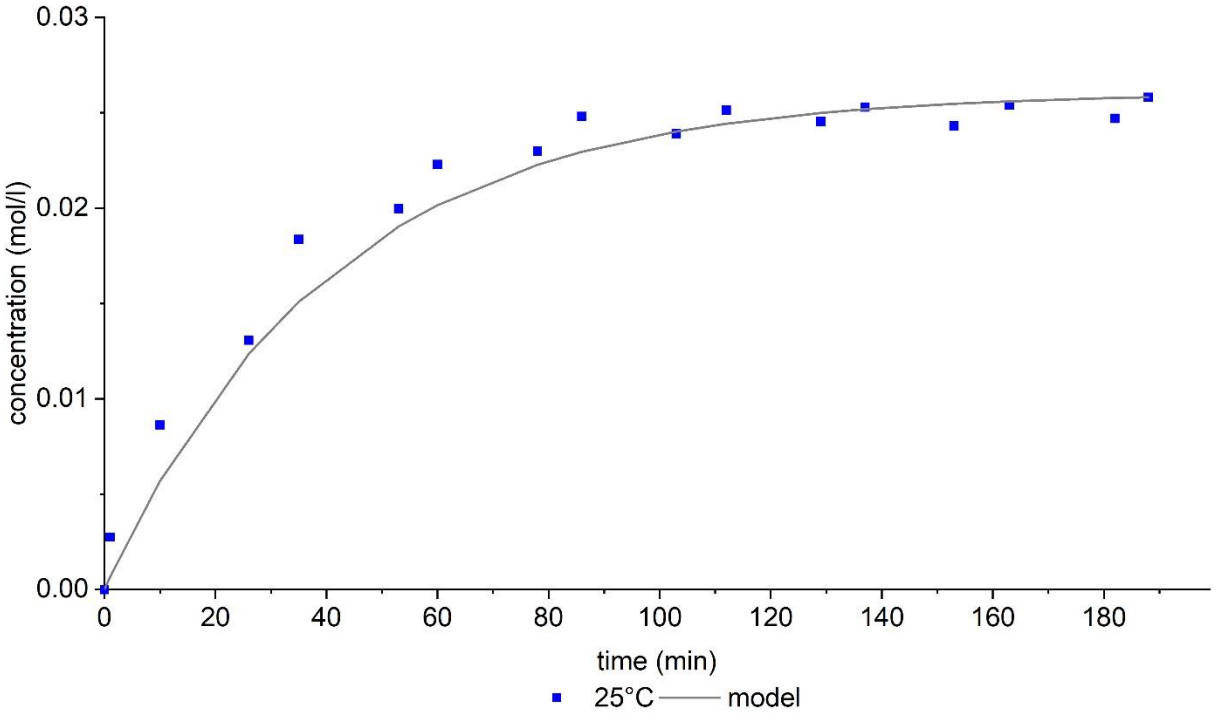

Figure 4-5: Composition of DAA over time at 25°C and 1 atm with 6 w% starting concentration of acetone and 0.05M NaOH as catalyst and the fitted curve of the model.

Table 4-1: Reaction rate constants k_1 and k_2 for 3 w%, 6 w% and 12 w% starting concentration of acetone at 1 atm and the temperatures of 25°C and 40°C with 0.05M NaOH as catalyst.

$C_{0,\ acetone}$	T	k_1	k_2	c_{calc}-c_{exp}
[w%]	[°C]	[l/mols]	[1/s]	[mol/l]
3	40	4.7E-06	8.7E-04	1.34E-04
	25	4.5E-06	4.7E-04	2.25E-04
6	40	5.2E-06	8.0E-04	6.67E-04
	25	3.4E-06	4.0E-04	7.81E-04
12	40	6.3E-06	7.9E-04	2.84E-03
	25	5.1E-06	4.2E-04	2.39E-04

4.1.4 Influence of the temperature

Additionally, an Arrhenius diagram is created to illustrate the influence of the temperature on the reaction kinetics and to determine the activation energy. In this diagram the linearization of the Arrhenius equation is shown. This results from the Arrhenius equation as mentioned in chapter 2.3.2.

$$k = A * e^{\frac{-E_A}{RT}} \tag{4-9}$$

Applying the natural logarithm results in

$$ln(k) = \ln(A) + \frac{-E_A}{RT} \tag{4-10}$$

In Table 4-2 the results for the activation energy and the frequency factor for the forward as well as the reverse reaction are shown.

Table 4-2: Values for E_A and A from the Arrhenius equation.

$C_{0,\ acetone}$		E_A	A
[w%]		[J/mol]	[l/mols]
3	k_1	2642	1.310E-05
	k_2	31865	179.873
6	k_1	22882	3.444E-02
	k_2	35870	770.128
12	k_1	11592	5.449E-04
	k_2	32694	224.566

The straight line that results from the Arrhenius equation is shown in Figure 4-6 exemplarily for the 6 w% starting concentration of acetone. To determine the activation energy and the frequency factor from the Arrhenius equation, three values at three different temperatures are usually measured. To examine a third temperature for the aldol self-condensation of acetone would go beyond the scope of the discussion of this thesis. These are results for estimating the activation energy and the frequency factor.

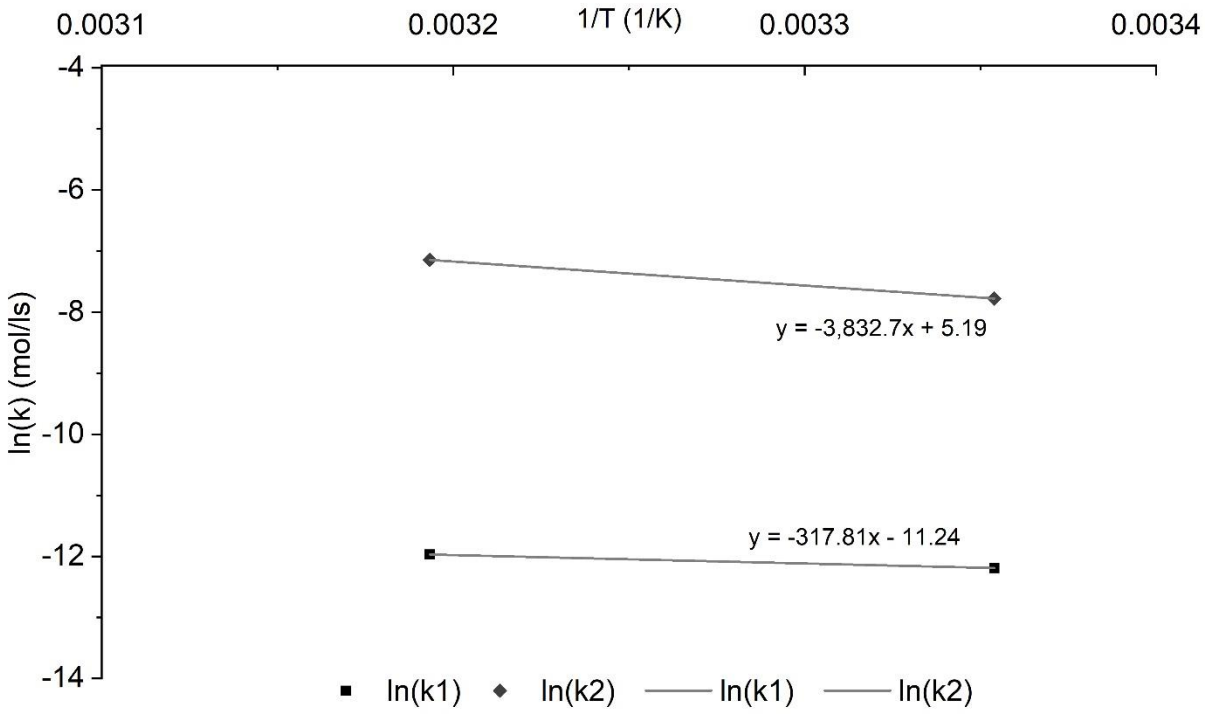

Figure 4-6: Arrhenius plot for 6 w% starting concentration of acetone.

4.2 Liquid-liquid equilibria

For an accurate representation of a system for a reactive extraction, the liquid-liquid-equilibria (LLE) data are necessary. The investigated system is the quaternary system of reactive components, acetone and DAA, in the extractive system water + toluene. Water and toluene are the phase forming components and acetone and DAA are the target components. The experiments are conducted at 25°C and 40°C. The equilibrated samples are subsequently used to determine the interfacial tension at the respective tie lines within the phase tetrahedron.

4.2.1 LLE

In Figure 4-7, the tie lines 1-5 of plane 1 of the quaternary system water/toluene/acetone/DAA at 25°C are shown. The ratio of acetone and DAA in this plane is 1:1.

The grey spheres show the mixing points for the original mixtures. The tie lines result from the separated phases after equilibrium is reached. On the top of the tetrahedron diagram acetone is plotted, on the left corner DAA is plotted. The spheres in the front of the tetrahedron represent the composition in the aqueous phase, the spheres in the back right corner represent the composition in the organic phase.

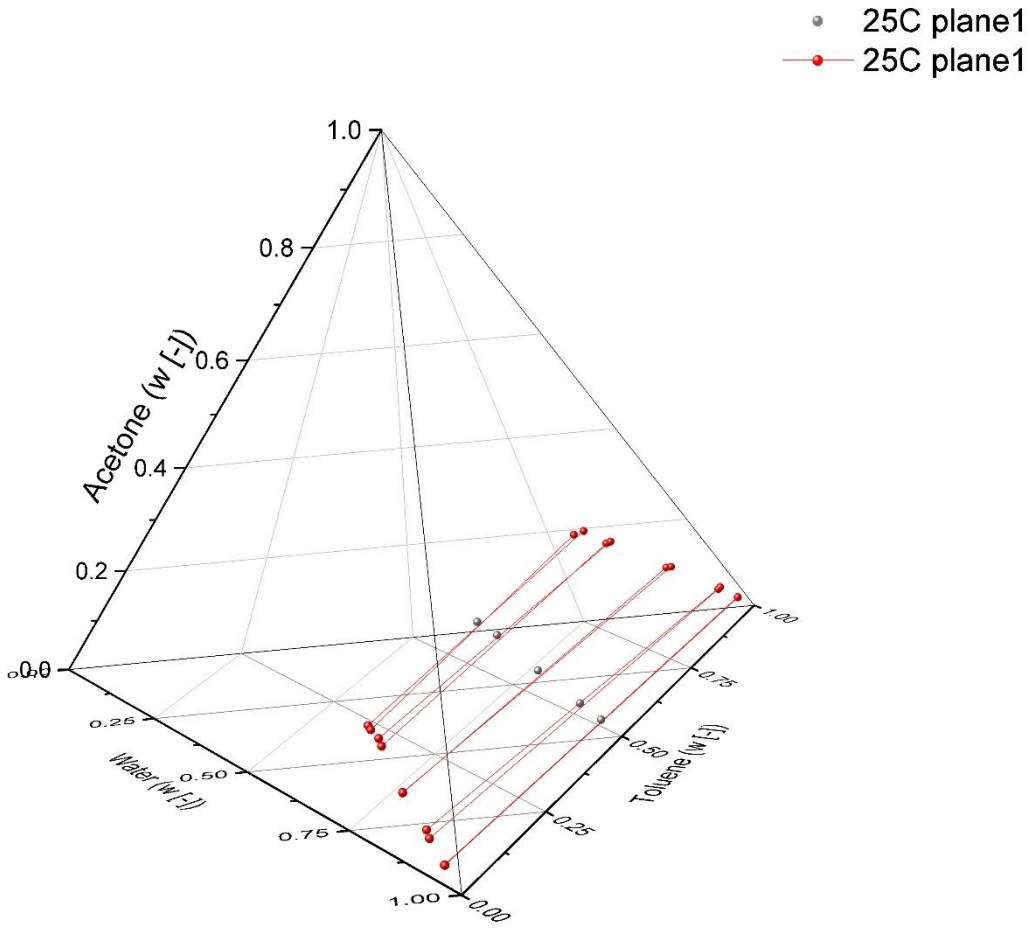

Figure 4-7: LLE at 25°C, plane 1, tie lines 1-5, after 68 hours and 92 hours.

In Figure 4-8, the tie lines 1-3 of plane 2 of the quaternary system at 25°C are shown. The ratio in plane 2 for acetone and DAA is 1:3.

The difference between the results after 68 hours and 92 hours are within reasonable deviation. This deviation is shown by the difference between the corresponding lines for each mixing point. The deviation of tie lines and mixing points, especially for plane 2 and 3, where the ratio of acetone and DAA is not equal, is likely caused by the analytical method (GC). DAA is not measured properly by the GC, the results show an acetone peak for pure DAA. This can result from DAA conversion to acetone over time due to the high temperature in the GC or from interaction between the target components in the mixture. The higher the amount of target components in the system, the higher the deviations are.

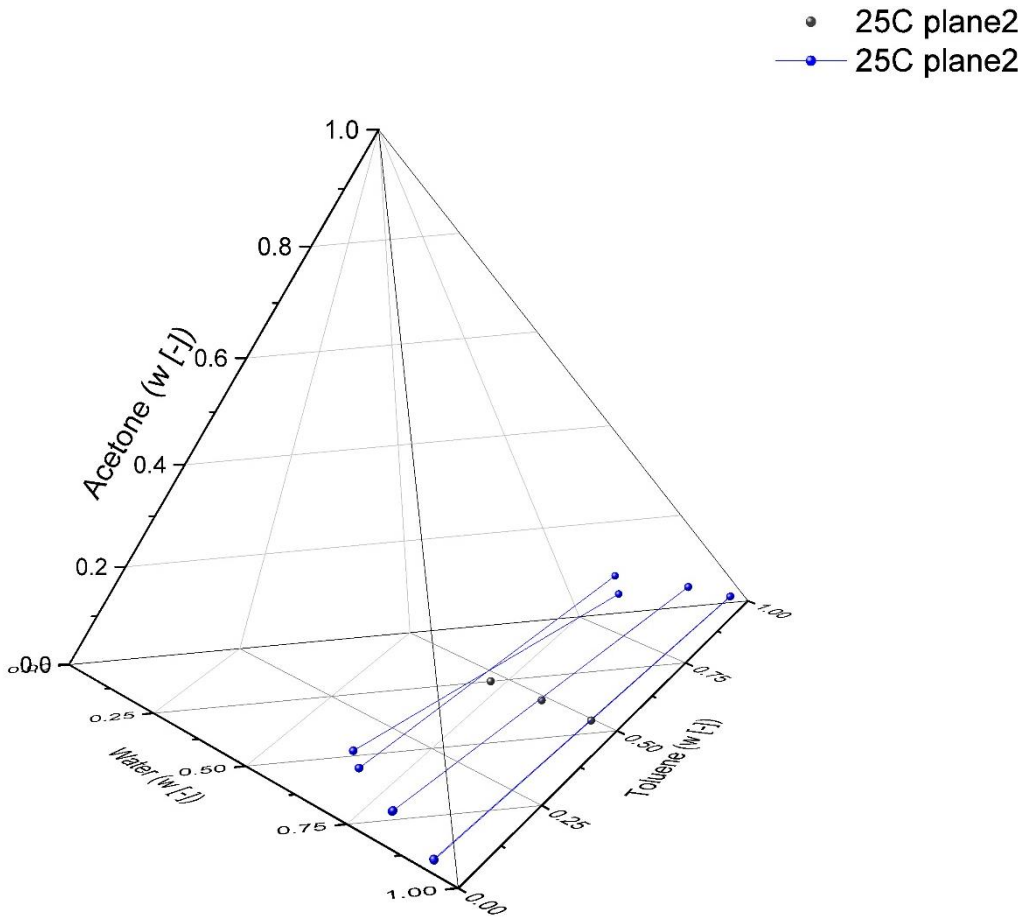

Figure 4-8: LLE at 25°C, plane 2, tie lines 1-3, after 68 hours and 92 hours.

In Figure 4-9, the tie lines 1-3 of plane 3 of the quaternary system at 25°C are shown. In plane 3 the ratio of acetone to DAA is 3:1. The mass ratios of all components are shown in Table 3-5.

The tetrahedron diagrams show that the solubility of acetone is similar in both phases, hence the tie lines are almost horizontal. The solubility of DAA is slightly smaller in the organic phase than in the aqueous phase. Due to that, the tie lines are slightly tilted. This tilting effect is more pronounced at 40°C. The phase forming components of the mixture are water and toluene. Since the properties of these components do not change significantly at a higher temperature, the difference between the results at 25°C and 40°C is minor. The higher the amount of target component in the system, the more water is soluble in the organic phase and the higher the amount of toluene in the aqueous phase. The red spheres connecting the tie lines show the border of the miscibility gap in the quaternary system.

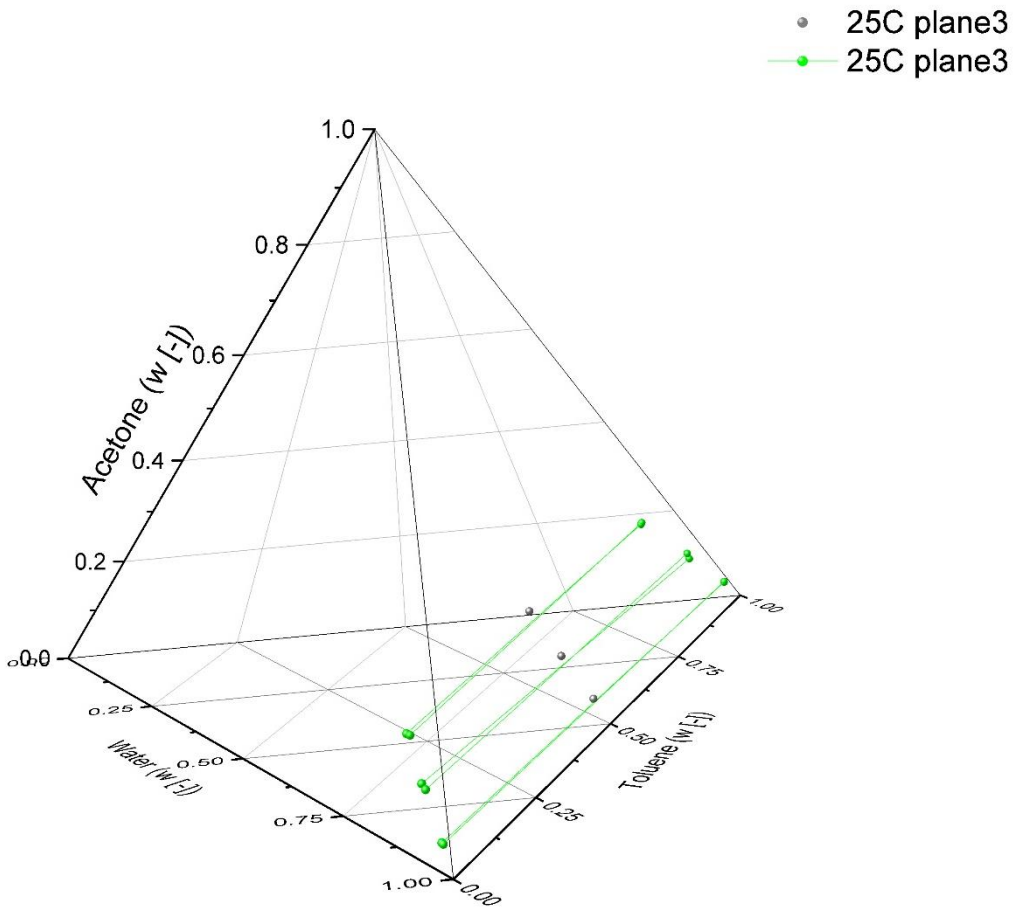

Figure 4-9: LLE at 25°C, plane 3, tie lines 1-3, after 68 hours and 92 hours.

For a better overview, the results for the conducted LLE experiments at 40°C after 92 hours are shown in Table 4-3 and Table 4-4.

Table 4-3: Results of LLE at 40°C in the organic phase after 92 hours.

Plane	Sample	Water	Toluene	DAA	Acetone
		w [-]	w [-]	w [-]	w [-]
1	1	0.0016	0.9602	0.0160	0.0223
1	2	0.0023	0.9128	0.0389	0.0460
1	3	0.0063	0.7903	0.0980	0.1054
1	4	0.0117	0.6702	0.1474	0.1707
1	5	0.0183	0.6122	0.1779	0.1917
2	6	0.0011	0.9548	0.0268	0.0173
2	7	0.0033	0.8635	0.0833	0.0498
2	8	0.0076	0.7266	0.1708	0.0951
3	9	0.0015	0.9573	0.0093	0.0318
3	10	0.0038	0.8578	0.0321	0.1063
3	11	0.0081	0.7500	0.0587	0.1832

Table 4-4: Results of LLE at 40°C in the aqueous phase after 92 hours.

Plane	Sample	Water	Toluene	DAA	Acetone
		w [-]	w [-]	w [-]	w [-]
1	1	0.9514	0.0001	0.0274	0.0211
1	2	0.8994	0.0002	0.0552	0.0452
1	3	0.8060	0.0001	0.1174	0.0764
1	4	0.7331	0.0015	0.1427	0.1227
1	5	0.7031	0.0036	0.1582	0.1351
2	6	0.9401	0.0001	0.0430	0.0168
2	7	0.8300	0.0004	0.1218	0.0479
2	8	0.7296	0.0001	0.1940	0.0763
3	9	0.9571	0.0001	0.0148	0.0280
3	10	0.8868	0.0001	0.0385	0.0746
3	11	0.8138	0.0007	0.0604	0.1251

4.2.2 Interfacial tension

In Figure 4-10 the interfacial tension in correlation to the weight percent for DAA in the organic phase at 25°C is shown. The higher the concentration of the target component is in the system, the closer the tie lines are to the critical point. At the critical point there is only one thermodynamically stable phase, hence the interfacial tension decreases with increasing concentration of the target component and approaches zero at the critical point. Figure 4-11 shows the interfacial tension for plane 1 at 25°C and 40°C with respect to DAA in the organic phase. Between 25°C and 40°C almost no changes are observed in the interfacial tension. For the subsystem water/toluene, the influence of the temperature on the LLE and the interfacial tension is very small. The phase forming components are water and toluene, hence the temperature has a small impact on the interfacial tension. The interfacial tension displayed in the organic phase at 40°C seems to be slightly higher than at 25°C, which can be due to the measuring tolerance.

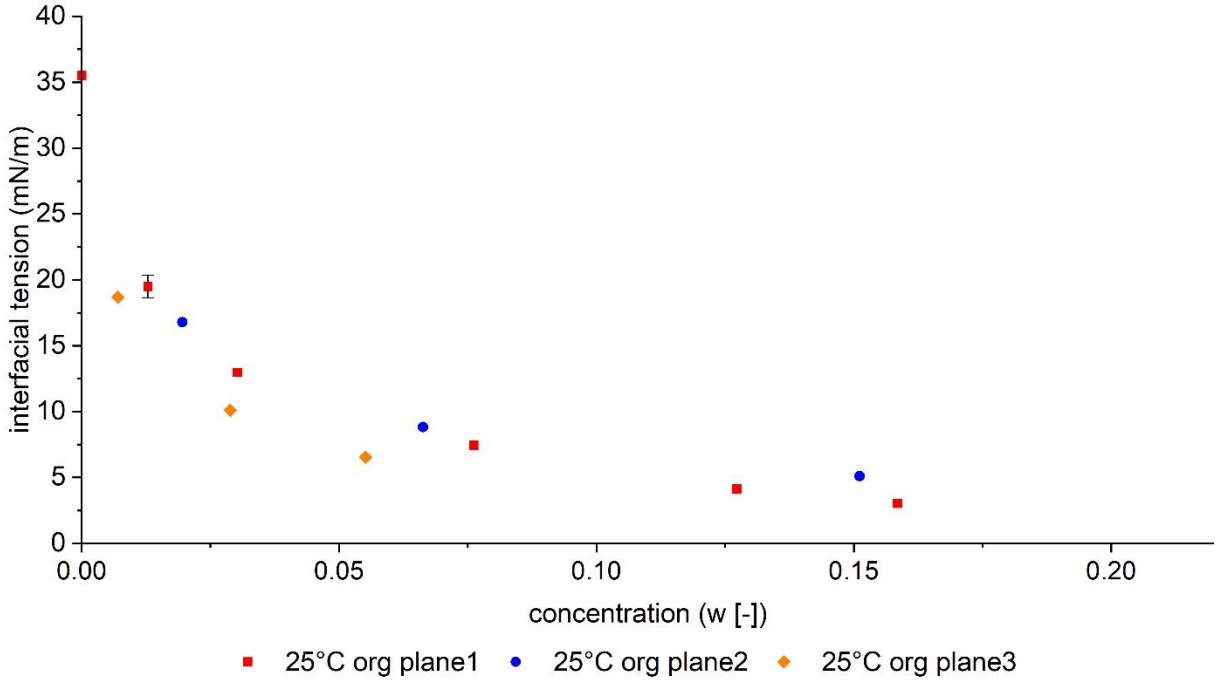

Figure 4-10: Interfacial tension with respect to DAA concentration in the organic phase at 25°C.

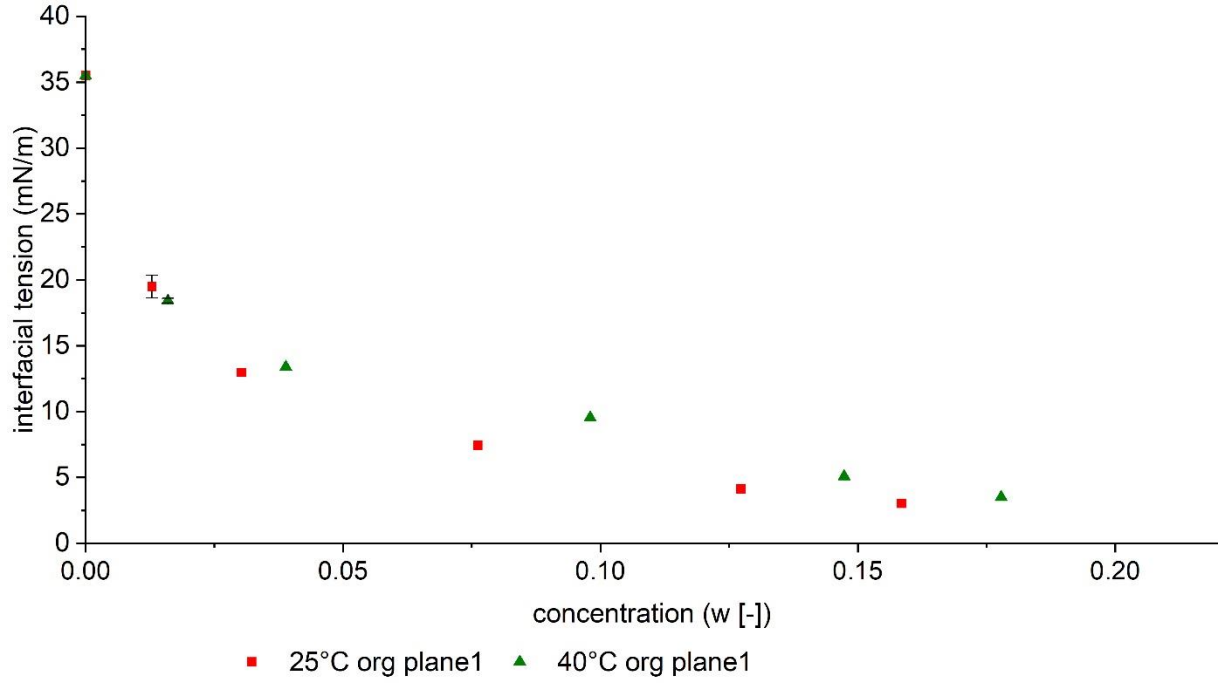

Figure 4-11: Interfacial tension with respect to DAA concentration for plane 1 in the organic phase at 25°C and 40°C.

4.3 Interfacial mass transfer

As described in chapter 3.7.2, eight different experiments are conducted to determine the mass transfer between the organic and the aqueous phase. First, the purely diffusive mass transfer in the water/toluene/acetone/DAA system is investigated. Subsequently, the mass transfer for simultaneous diffusion and reaction is studied by conducting mass transfer experiments in the presence of NaOH as a catalyst for the aldol self-condensation reaction.

4.3.1 Diffusive interfacial mass transfer

In Figure 4-12 the development of the concentration over time for both phases and both target components, acetone and DAA, is shown. In experiment 1 the ternary system water/toluene/acetone is in equilibrium when the target component DAA is injected into the top (organic) phase. Therefore, the composition of acetone in both phases is relatively constant over time. The composition of DAA in the organic phase decreases over time, due to the transfer into the aqueous phase. In the aqueous phase, the amount of DAA is increasing until the equilibrium is reached. The DAA concentration in both phases levels off after 3 hours, when the equilibrium composition is approached.

It is also shown that the equilibrium value of DAA in the aqueous phase is higher than in the organic phase. The equilibrium value of acetone is roughly the same in both phases.

To improve the readability, the error indicators are not shown in the diagrams. All experiments with error indicators are shown in Appendix C3.

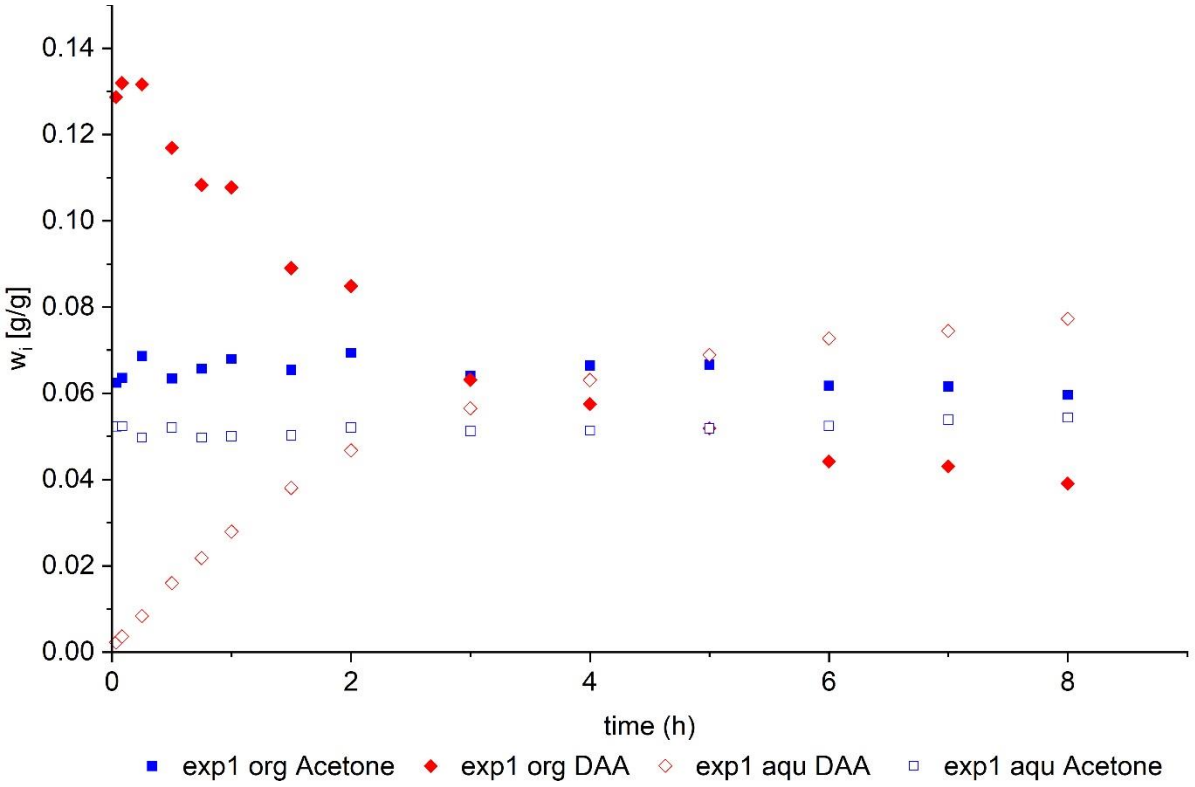

Figure 4-12: Composition over time for Nitsch cell experiment 1, 25°C, 1 atm, ternary system water/toluene/acetone, target component DAA injected in the organic phase.

In Nitsch cell experiments 1 and 2 DAA is the target component at 25°C. In experiment 1 DAA is injected in the organic phase, in experiment 2 DAA is injected in the aqueous phase of the pre-equilibrated ternary system water/toluene/acetone. The comparison of these two experiments is shown in Figure 4-13.

The composition of acetone over time is constant for both phases and experiments, whereas the composition of DAA changes over time. In experiment 2, DAA is injected into the aqueous phase. Therefore, due to the interfacial mass transfer, the composition in the organic phase increases, while it decreases in the aqueous phase. The equilibrium is reached after 3 hours in both experiments. The equilibrium value for DAA in the organic phase is lower than in the aqueous phase. The development of the concentration of DAA in the organic and aqueous phase converge to the same value for both experiments.

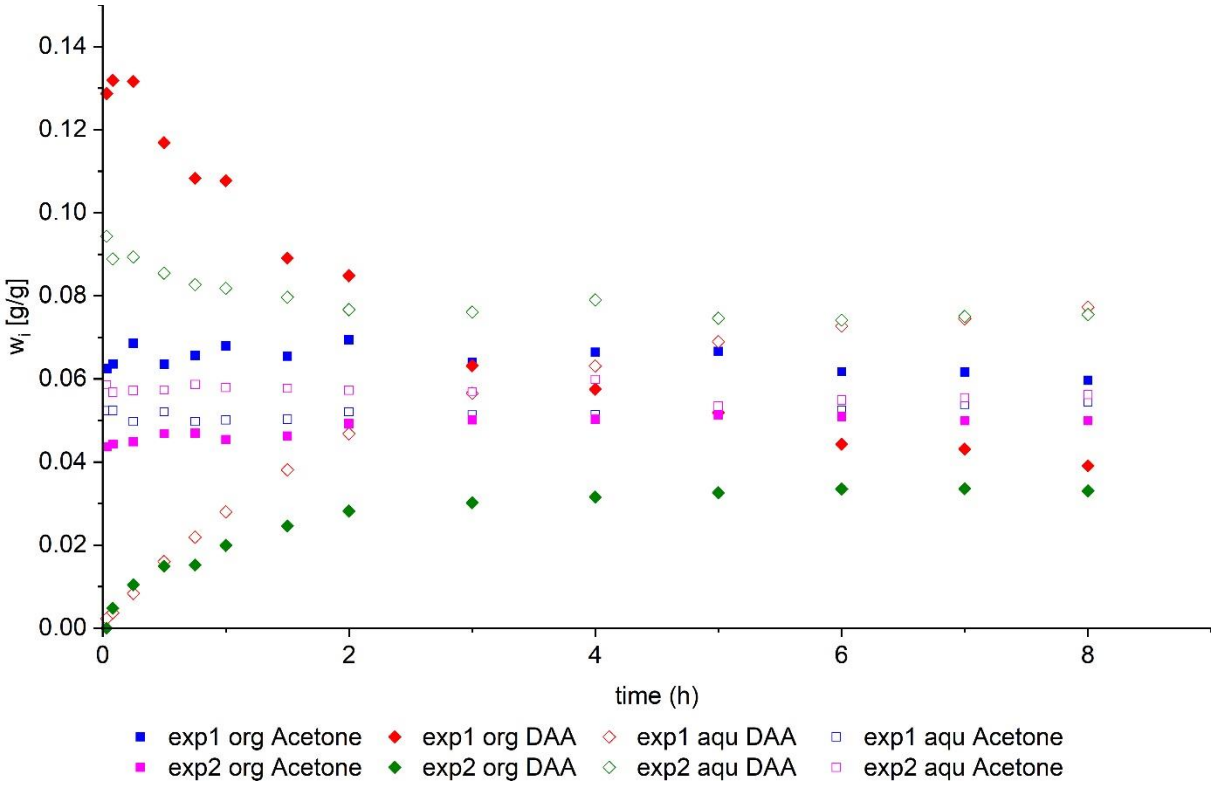

Figure 4-13: Composition over time for Nitsch cell experiment 1 and 2, 25°C, 1 atm, ternary system water/toluene/acetone, target component DAA injected in the organic phase and the aqueous phase.

In experiment 1 DAA is injected into the organic phase, while in experiment 3 acetone is injected into the organic phase. In Figure 4-14 the results are shown.

As previously described, the composition of acetone is constant for experiment 1. In experiment 3 the pre-equilibrated ternary system is water/toluene/DAA, hence the composition of DAA is constant in both phases. The decreasing compositions in the organic phases are DAA in experiment 1 and acetone in experiment 3. The increasing compositions in the aqueous phases are DAA in experiment 1 and acetone in experiment 3. The concentration of DAA in the aqueous phase is again higher when in equilibrium than the concentration of DAA in the organic phase. The equilibrium values for acetone approach the same value in each phase for both experiment 1 and experiment 2.

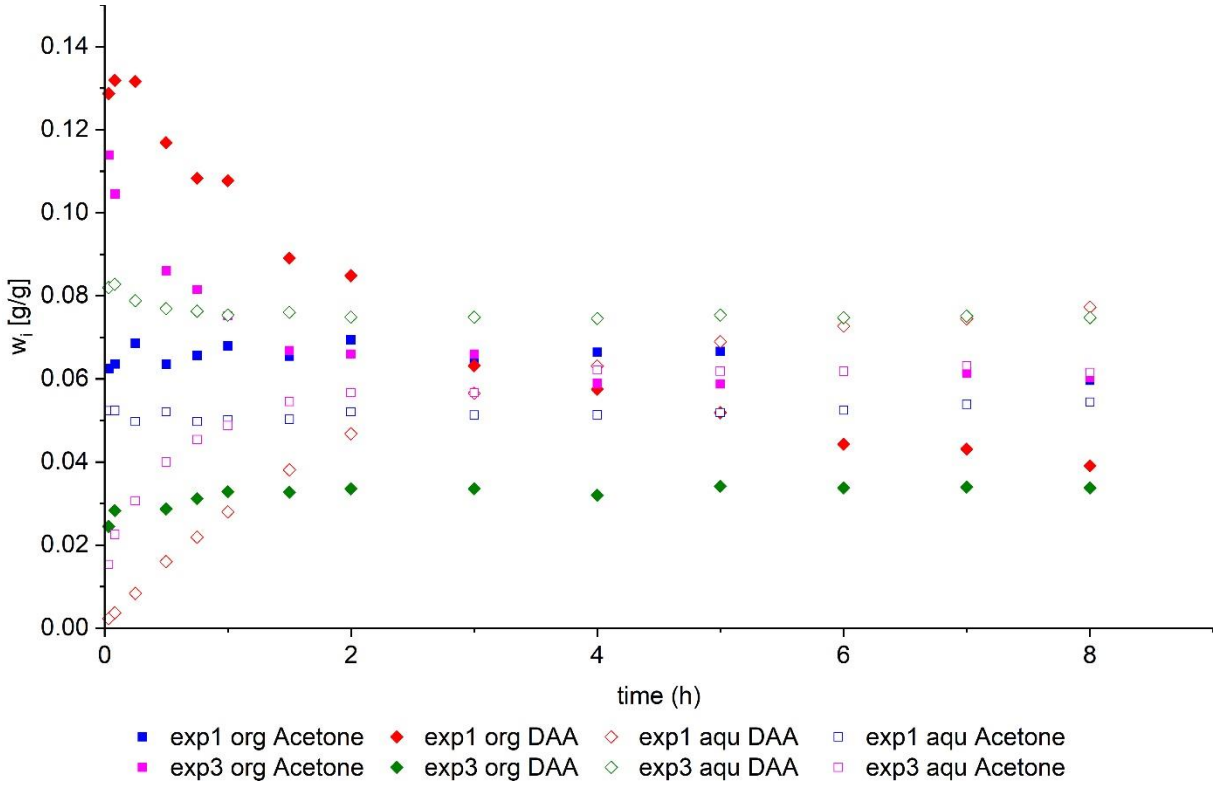

Figure 4-14: Composition over time for Nitsch cell experiment 1 and 3, 25°C, 1 atm, ternary system water/toluene/acetone for 1 and water/toluene/DAA for 3, target component DAA or acetone injected in the organic phase.

As the results from the kinetic study in chapter 4.1.2 show, higher temperature increases the reaction rate. This is also valid for the mass transfer experiments. In Figure 4-15 the results of experiment 2 and 5 are shown. Experiment 2 is conducted at 25°C and experiment 5 is conducted at 40°C. The target component DAA is injected into the aqueous phase in both experiments. Since the values for acetone are almost constant over the whole running time, only the composition for DAA is shown in the graph. Due to the mass transfer to the organic phase, the concentration of DAA in the aqueous phase decreases after the injection. This is valid for both temperatures. The equilibrium is reached faster with higher temperature and the difference between the starting values and the equilibrium values is smaller at 40°C than at 25°C.

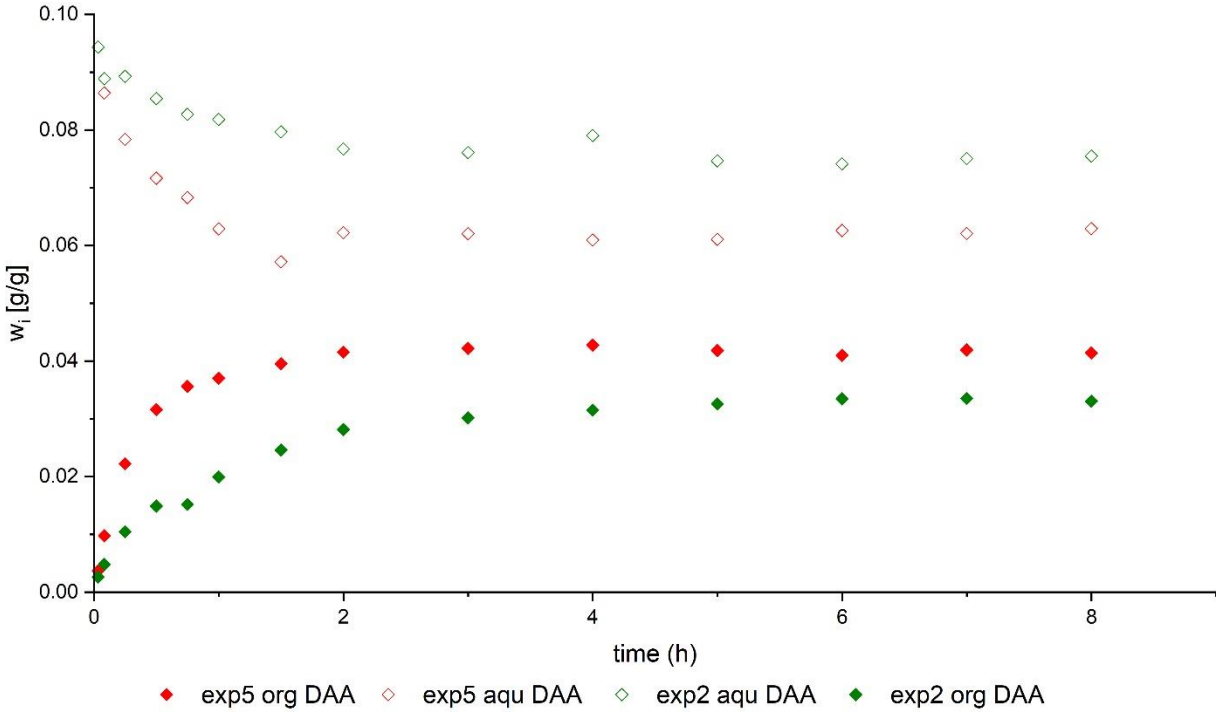

Figure 4-15: Composition over time for Nitsch cell experiment 2 and 5, 25°C and 40°C, 1 atm, ternary system water/toluene/acetone, target component DAA injected in the aqueous phase.

4.3.2 Interfacial mass transfer with overlaid reaction

After determining the purely diffusive mass transfer of acetone and DAA, another set of mass transfer experiments is conducted to determine the influence of the reaction kinetics of the aldol self-condensation on the overall mass transfer. For these experiments, NaOH is added to the aqueous phase and the concentration of formed DAA in both phases is investigated.

In Figure 4-16 the development of DAA concentration for experiment 7 at 25°C is shown. The amount of acetone is much higher than the formed amount of DAA and it is almost constant. Due to that, only the composition of DAA is shown in the graph. In the aqueous phase the development of DAA concentration over time resembles the kinetic study described in chapter 4.1.2. At first the amount of DAA increases fast, yielding a steep DAA concentration curve. When reaching equilibrium after 2 hours, the concentration levels off. In the organic phase DAA increases even after the equilibrium value is reached in the aqueous phase, because the mass transfer continues and the true equilibrium in both phases has not been reached yet. The development in

the organic phase shows an inflection point at the same time as the slope of DAA in the aqueous phase levels off. It can be concluded that the more DAA is formed, the faster the mass transfer to the organic phase takes place.

The interfacial mass transfer with overlaid reaction is investigated at 25°C and 40°C.

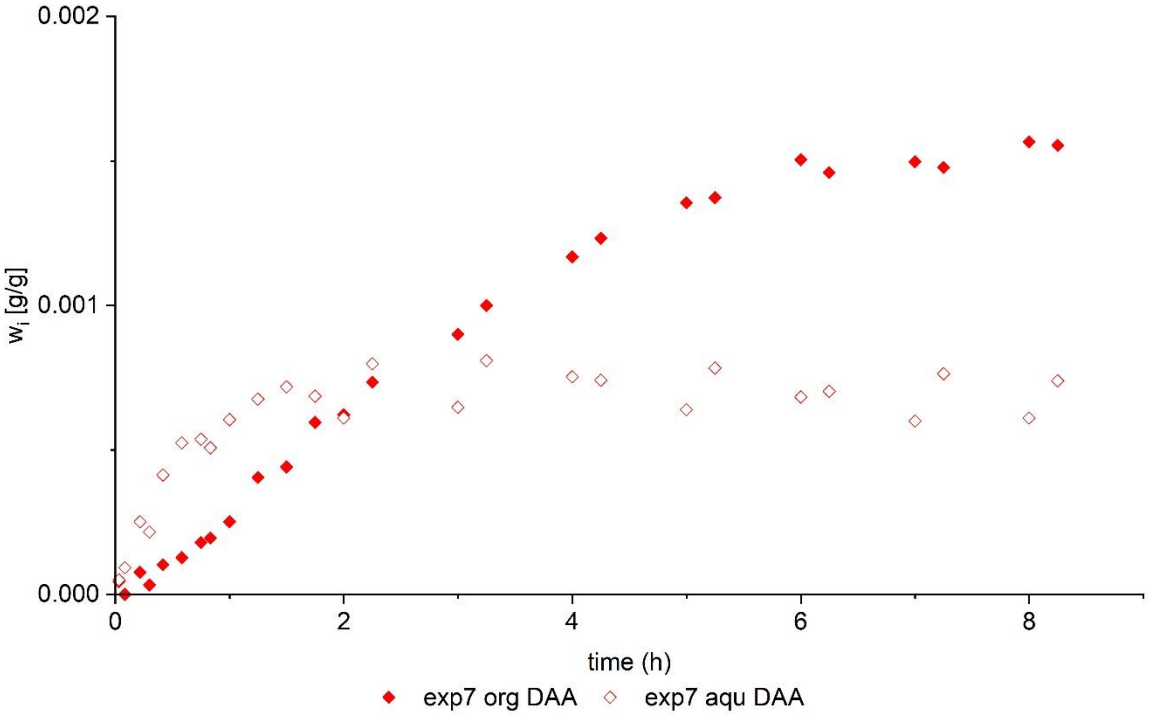

Figure 4-16: Figure 4 14: Composition over time for Nitsch cell experiment 7, 25°C, 1 atm, ternary system water/toluene/acetone, target component DAA, with NaOH injected in the aqueous phase.

Experiment 8 is conducted with NaOH being injected into the aqueous phase of a pre-equilibrated ternary system water/toluene/acetone. The comparison of experiment 7 at 25°C and experiment 8 at 40°C is shown in Figure 4-17.

Experiments 7 and 8 both show similar results for the composition of DAA. With higher temperature the reaction is faster. The comparison of the concentration of DAA shows again, that the equilibrium value for DAA in the organic as well as the aqueous phase is lower at a higher temperature. At 40°C the equilibrium in the aqueous phase is reached after 1 hour, while in the organic phase the equilibrium, and therefore the overall equilibrium, has not been reached after 8 hours of running time.

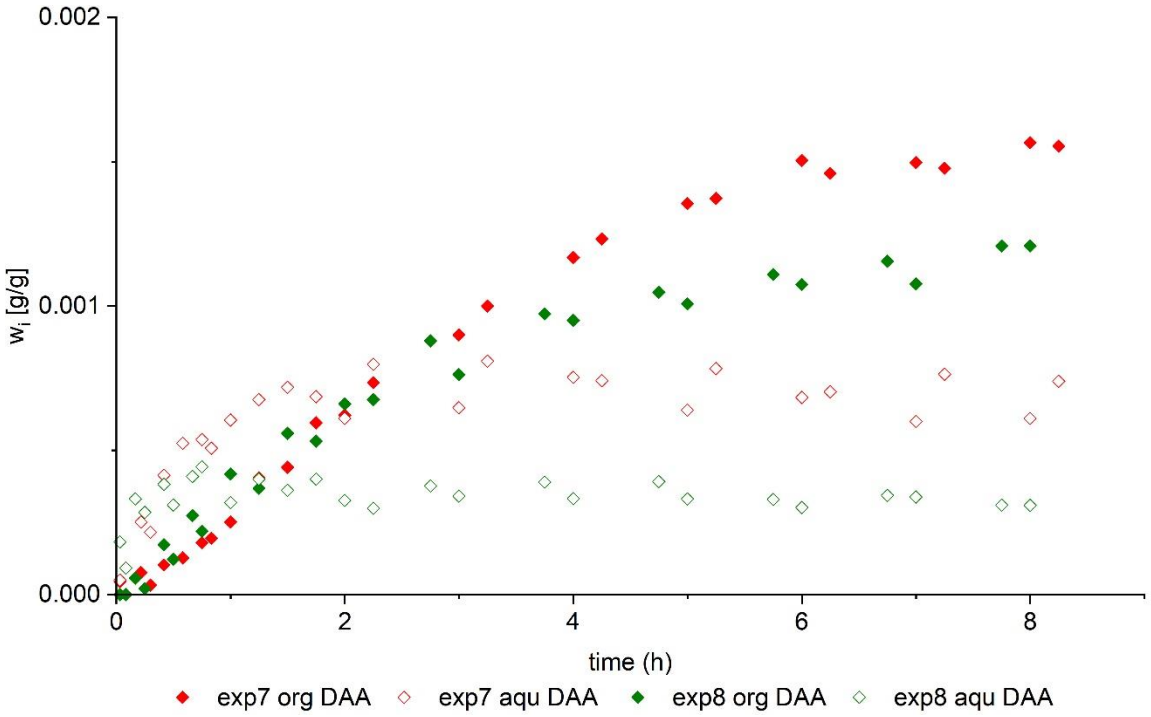

Figure 4-17: Composition over time for Nitsch cell experiment 7 and 8, 25°C and 40°C, 1 atm, ternary system water/toluene/acetone, target component DAA, with NaOH injected in the aqueous phase.

The concentration of formed DAA in the experiments with ongoing reaction is very small, hence a comparison of experiment 2 and experiment 7 is plotted with a secondary axis. On the left side of the diagram, the concentration of DAA for experiment 7 is plotted, while on the right side, the concentration of DAA for experiment 2 is plotted. In experiment 2, DAA is injected into the aqueous phase at 25°C and in experiment 7, DAA is formed in the aqueous phase in the presence of NaOH at 25°C. In Figure 4-18 the comparison is shown.

DAA is transferred from the aqueous to the organic phase in both experiments. The increase of DAA in the organic phases without ongoing reaction is similar to composition of DAA in the aqueous phase with ongoing reaction, where DAA is formed. The mass transfer from the aqueous phase to the organic phase in experiment 2 leads to a steep curve for the DAA concentration at the beginning in the organic phase. At the same time, the DAA concentration in the aqueous phase decreases. In experiment 7 DAA is formed from acetone in the aqueous phase and then transferred into the organic phase, hence the DAA concentration in both phases increases over time. The increase of DAA concentration in the organic phases is different for each experiment.

Experiment 7 shows that the formation of DAA in the aqueous phase is faster than the interfacial mass transfer, which leads to an inflection point in the curve.

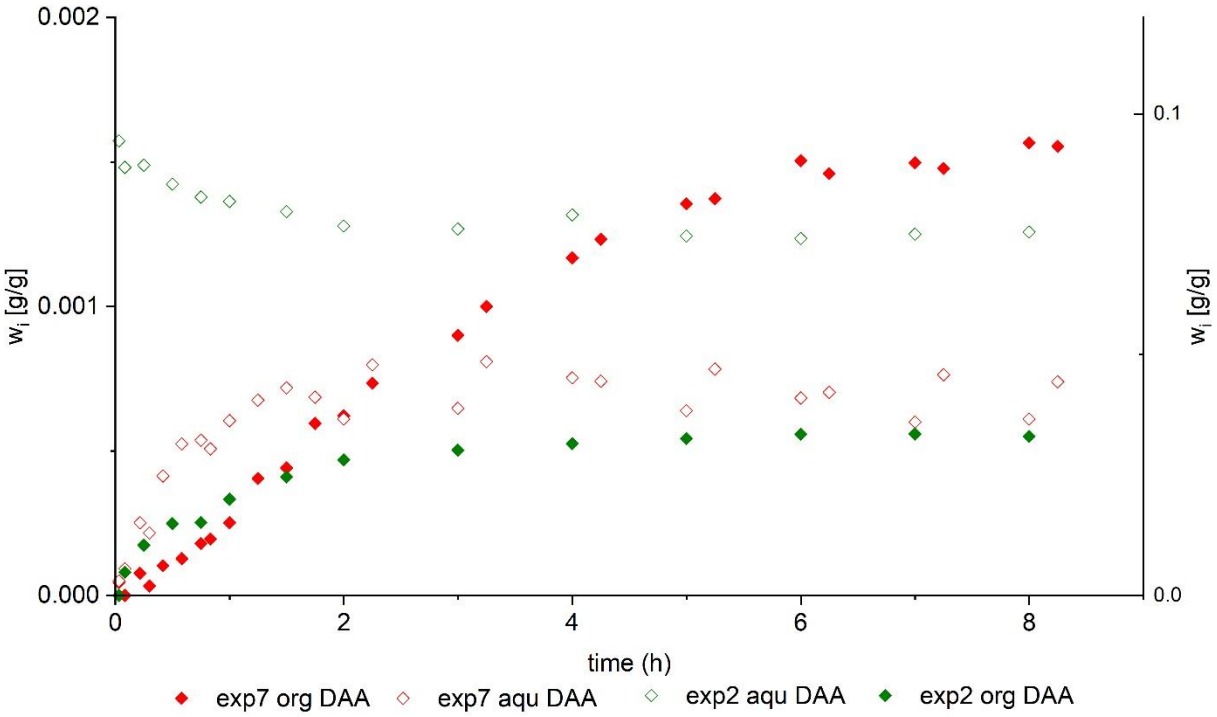

Figure 4-18: Composition over time for Nitsch cell experiment 2 and 7, 25°C and 40°C, 1 atm, ternary system water/toluene/acetone, target component DAA, with NaOH injected in the aqueous phase.

5 Summary and outlook

Within the scope of this thesis a kinetic study of the aldol self-condensation of acetone to diacetone alcohol in a water/toluene system was conducted. The reaction kinetics and LLE in the quaternary system were investigated and mass transfer experiments in a Nitsch cell with and without overlaid aldol self-condensation of acetone were conducted.

At first, a catalyst screening with basic and acidic catalysts was conducted. After choosing 0.5M NaOH as catalyst, the reaction kinetics were determined.

The experiments to determine the reaction rate constants at different temperatures and with various amounts of acetone were conducted in the aqueous phase. The catalyst is only soluble in water, hence the reaction only takes place in the aqueous phase. The chosen reaction was investigated at 25°C and 40°C. The amounts of acetone in the aqueous phase were varied for both temperatures between 3 w%, 6 w% and 12 w% with respect to the overall mass. The results showed that a higher temperature leads to a higher reaction rate and a smaller conversion. The activation energy and the frequency factor were determined from the Arrhenius equation.

The model for the reaction kinetics was based on the work of Kuśtrowski et al. [4]. The results showed good accordance with the experimental data.

For the LLE , eleven different mixtures were prepared and analyzed. Due to the catalyst and the reactive substances, the analytical procedure was challenging. Therefore, some deviations were observed in the results. Despite the difficulties with the analytical method, the mixing points were met in good accordance. It was observed that the solubility of acetone is almost the same in the aqueous and organic phase, whereas the solubility of DAA is higher in the aqueous phase than in the organic phase. The solubility increases slightly with higher temperature. The interfacial tension is also dependent on the amount of target component (acetone and DAA) in the system. The higher the concentration of target component, the lower is the interfacial tension. The impact of the temperature on the interfacial tension is very small, due to the low influence of temperature on the subsystem water/toluene.

These data are important to design a reactive extraction process and the conclusions can also be observed in the results of the mass transfer experiments.

A Nitsch cell was used to determine the interfacial mass transfer of the target components in a quaternary system between the aqueous and the organic toluene phase. These experiments were conducted at 25°C and 40°C with an amount of 6 w% starting concentration of acetone with respect to the overall mass. The results showed that at a higher temperature, the mass transfer as well as the overlaid aldol self-condensation of acetone was faster. The equilibrium conversion, however, decreased with increasing temperature Moreover, the overlaid reaction led to a different development of bulk phase composition compared to the purely diffusive mass transfer. It showed an inflection point in the organic phase at the same time as the equilibrium concentration was reached in the aqueous phase. In the aqueous phase the formed DAA concentration resembles the kinetic study. After two hours the equilibrium concentration was reached in the aqueous phase. In the organic phase the equilibrium concentration was not reached within that time, because the mass transfer continued and the overall equilibrium was not reached yet. After eight hours the overall equilibrium was approximated in the organic phase.

Appendix

Appendix A

Abbreviations

ICVT	Institute of Chemical Engineering and Environmental Technology
LLE	liquid-liquid-equilibrium
DAA	diacetone alcohol
MO	mesityl oxide
E1cB	elimination mechanism
OH-	hydroxide ion
DGT	density gradient theory
NMR	nuclear magnetic resonance
GC	gas chromatography
FID	flame ionization detector
DMSO	dimethyl sulfoxide
THF	tetrahydrofuran
NaOH	sodium hydroxide
Ba(OH)2	barium hydroxide
KOH	potassium hydroxide
H2SO4	sufuric acid
H3PO4	o-phosphoric acid
HCl	hydrochloric acid
Ca(OH)2	calcium hydroxide
A	acetone
W	water
T	toluene
aqu	aqueous
org	organic
exp	experiment
std	standard

Symbols

Symbol	unit	description
a	-	activity
a,b,c,d	-	stoichiometric coefficients
A,B,C,D,R	-	components
A	mol/(l*s)	frequency factor
c	mol/l	concentration
D	m^2/s	diffusion coefficient
E_A	J/mol	activation energy
f	Pa	fugacity
g	m/s^2	gravitational force
g^*	m/s^2	force due to rotational acceleration
I	-	phase in a system
j	mol/m^2s	flux
k	mol/(l*s)	reaction rate constant
k	m/s	mass transfer coefficient
K	-	equilibrium constant
L	m	length
n	-	reaction order
n	rpm	rotational speed
N	mol/m^2s	flux at interface
p	MPa	pressure
r	mol/m^3s	reaction rate
R	J/(mol*K)	gas constant
R	mm	radius
t	s	time
T	°C	temperature
v	m/s	velocity
x	mol/mol	amount-of-substance fraction
X	-	conversion

Greek symbols

α, β, γ	-	reaction order
γ	-	activity coefficient
δ	mm	layer thickness
η	Pa*s	dynamic viscosity
λ	mm	potential distance
ϑ	°C	temperature
μ	J/mol	chemical potential
ρ	kg/m^3	density
σ	kg/s^2	interfacial tension
υ	m^2/s	kinematic viscosity
φ	-	fugacity coefficient

Subscript character

0	start value
0	pure component
i	component in the system
i	interface
j	medium
∞	equilibrium
I,II	phase I, phase II

References

[1] K. Sattler, *Thermische Trennverfahren*. Mannheim: Wiley-VCH Verlag, 2001.

[2] O. B. B. Thoma J., *Modelling and Simulation in Thermal and Chemical Engineering*. Springer-Verlag, 2000.

[3] G. S. Salvapati, K. V. Ramanamurty, and M. Janardanarao, “Selective catalytic self-condensation of acetone,” *J. Mol. Catal.*, vol. 54, no. 1, pp. 9–30, 1989, doi: 10.1016/0304-5102(89)80134-8.

[4] P. Kuśtrowski, D. Sułkowska, R. Pytlowany, and R. Dziembaj, “Kinetics of self-condensation of acetone over heterogeneous Ba(OH)2 and Sr(OH)2 catalysts,” *React. Kinet. Catal. Lett.*, vol. 81, no. 1, pp. 3–11, 2004, doi: 10.1023/B:REAC.0000016510.02042.8d.

[5] H.-J. Bart, *Reactive Extraction*. Springer-Verlag, 2001.

[6] R. Marr and H.-J. Bart, “Metallsalz-Extraktion,” *Chemie Ing. Tech.*, vol. 54, no. 2, pp. 119–129, 1982, doi: 10.1017/CBO9781107415324.004.

[7] J. Hartl and R. Marr, “Dreiphasenextraktion zur Anreicherung bei der Flüssig/Flüssig-Extraktion von Carbonsäuren,” *Chemie Ing. Tech.*, vol. 65, no. 7, pp. 810–818, 1993, doi: 10.1002/cite.330650706.

[8] H. P. Latscha, U. Kazmaier, and H. A. Klein, *Organische Chemie*. Springer-Verlag, 2016.

[9] G. G. Podrebarac, F. T. T. Ng, and G. L. Rempel, “A kinetic study of the aldol condensation of acetone using an anion exchange resin catalyst,” *Chem. Eng. Sci.*, vol. 52, no. 17, pp. 2991–3002, 1997, doi: 10.1016/S0009-2509(97)00098-5.

[10] J. Clayden, N. Greeves, and S. Warren, *Organic Chemistry*, vol. 85, no. 9. Oxford University Press, 2012.

[11] O. Levenspiel, *Chemical Reaction Engineering*. John Wiley & Sons, 1999.

[12] M. Jakubith, *WILEY-VCH*. Weinheim: Wiley-VCH Verlag, 1998.

[13] S. R. Maple and A. Allerhand, “Analysis of Minor Components by Ultrahigh Resolution NMR 2. Detection of 0.01% Diacetone Alcohol in ‘Pure’ Acetone and Direct Measurement of the Rate of the Aldol Condensation of Acetone,” *J. Am. Chem. Soc.*, vol. 109, no. 22, pp. 6609–6614, 1987, doi: 10.1021/ja00256a008.

[14] A. Mersmann, M. Kind, and J. Stichlmair, *Thermal Seperation Technology*. Heidelberg: Springer-Verlag, 2011.

[15] P. Stephan, K. Schaber, K. Stephan, and F. Mayinger, *Thermodynamik*. Heidelberg: Springer-Verlag, 2010.

[16] R. Bock and A. Monerjan, “Über die Gültigkeit des Nernstschen Verteilungsgesetzes bei kleinen Konzentrationen *,” 1966.

[17] F. Ruiz, D. Prats, and V. Gomls, “Quaternary liquid-liquid equilibrium. water-ethanol-1-butanol-chloroform at 25 °C. experimental determination and graphical representation of equilibrium data,” *J. Chem. Eng. Data*, vol. 29, no. 2,

pp. 147–151, 1984, doi: 10.1021/je00036a015.

[18] J. Spurk, *Strömungslehre*. Berlin: Springer Vieweg, 2019.

[19] E. L. Cussler, *Diffusion Mass Transfer in Fluid Systems*. Cambridge University Press, 2009.

[20] R. Nagl, P. Zimmermann, and T. Zeiner, “Interfacial Mass Transfer in Water-Toluene Systems,” *J. Chem. Eng. Data*, 2019, doi: 10.1021/acs.jced.9b00672.

[21] A. Friebel, A. Fröscher, K. Münnemann, E. von Harbou, and H. Hasse, “In situ measurement of liquid-liquid equilibria by medium field nuclear magnetic resonance,” *Fluid Phase Equilib.*, vol. 438, pp. 44–52, 2017, doi: 10.1016/j.fluid.2017.01.027.

[22] J. Thien, C. Peters, T. Brands, H. J. Koß, and A. Bardow, “Efficient Determination of Liquid-Liquid Equilibria Using Microfluidics and Raman Microspectroscopy,” *Ind. Eng. Chem. Res.*, vol. 56, no. 46, pp. 13905–13910, 2017, doi: 10.1021/acs.iecr.7b03230.

[23] W. Nitsch, M. Raab, and R. Wiedholz, “Zum Transportmechanismus der Wärme- und Stoffübertragung zwischen turbulent bewegten flüssigen Phasen,” *Chemie Ing. Tech.*, vol. 45, no. 16, pp. 1026–1032, 1973, doi: 10.1002/cite.330451606.

[24] E. Bertakis, M. Kalem, and A. Pfennig, “Model-based geometry optimization of a Nitsch cell using the Fisher information matrix,” *Chem. Eng. Sci.*, vol. 63, no. 19, pp. 4881–4887, 2008, doi: 10.1016/j.ces.2007.07.043.

[25] D. C. Harris, *Lehrbuch der Quantitativen Analyse*, 8. Auflage., vol. 41, no. 11. Springer Spektrum, 2014.

[26] J. Viades-Trejo and J. Gracia-Fadrique, “Spinning drop method. From Young-Laplace to Vonnegut,” *Colloids Surfaces A Physicochem. Eng. Asp.*, vol. 302, no. 1–3, pp. 549–552, 2007, doi: 10.1016/j.colsurfa.2007.03.033.

List of figures

List of tables

Appendix B

Weighing

All devices that are used have a specific deviation. The accuracy and deviation of all scales are shown in Table 3-3. The weighing cannot be completely exact, therefore the actually weighed masses are shown in the following tables.

Table B-1: Weighed masses for the kinetic experiments.

T	c	Acetone	Water	NaOH
[°C]	[w%]	[g]	[g]	[g]
25	3	8.98	149.93	0.3081
		8.95	149.73	0.3070
	6	18.01	151.14	0.3068
		17.99	149.78	0.3078
	12	35.83	149.91	0.3077
		35.88	150.41	0.3085
40	3	8.99	150.96	0.3079
		8.95	150.08	0.3081
	6	18.07	150.01	0.304
		17.99	149.81	0.3082
	12	35.92	149.95	0.3065
		35.86	149.90	0.3078

Table B-2: Weighed mixing points for the LLE at 25°C.

Plane	Sample	Water	Toluene	DAA	Acetone
		[g]	[g]	[g]	[g]
1	1	19.02	19.04	1.01	1.01
1	2	18.02	18.03	2.03	2.00
1	3	16.01	16.03	4.09	4.01
1	4	14.01	14.01	6.01	6.24
1	5	13.02	13.01	7.01	7.00
2	6	19.02	19.05	1.56	0.51
2	7	17.01	17.01	4.51	1.56
2	8	15.02	15.01	7.68	2.52
3	9	19.04	19.02	0.51	1.68
3	10	17.04	17.02	1.59	4.52
3	11	15.04	15.00	2.60	7.51

Table B-3: Weighed mixing points for the LLE at 40°C.

Plane	Sample	Water	Toluene	DAA	Acetone
		[g]	[g]	[g]	[g]
1	1	19.81	19.20	1.02	1.00
1	2	18.19	18.05	2.04	2.03
1	3	16.00	16.02	4.04	4.69
1	4	14.14	14.04	6.01	6.06
1	5	13.25	13.02	7.18	7.02
2	6	19.11	19.25	1.51	0.49
2	7	17.03	17.05	4.56	1.50
2	8	15.04	15.05	7.51	2.52
3	9	19.02	19.09	0.51	1.51
3	10	17.01	17.14	1.49	4.50
3	11	15.06	15.08	2.50	7.50

Table B-4 Weighed masses for the mass transfer experiments in the Nitsch cell.

Number	T	Water	Toluene	Acetone	DAA	NaOH
	[°C]	[g]	[g]	[g]	[g]	[g]
1	25	348.58	304.5	45.68	45.35	-
2	25	354.17	308.9	39.5	39.49	-
3	25	354.02	309.2	39.79	39.66	-
4	25	354.48	308.79	39.7	39.48	-
		354.23	308.51	39.53	39.57	-
5	40	352.9	301.73	39.18	39.37	-
6	40	352.28	301.89	39.07	39.21	-
7	25	358.06	299.83	78.05	-	0.72
		358.15	301.36	78.2	-	0.72
8	40	355.47	293.91	77.25	-	0.72
		355.96	294.6	77.58	-	0.72

Calibration lines

All calibration lines are straight lines through the origin, which results in an intercept of 0. All values apply to the unit ppm.

Table B-5: Slopes for all calibration lines used for this thesis.

Use	Calibration	Component	Slope
Catalyst screening	Acetone, DAA, Toluene, MO in Water	Acetone	1815.80
		Toluene	4044.10
		MO	963.89
		DAA	112.66
	Acetone, DAA, Toluene, MO in THF	Acetone	1859.50
		Toluene	4229.40
		MO	2664.46
		DAA	1729.40
Reaction kinetics	Acetone, MO, DAA in Water	Acetone	1218.03
		MO	1225.80
		DAA	1269.51
LLE	Acetone, Toluene, DAA, DMSO in THF	Acetone	1549.88
		Toluene	3644.95
		DAA	1837.77
		DMSO	1512.07
Mass transfer in the Nitsch cell	Acetone, Toluene, DAA in THF	Acetone	2093.40
		Toluene	5720.79
		DAA	2565.42
	Acetone, Toluene, DAA in THF	Acetone	1369.97
		Toluene	3645.39
		DAA	1874.13
	Acetone, Toluene, DAA in THF	Acetone	1793.66
		Toluene	4258.70
		DAA	1995.06

Density and refraction

Before determining the interfacial tension, the density of all samples and the refraction of the aqueous samples have to be determined.

Table B-6: Density and refraction for the LLE samples at 25°C.

Phase	Sample	Density	Phase	Sample	Density	Refraction
		[g/cm^3]			[g/cm^3]	[-]
	1	0.8614		1	0.9942	1.3383
	2	0.8604		2	0.9914	1.3450
	3	0.8591		3	0.9852	1.3560
	4	0.8586		4	0.9771	1.3643
	5	0.8597		5	0.9736	1.3697
organic	6	0.8628	aqueous	6	0.9962	1.3408
	7	0.8635		7	0.9886	1.3542
	8	0.8664		8	0.9908	1.3647
	9	0.8596		9	0.9913	1.3383
	10	0.8567		10	0.9825	1.3475
	11	0.8518		11	0.9730	1.3550

Table B-7: Density and refraction for the LLE samples at 40°C.

Phase	Sample	Density	Phase	Sample	Density	Refraction
		[g/cm^3]			[g/cm^3]	[-]
	1	0.8464		1	0.9860	1.3373
	2	0.8460		2	0.9852	1.3433
	3	0.8109		3	0.9792	1.3513
	4	0.8323		4	0.9694	1.3603
	5	0.8458		5	0.9653	1.3428
organic	6	0.8486	aqueous	6	0.9912	1.3385
	7	0.8495		7	0.9865	1.3513
	8	0.8530		8	0.9823	1.3623
	9	0.8454		9	0.9864	1.3364
	10	0.8400		10	0.9783	1.3443
	11	0.8355		11	0.9671	1.3514

Appendix C

Appendix C1

The corresponding results of the kinetic experiments and the modeling are shown in this section.

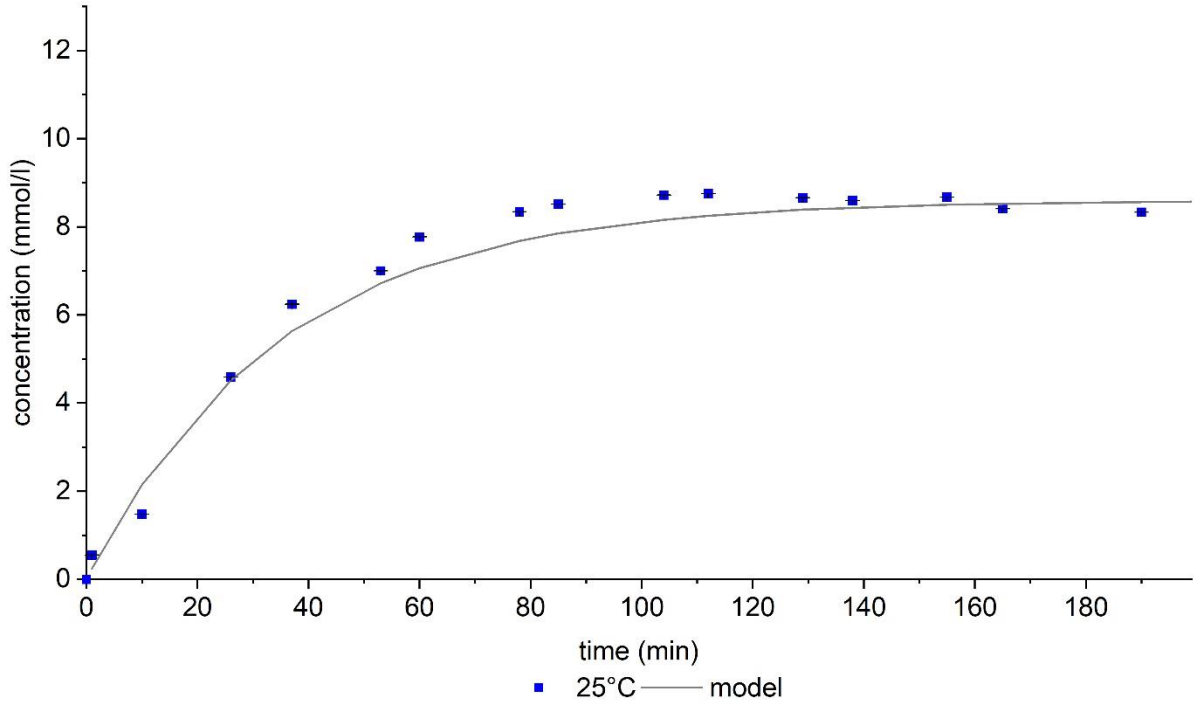

Figure C-1: Composition of DAA over time at 25°C and 1 atm with 3 w% starting concentration of acetone and 0.05M NaOH as catalyst and the fitted curve of the model.

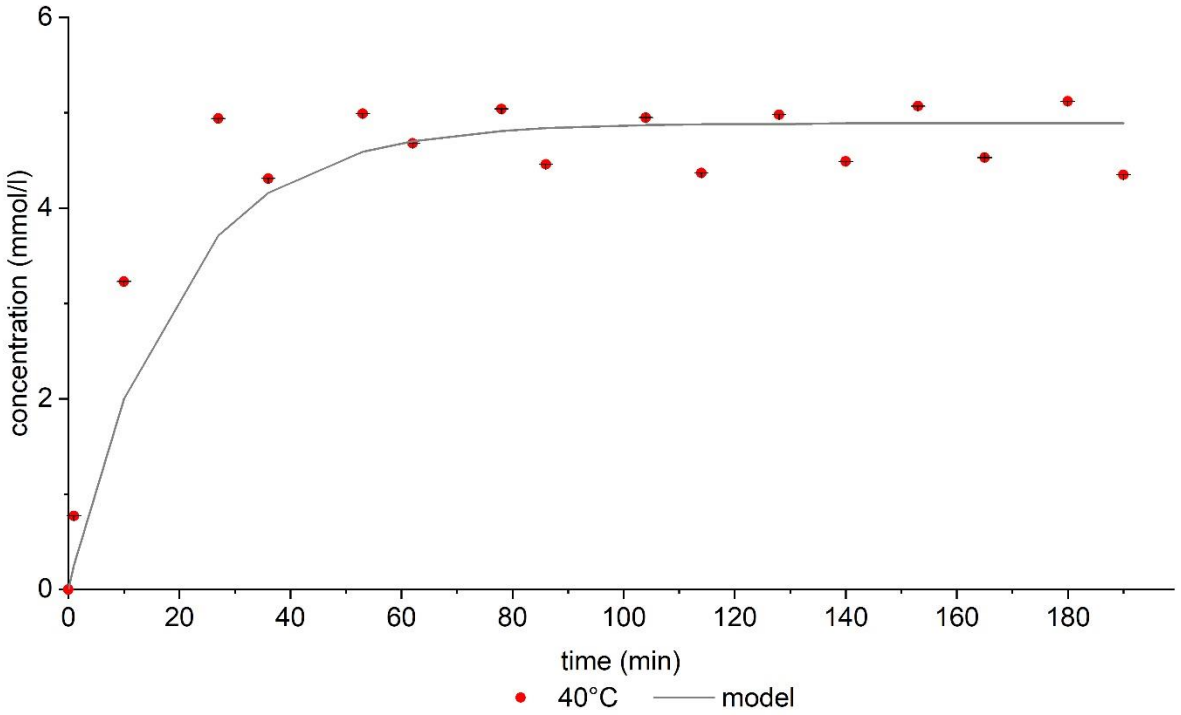

Figure C-2: Composition of DAA over time at 40°C and 1 atm with 3 w% starting concentration of acetone and 0.05M NaOH as catalyst and the fitted curve of the model.

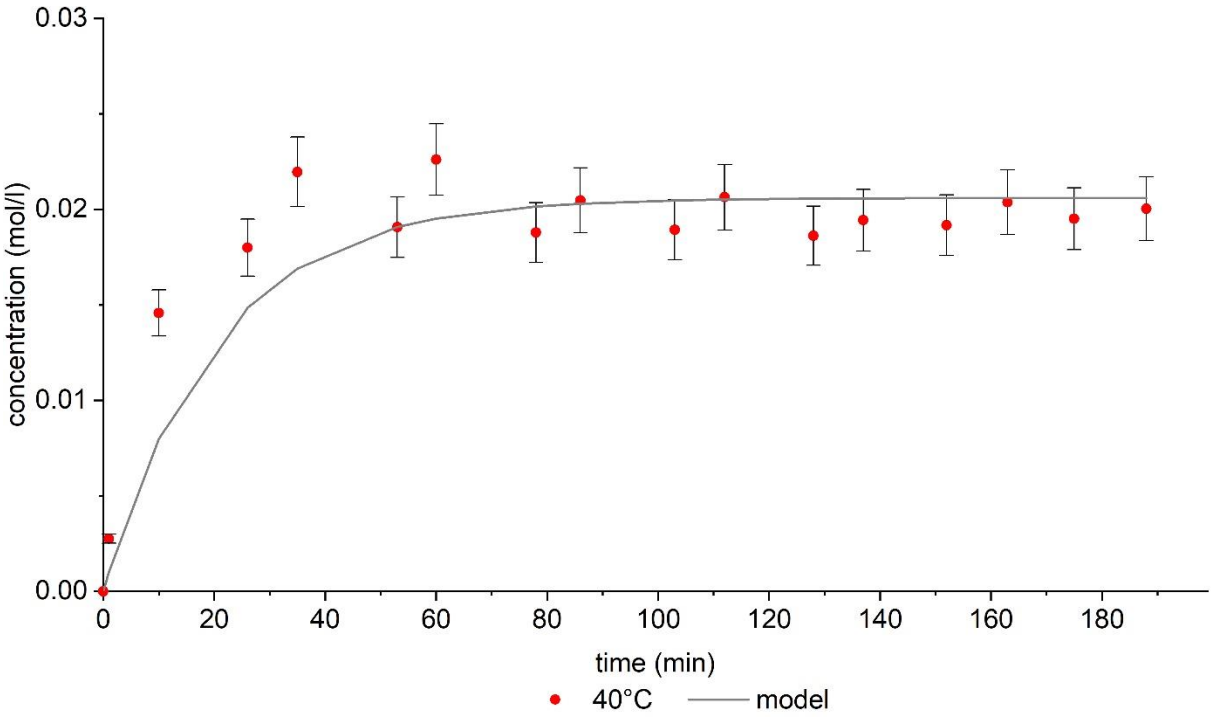

Figure C-3: Composition of DAA over time at 40°C and 1 atm with 6 w% starting concentration of acetone and 0.05M NaOH as catalyst and the fitted curve of the model.

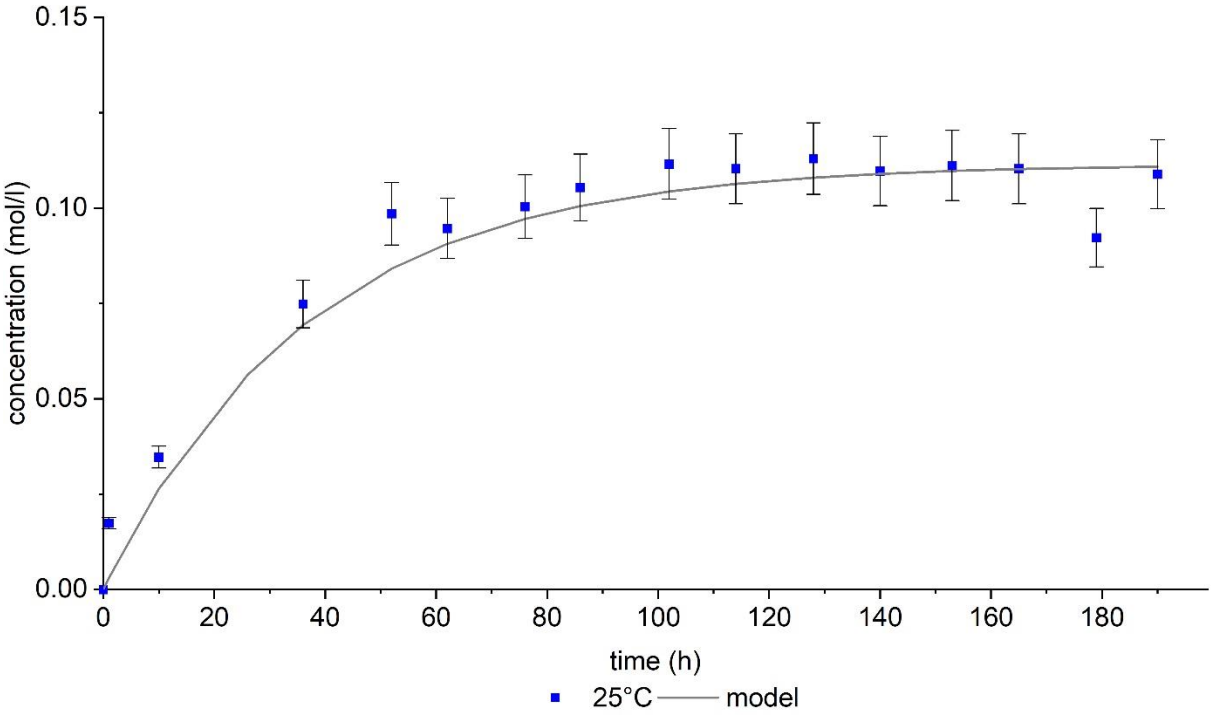

Figure C-4: Composition of DAA over time at 25°C and 1 atm with 12 w% starting concentration of acetone and 0.05M NaOH as catalyst and the fitted curve of the model.

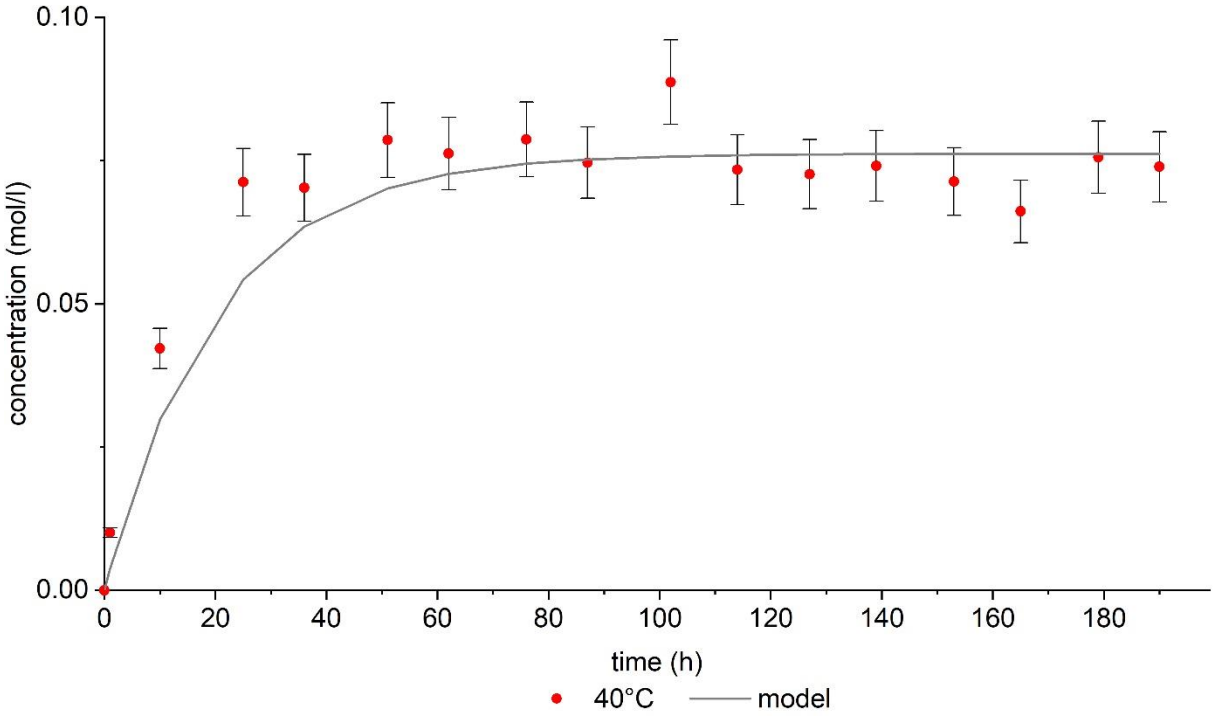

Figure C-5: Composition of DAA over time at 40°C and 1 atm with 12 w% starting concentration of acetone and 0.05M NaOH as catalyst and the fitted curve of the model.

Appendix C2

The corresponding results of the LLE experiments and interfacial tension are shown in this section.

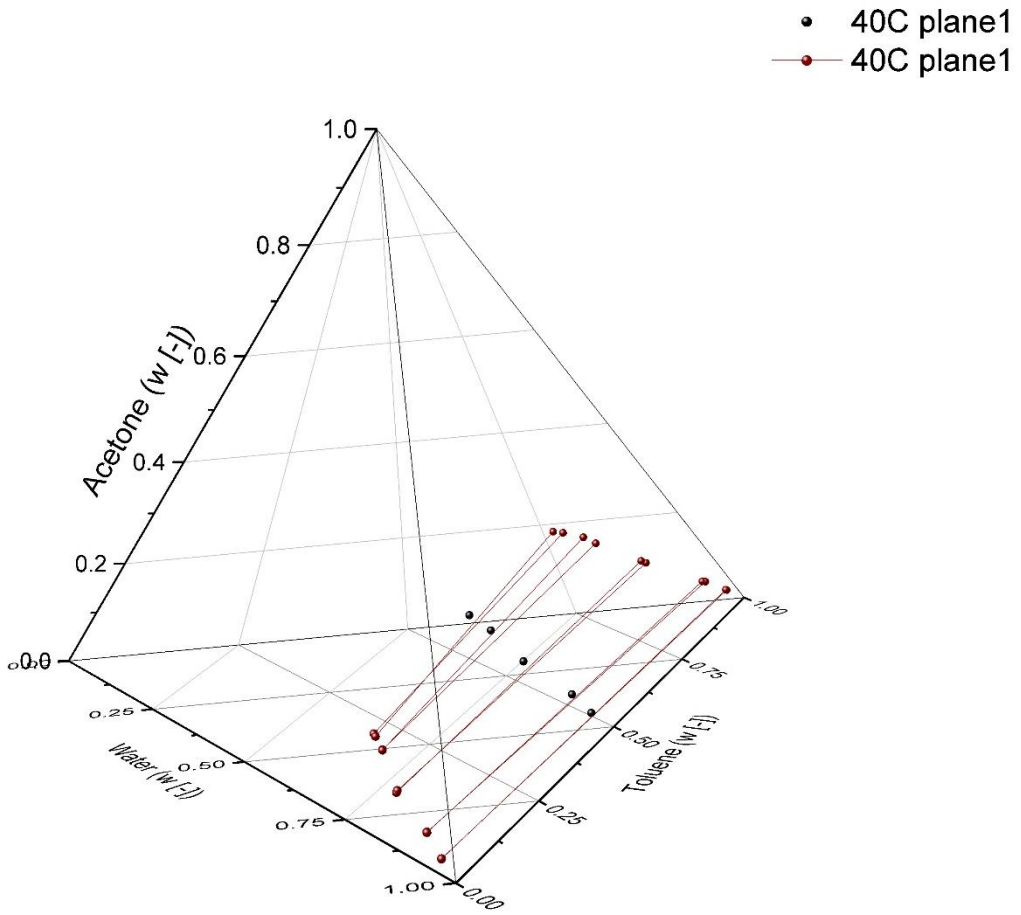

Figure C-6: LLE at 40°C, plane 1, tie lines 1-5, after 68 hours and 92 hours.

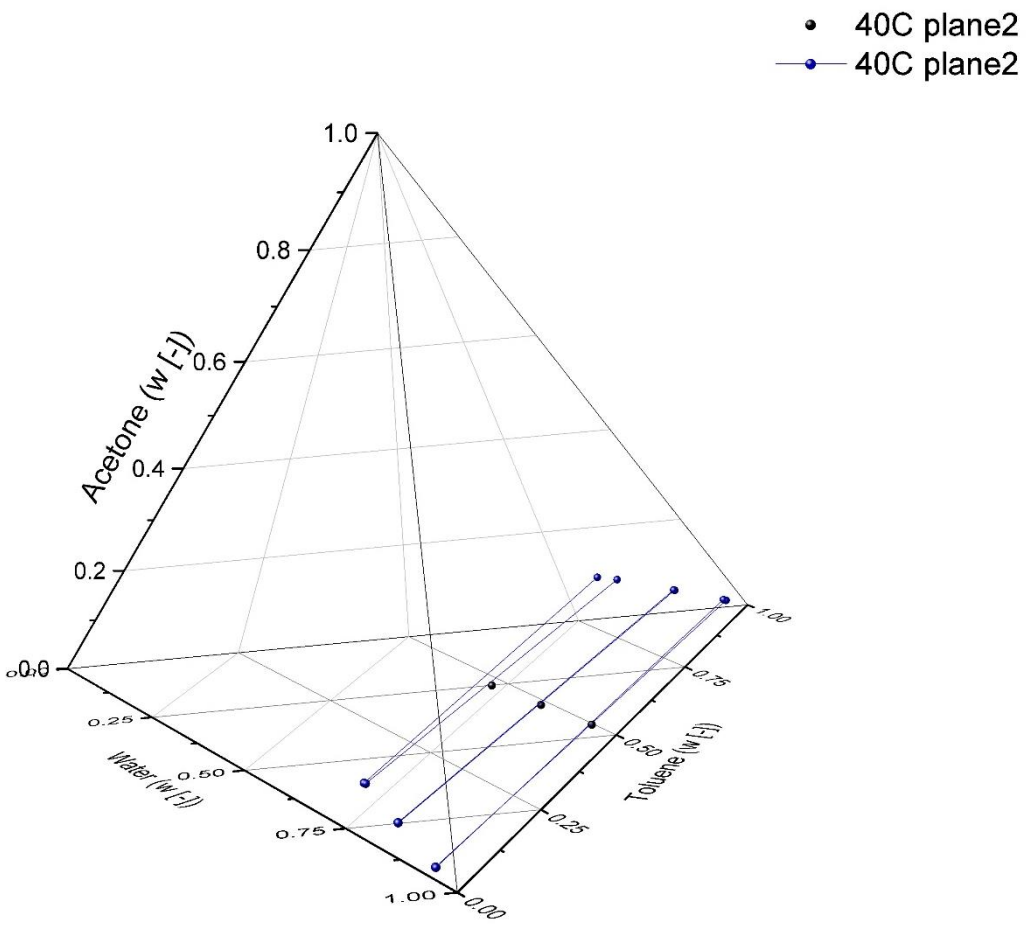

Figure C-7: LLE at 40°C, plane 2, tie lines 1-3, after 68 hours and 92 hours.

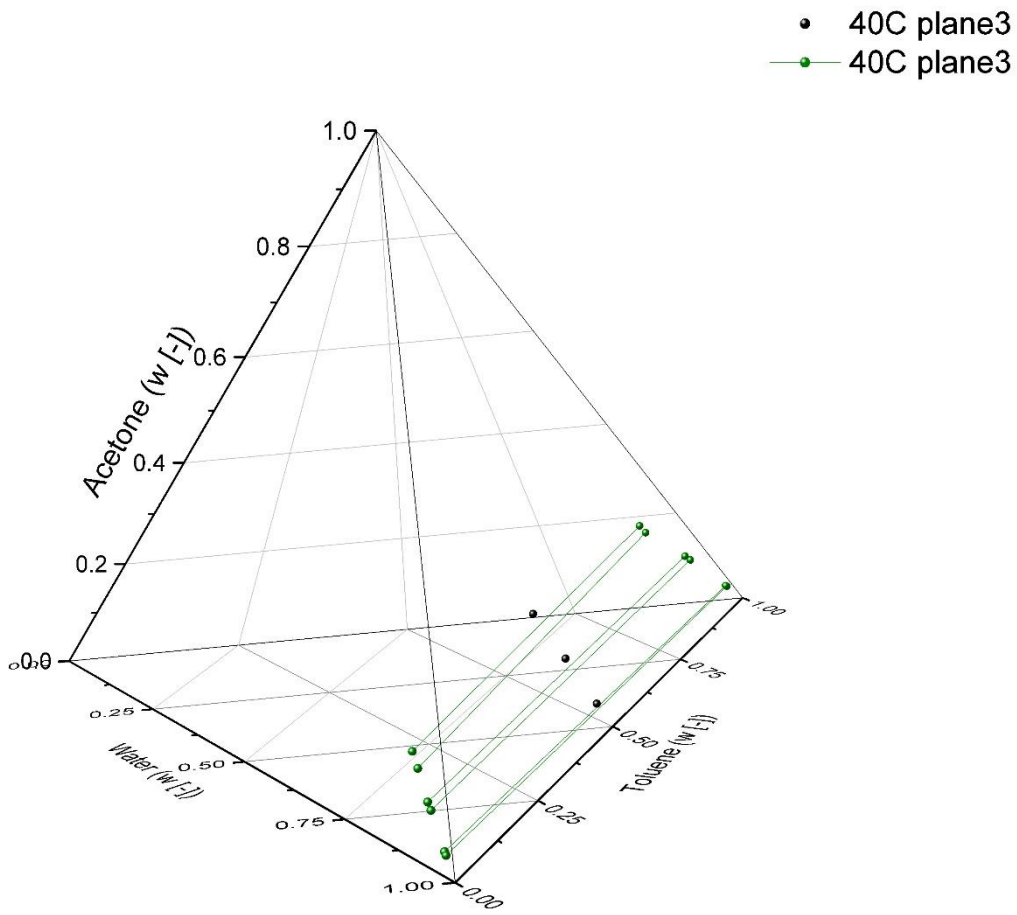

Figure C-8: LLE at 40°C, plane 3, tie lines 1-3, after 68 hours and 92 hours.

Table C-1: Results of LLE at 25°C in the organic phase after 68 hours.

Plane	Sample	Water	Toluene	DAA	Acetone
		w [-]	w [-]	w [-]	w [-]
1	1	0.0017	0.9639	0.0129	0.0215
1	2	0.0019	0.9237	0.0303	0.0441
1	3	0.0046	0.8166	0.0762	0.1026
1	4	0.0101	0.6941	0.1273	0.1686
1	5	0.0141	0.6323	0.1585	0.1951
2	6	0.0012	0.9653	0.0195	0.0140
2	7	0.0024	0.8873	0.0663	0.0440
2	8	0.0060	0.7572	0.1512	0.0856
3	9	0.0016	0.9576	0.0071	0.0337
3	10	0.0031	0.8742	0.0289	0.0938
3	11	0.0075	0.7570	0.0552	0.1803

Table C-2: Results of LLE at 25°C in the aqueous phase after 68 hours.

Plane	Sample	Water	Toluene	DAA	Acetone
		w [-]	w [-]	w [-]	w [-]
1	1	0.9420	0.0003	0.0317	0.0259
1	2	0.8891	0.0005	0.0607	0.0498
1	3	0.7956	0.0010	0.1130	0.0904
1	4	0.7074	0.0022	0.1534	0.1370
1	5	0.6695	0.0030	0.1764	0.1510
2	6	0.9306	0.0002	0.0496	0.0197
2	7	0.8120	0.0001	0.1339	0.0540
2	8	0.7049	0.0017	0.2082	0.0851
3	9	0.9503	0.0001	0.0155	0.0340
3	10	0.8641	0.0005	0.0449	0.0904
3	11	0.7881	0.0013	0.0678	0.1428

Table C-3: Results of LLE at 40°C in the organic phase after 68 hours.

Plane	Sample	Water	Toluene	DAA	Acetone
		w [-]	w [-]	w [-]	w [-]
1	1	0.0012	0.9625	0.0153	0.0211
1	2	0.0019	0.9184	0.0352	0.0446
1	3	0.0053	0.8007	0.0943	0.0997
1	4	0.0105	0.6969	0.1378	0.1548
1	5	0.0159	0.6306	0.1673	0.1862
2	6	0.0010	0.9599	0.0240	0.0151
2	7	0.0025	0.8662	0.0827	0.0486
2	8	0.0060	0.7612	0.1474	0.0854
3	9	0.0011	0.9601	0.0088	0.0300
3	10	0.0029	0.8711	0.0294	0.0966
3	11	0.0073	0.7672	0.0583	0.1671

Table C-4: Results of LLE at 40°C in the aqueous phase after 68 hours.

Plane	Sample	Water	Toluene	DAA	Acetone
		w [-]	w [-]	w [-]	w [-]
1	1	0.9513	0.0001	0.0272	0.0214
1	2	0.8987	0.0005	0.0555	0.0454
1	3	0.8049	0.0001	0.1152	0.0797
1	4	0.7316	0.0024	0.1432	0.1228
1	5	0.6965	0.0039	0.1622	0.1375
2	6	0.9384	0.0003	0.0445	0.0168
2	7	0.8306	0.0005	0.1213	0.0475
2	8	0.7310	0.0017	0.1916	0.0756
3	9	0.9551	0.0010	0.0157	0.0283
3	10	0.8830	0.0003	0.0391	0.0776
3	11	0.8143	0.0011	0.0606	0.1240

Table C-5: Results of LLE at 25°C in the organic phase after 92 hours.

Plane	Sample	Water	Toluene	DAA	Acetone
		w [-]	w [-]	w [-]	w [-]
1	1	0.0017	0.9639	0.0129	0.0215
1	2	0.0019	0.9237	0.0303	0.0441
1	3	0.0046	0.8166	0.0762	0.1026
1	4	0.0101	0.6941	0.1273	0.1686
1	5	0.0141	0.6323	0.1585	0.1951
2	6	0.0012	0.9653	0.0195	0.0140
2	7	0.0024	0.8873	0.0663	0.0440
2	8	0.0060	0.7572	0.1512	0.0856
3	9	0.0016	0.9576	0.0071	0.0337
3	10	0.0031	0.8742	0.0289	0.0938
3	11	0.0075	0.7570	0.0552	0.1803

Table C-6: Results of LLE at 25°C in the aqueous phase after 92 hours.

Plane	Sample	Water	Toluene	DAA	Acetone
		w [-]	w [-]	w [-]	w [-]
1	1	0.9420	0.0003	0.0317	0.0259
1	2	0.8891	0.0005	0.0607	0.0498
1	3	0.7956	0.0010	0.1130	0.0904
1	4	0.7074	0.0022	0.1534	0.1370
1	5	0.6695	0.0030	0.1764	0.1510
2	6	0.9306	0.0002	0.0496	0.0197
2	7	0.8120	0.0001	0.1339	0.0540
2	8	0.7049	0.0017	0.2082	0.0851
3	9	0.9503	0.0001	0.0155	0.0340
3	10	0.8641	0.0005	0.0449	0.0904
3	11	0.7881	0.0013	0.0678	0.1428

Table C-7: Results of LLE at 40°C in the organic phase after 92 hours.

Plane	Sample	Water	Toluene	DAA	Acetone
		w [-]	w [-]	w [-]	w [-]
1	1	0.0016	0.9602	0.0160	0.0223
1	2	0.0023	0.9128	0.0389	0.0460
1	3	0.0063	0.7903	0.0980	0.1054
1	4	0.0117	0.6702	0.1474	0.1707
1	5	0.0183	0.6122	0.1779	0.1917
2	6	0.0011	0.9548	0.0268	0.0173
2	7	0.0033	0.8635	0.0833	0.0498
2	8	0.0076	0.7266	0.1708	0.0951
3	9	0.0015	0.9573	0.0093	0.0318
3	10	0.0038	0.8578	0.0321	0.1063
3	11	0.0081	0.7500	0.0587	0.1832

Table C-8: Results of LLE at 40°C in the aqueous phase after 92 hours.

Plane	Sample	Water	Toluene	DAA	Acetone
		w [-]	w [-]	w [-]	w [-]
1	1	0.9514	0.0001	0.0274	0.0211
1	2	0.8994	0.0002	0.0552	0.0452
1	3	0.8060	0.0001	0.1174	0.0764
1	4	0.7331	0.0015	0.1427	0.1227
1	5	0.7031	0.0036	0.1582	0.1351
2	6	0.9401	0.0001	0.0430	0.0168
2	7	0.8300	0.0004	0.1218	0.0479
2	8	0.7296	0.0001	0.1940	0.0763
3	9	0.9571	0.0001	0.0148	0.0280
3	10	0.8868	0.0001	0.0385	0.0746
3	11	0.8138	0.0007	0.0604	0.1251

Table C-9: Interfacial tension at 25°C for DAA and acetone in the aqueous phase.

Sample	DAA	Acetone	Interfacial tension	Deviation
	w [-]	w [-]	[mN/m]	
-	0	0	35.50	
1	0.0317	0.0259	19.49	0.856
2	0.0607	0.0498	12.97	
3	0.1130	0.0904	7.43	
4	0.1534	0.1370	4.13	
5	0.1764	0.1510	3.04	
6	0.0496	0.0197	16.79	
7	0.1339	0.0540	8.82	
8	0.2082	0.0851	5.10	
9	0.0155	0.0340	18.69	
10	0.0449	0.0904	10.10	
11	0.0678	0.1428	6.53	

Table C-10: Interfacial tension at 40°C for DAA and acetone in the aqueous phase.

Sample	DAA	Acetone	Interfacial tension	Deviation
	w [-]	w [-]	[mN/m]	
-	0	0	35.50	
1	0.0274	0.0211	18.42	0.181
2	0.0552	0.0452	13.40	
3	0.1174	0.0764	9.55	
4	0.1427	0.1227	5.08	
5	0.1582	0.1351	3.51	
6	0.0430	0.0168	18.02	
7	0.1218	0.0479	9.98	
8	0.1940	0.0763	5.90	
9	0.0148	0.0280	19.26	
10	0.0385	0.0746	12.35	
11	0.0604	0.1251	7.33	

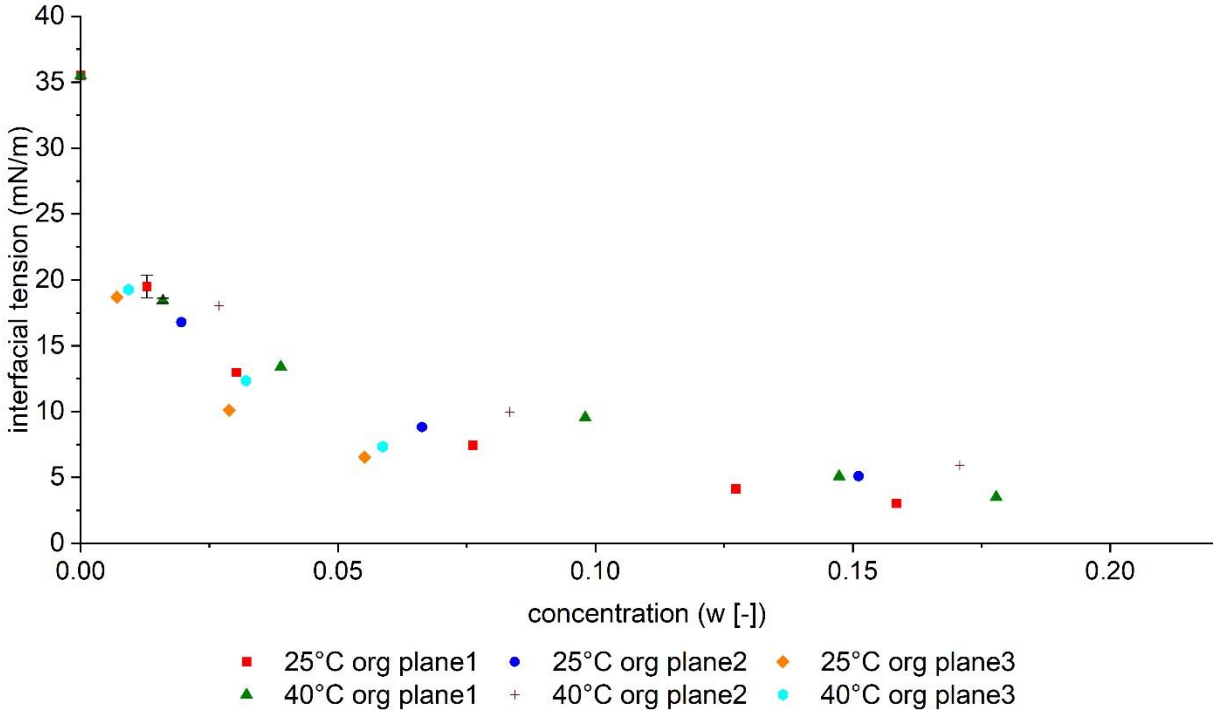

Figure C-9: Interfacial tension with respect to DAA concentration in the organic phase at 25°C and 40°C.

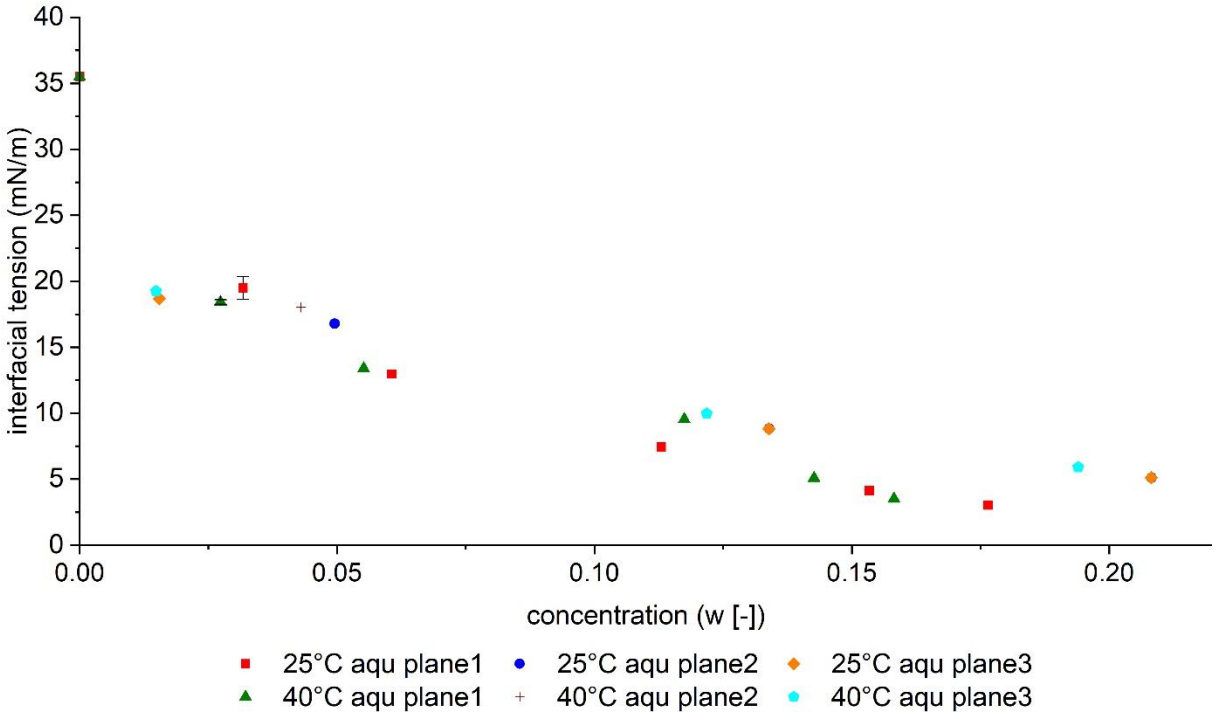

Figure C-10: Interfacial tension with respect to DAA concentration in the aqueous phase at 25°C and 40°C.

Appendix C3

The corresponding graphs from the mass transfer experiments in the Nitsch cell are shown in this section.

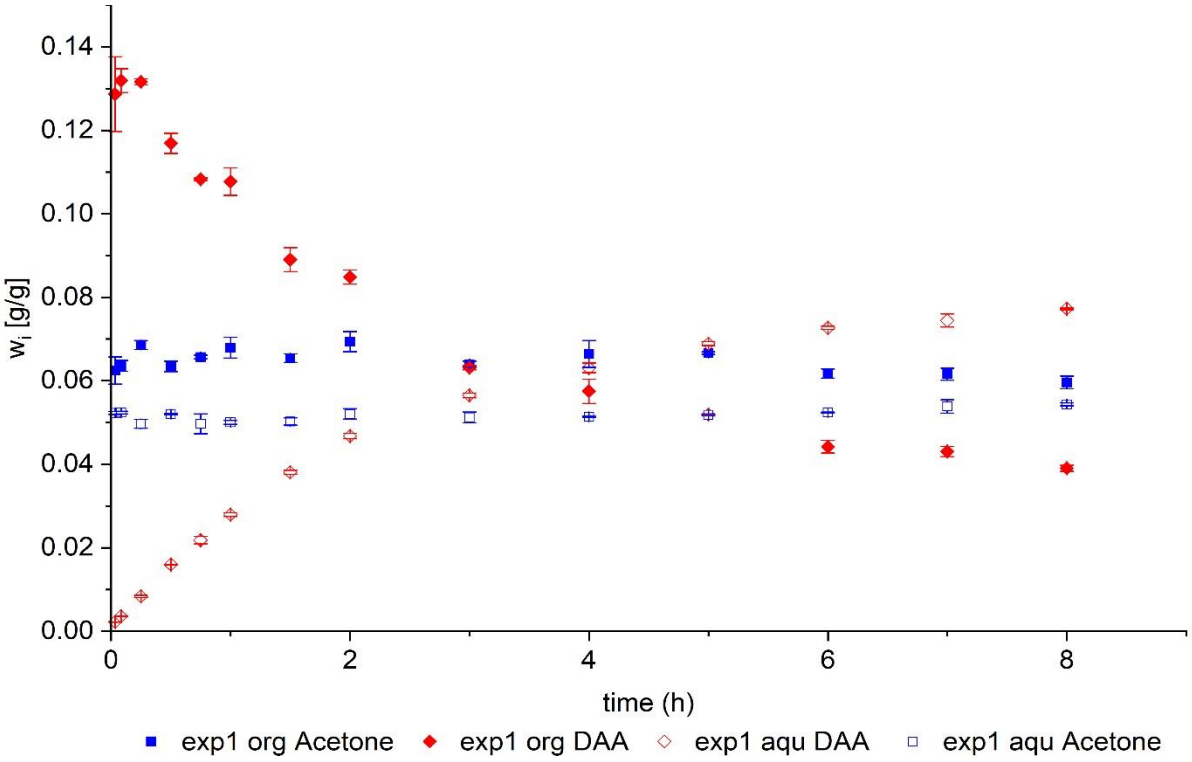

Figure C-11: Composition over time for Nitsch cell experiment 1, 25°C, 1 atm, ternary system water/toluene/acetone, target component DAA injected in the organic phase.

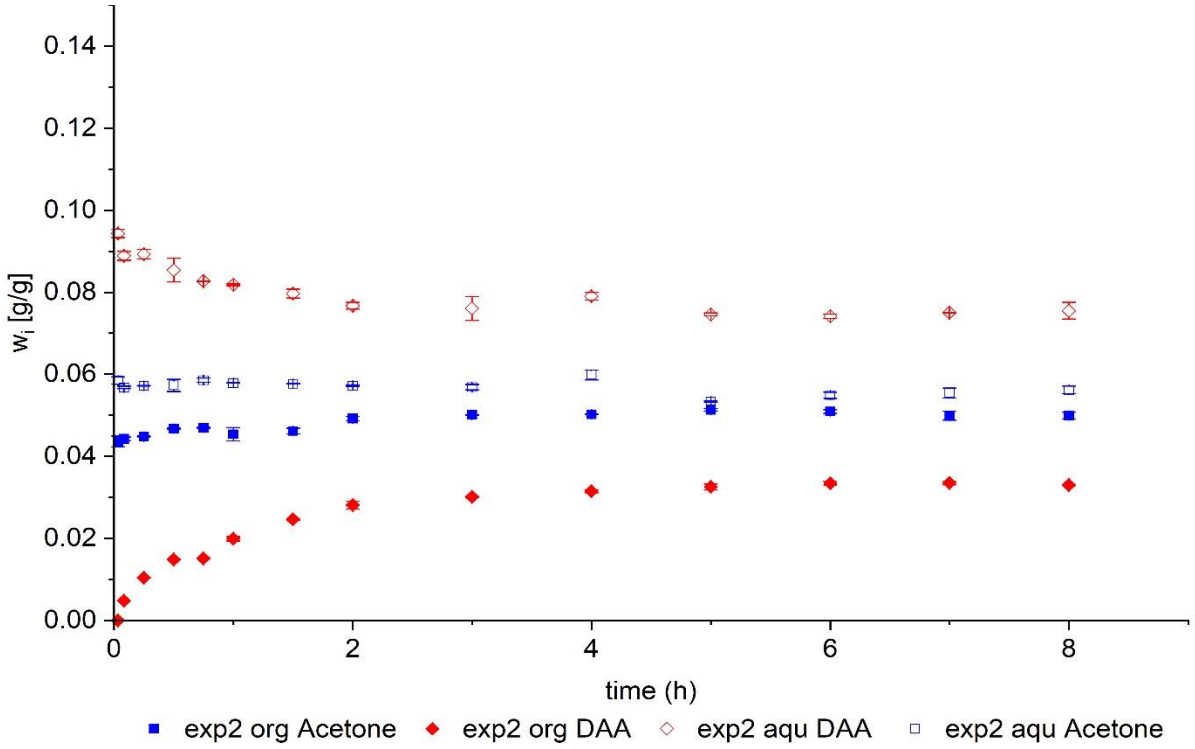

Figure C-12: Composition over time for Nitsch cell experiment 2, 25°C, 1 atm, ternary system water/toluene/acetone, target component DAA injected in the aqueous phase.

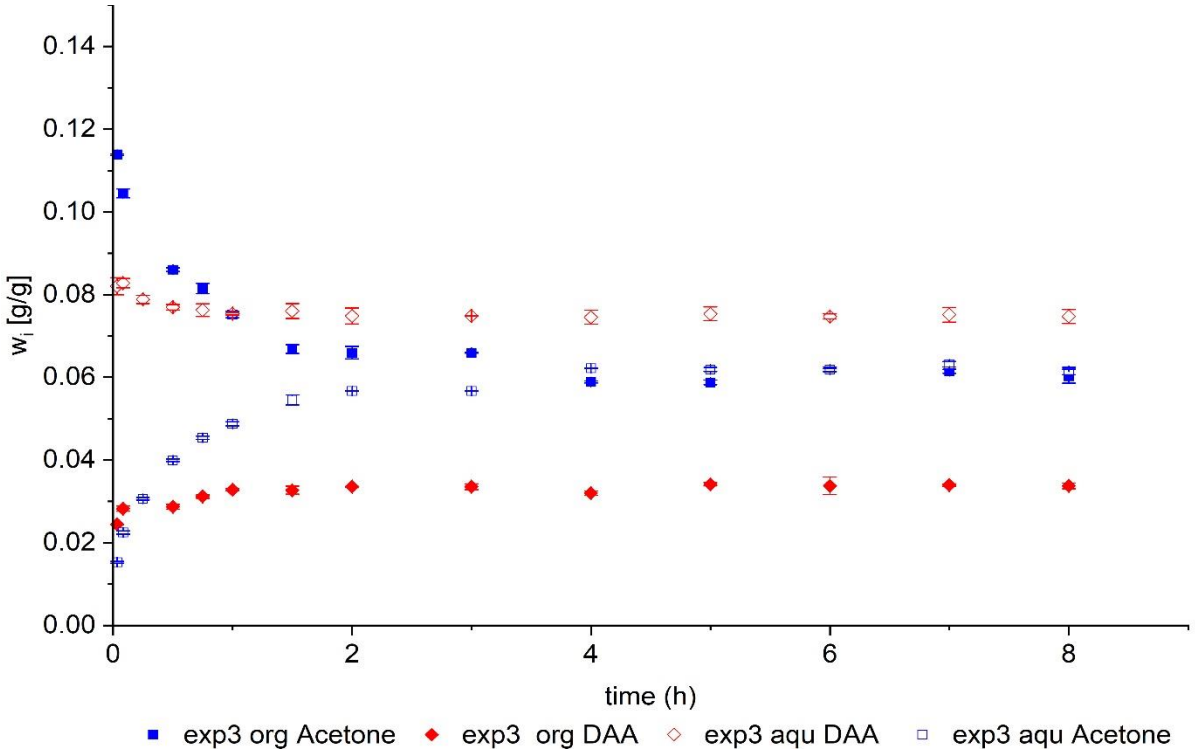

Figure C-13: Composition over time for Nitsch cell experiment 3, 25°C, 1 atm, ternary system water/toluene/DAA, target component acetone injected in the organic phase.

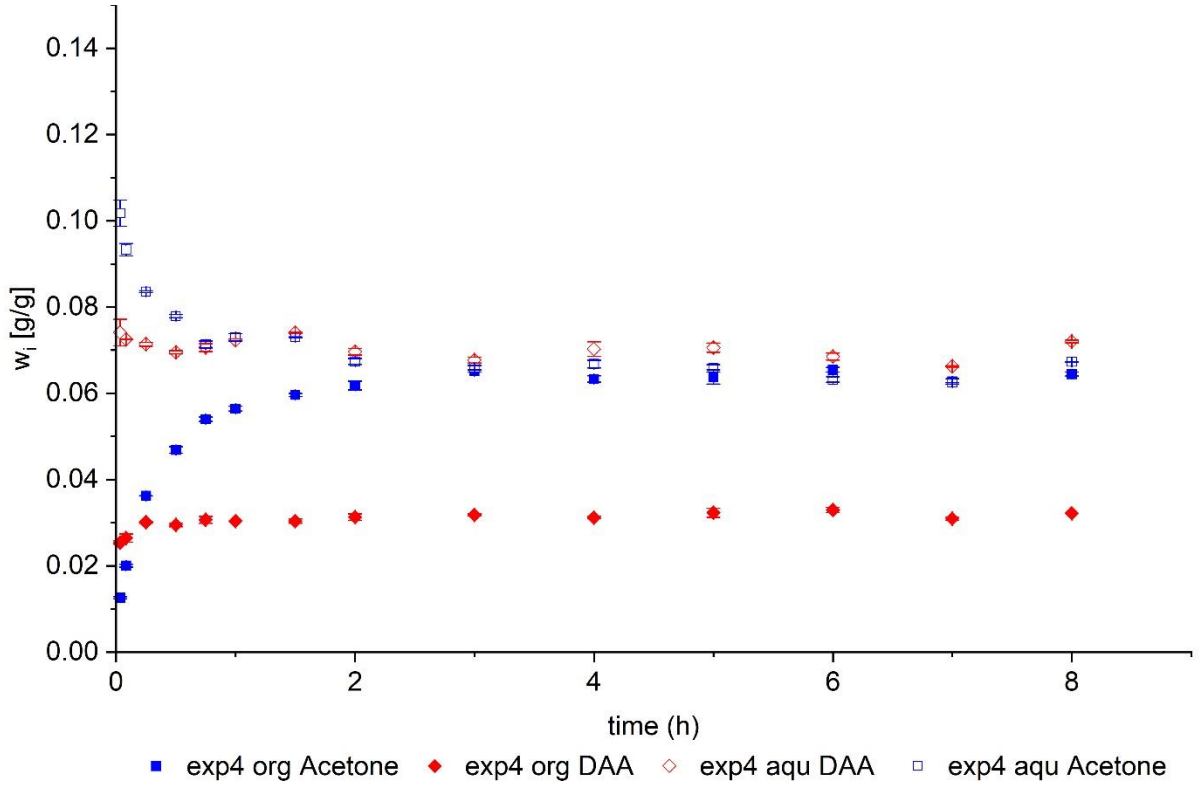

Figure C-14: Composition over time for Nitsch cell experiment 4, 25°C, 1 atm, ternary system water/toluene/DAA, target component acetone injected in the aqueous phase.

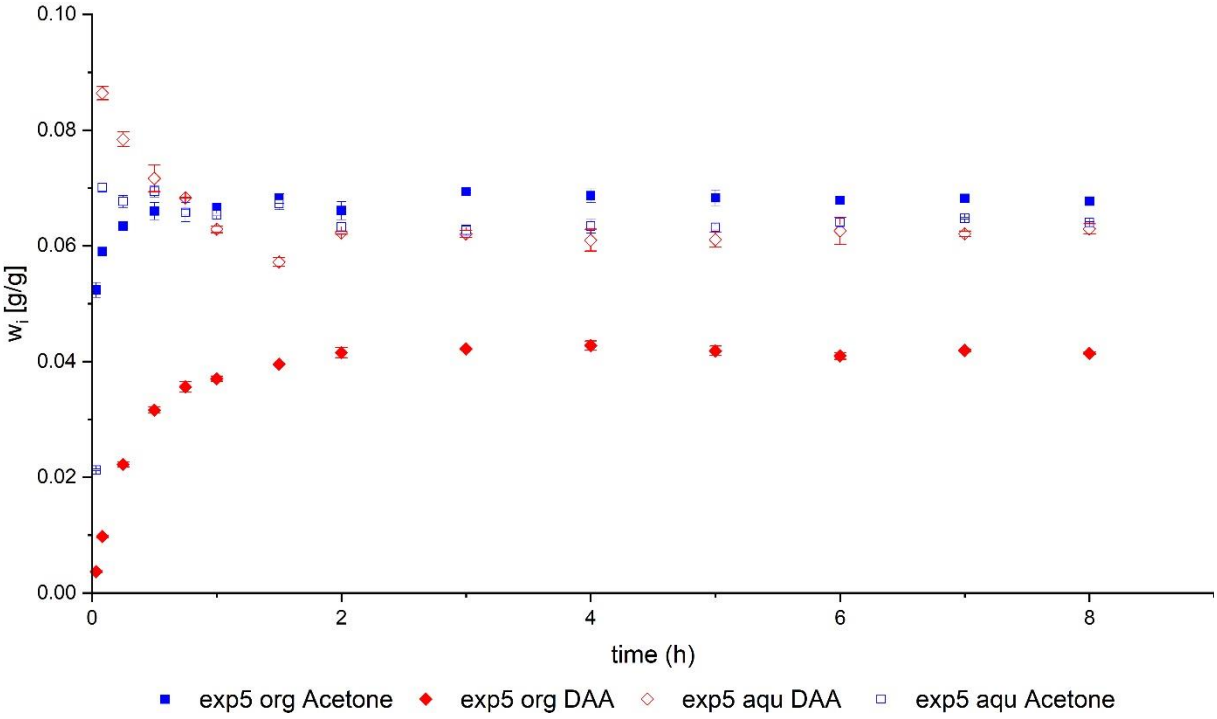

Figure C-15: Composition over time for Nitsch cell experiment 5, 40°C, 1 atm, ternary system water/toluene/acetone, target component DAA injected in the aqueous phase.

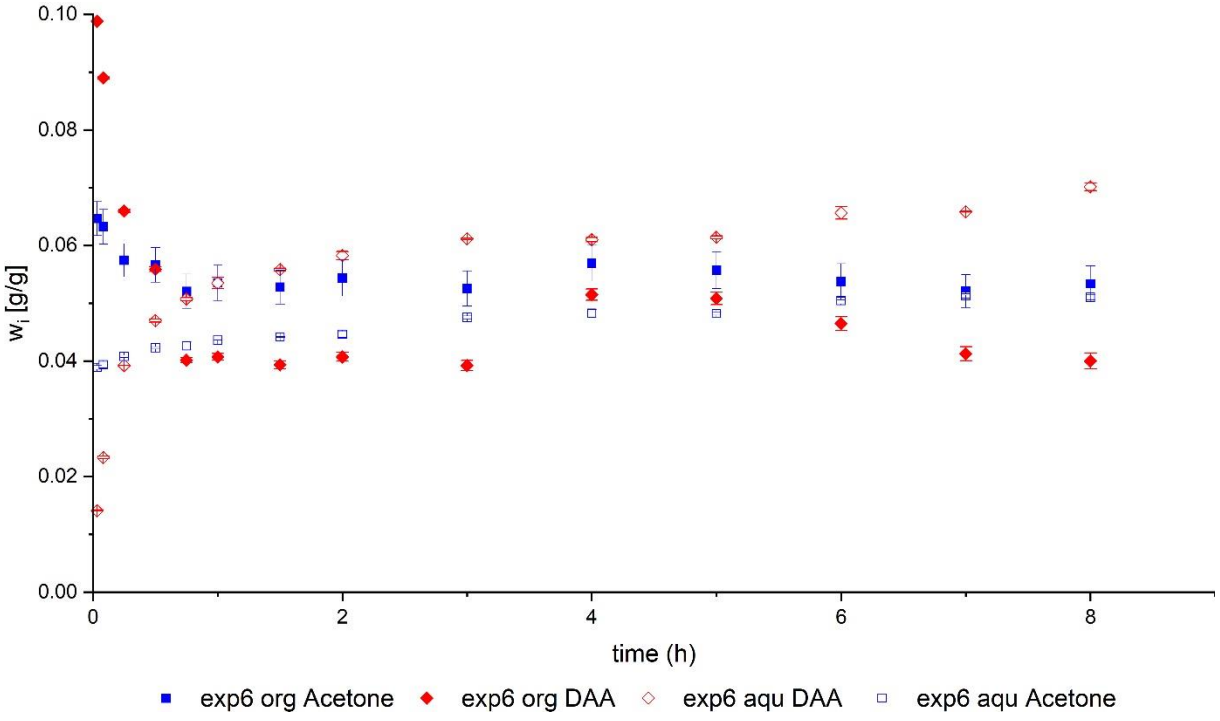

Figure C-16: Composition over time for Nitsch cell experiment 6, 40°C, 1 atm, ternary system water/toluene/acetone, target component DAA injected in the organic phase.

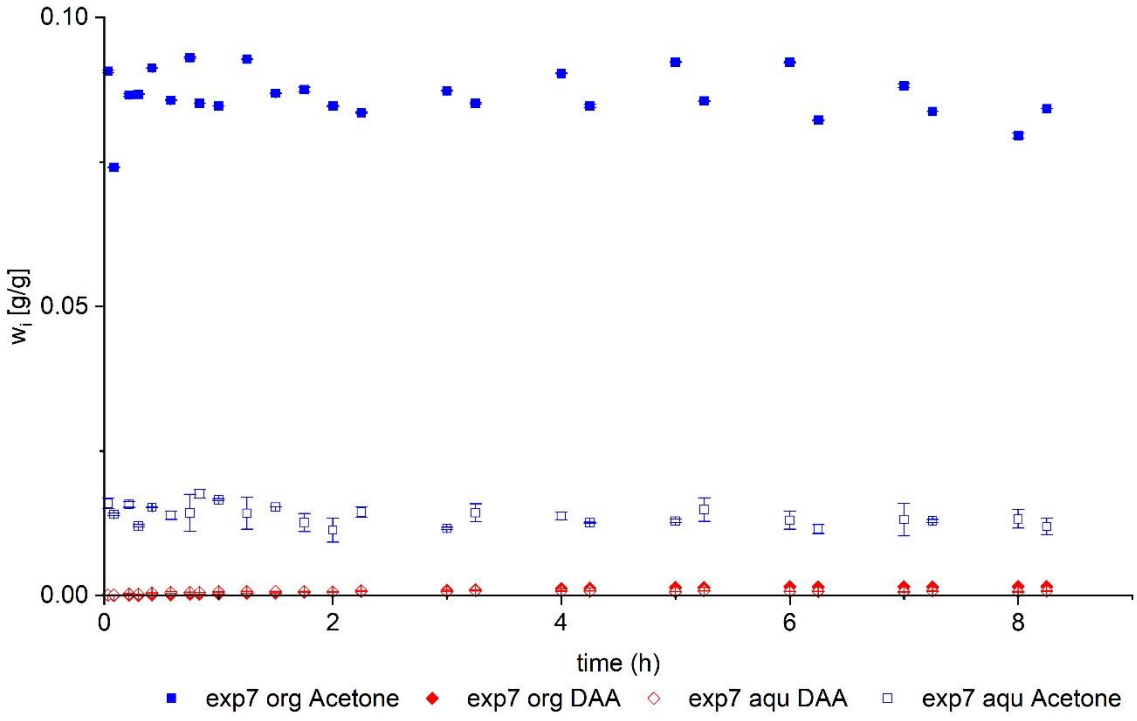

Figure C-17: Composition over time for Nitsch cell experiment 7, 25°C, 1 atm, ternary system water/toluene/acetone, target component DAA, NaOH injected in the aqueous phase.

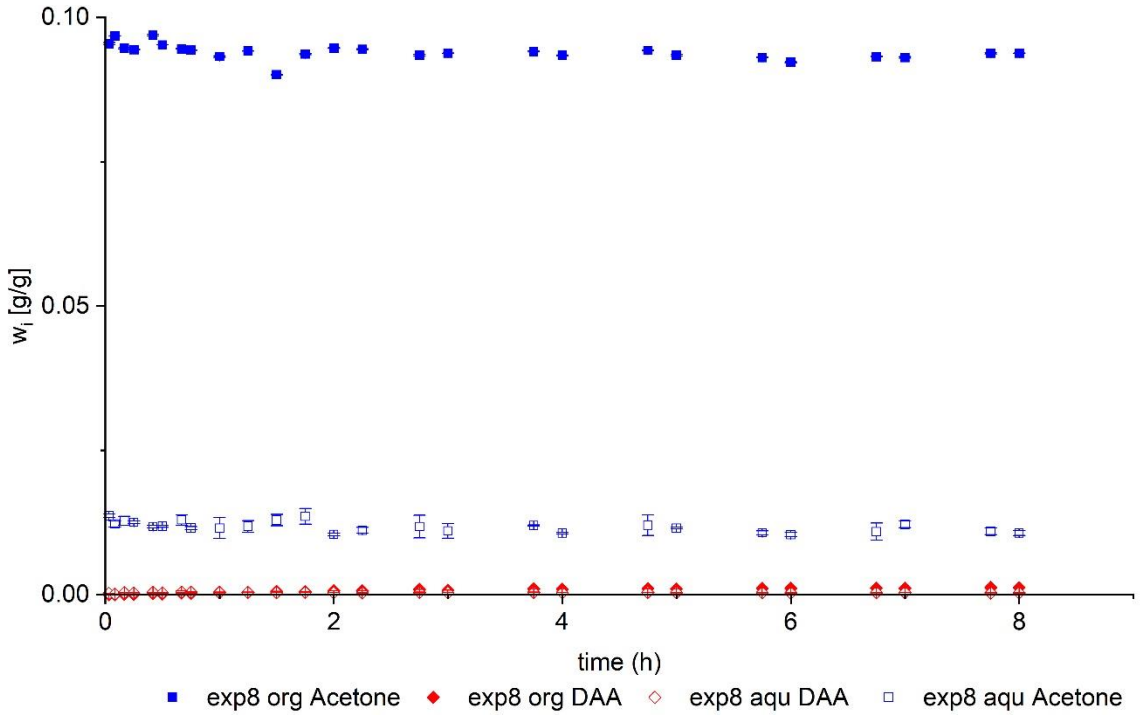

Figure C-18: Composition over time for Nitsch cell experiment 8, 40°C, 1 atm, ternary system water/toluene/acetone, target component DAA, NaOH injected in the aqueous phase.